

Transformation of Pharmaceutical and Personal Care Product Pollutants by
Wastewater Chlorine Disinfection and Aqueous Photolysis

A thesis
submitted to the faculty of the graduate school
of the University of Minnesota
by

Jeffrey M. Buth

In partial fulfillment of the requirements
for the degree of
Doctor of Philosophy

Co-advisors:
Kristopher McNeill
William Arnold

August, 2009

© Jeffrey M. Buth 2008

Acknowledgements

I'd like to start by thanking my advisors Kris McNeill and Bill Arnold for serving as my scientific mentors. Their insightful and complimentary approaches to science have challenged me to expand my ways of thinking through problems. Their excellence as advisors is matched by their kindness and generosity by which they make their labs great places to work.

The camaraderie with McNeill and Arnold group members, past and present, is much appreciated. I couldn't imagine working with a more helpful and friendly group of people. Special thanks to Matt Grandbois for synthesizing the compounds without which most of this research could not have been completed, and to Peter Steen for his constant willingness to help in obtaining environmental samples.

Don Winkler of the Metropolitan Wastewater Treatment Plant has been a great help in coordinating the wastewater sampling and a pleasure to work with. Pete Villalta of the Cancer Center mass spectrometry facility has gone above and beyond the call of duty to help get all our samples analyzed.

Funding from the U.S. Environmental Protection Agency STAR Fellowship Program has not only paid the bills and fed me, but has well-equipped me with supplies and opportunities for travel and scientific development.

Thanks to my parents, siblings, and friends who have been a huge support to me during grad school and throughout life.

Finally, I acknowledge the One through whom and for whom all things exist. He holds the bonds of every molecule together by His powerful word, and has held me together throughout my graduate school career.

Abstract

Concern has grown over the presence of pharmaceutical and personal care products (PPCPs) as pollutants in aquatic systems because these chemicals are specifically designed to elicit biological effects. To fully assess the environmental impact of these pollutants, their transformations by engineered and environmental processes must be considered. The transformation of cimetidine, an antacid drug, and triclosan, an antimicrobial compound, by wastewater chlorine disinfection was studied, as well as the photochemical transformations and environmental occurrence of triclosan, its chlorinated derivatives, and their dioxin photoproducts.

Cimetidine was found to react rapidly with free chlorine, indicating that it will likely undergo significant degradation during wastewater chlorination. Four major products were identified, two of which were estimated to have lower predicted no-effect concentrations than cimetidine. Reaction pathways and reaction mechanisms were proposed.

The aquatic photochemistry of triclosan and three of its chlorinated derivatives was explored. Reaction kinetics were studied, quantum yields were measured, and photoproducts were identified. Notably, dioxin photoproducts were observed to form at yields of 0.5 to 2.5% from triclosan and its chlorinated derivatives. A method was developed to analyze for triclosan and its chlorinated derivatives throughout the wastewater treatment process. A five-fold increase in the chlorinated derivatives of triclosan was observed in wastewater effluent after the chlorine disinfection step, showing this process to be a significant source of these pre-dioxins. Two sediment cores from Lake Pepin, a wastewater-impacted depositional zone of the Mississippi

River, were analyzed for triclosan and the dioxin photoproducts of triclosan and its chlorinated derivatives. These dioxins were detected at levels that trended with levels of triclosan that increased over the last 45 years since its introduction in the mid-1960s, providing strong evidence for the photochemistry of triclosan and its chlorinated derivatives as their source. The triclosan-derived dioxins comprised an increasing percentage of the total mass of all dioxins detected in Lake Pepin, reaching as high as 31% in recent years.

Table of Contents

Acknowledgments	<i>i</i>
Abstract	<i>ii</i>
Table of Contents	<i>iv</i>
List of Figures	<i>viii</i>
List of Tables	<i>x</i>
List of Schemes	<i>xi</i>

Chapter 1:

Environmental Occurrence and Transformation Processes of Pharmaceutical and Personal Care Product Pollutants	1
1.1 Pharmaceuticals and personal care products in the environment	2
1.2 Chemical transformations of PPCP pollutants	4
1.2.1 Chlorine disinfection of wastewater	4
1.2.2 Environmental aquatic photochemistry	7
1.3 Environmental analysis of PPCP chlorination and photolysis products	12
1.4 Scope of dissertation	14

Chapter 2:

Reaction Kinetics and Mechanisms of the Aqueous Chlorination of Cimetidine	15
2.1 Introduction	16
2.2 Experimental	18
2.2.1 General	18
2.2.2 Wastewater procurement and analysis	18
2.2.3 Chlorination reactions	19
2.2.4 Ammonium chloride quenching control experiments	20
2.2.5 HPLC analysis	21
2.2.6 Product identification	22
2.2.7 ECOSAR analysis	22
2.3 Results and Discussion	23

2.3.1	Ammonium chloride quenching control experiments	23
2.3.2	Chlorination kinetics of cimetidine in DI water and wastewater	25
2.3.3	Product identification	27
2.3.4	Intermediacy of chlorination products	37
2.3.5	Proposed reaction pathways and mechanisms	39
2.3.6	Toxicity of products	42
2.3.7	Environmental significance	42

Chapter 3:

	Aquatic Photochemistry of Chlorinated Triclosan Derivatives: Potential Source of Polychlorodibenzo- <i>p</i> -dioxins	44
3.1	Introduction	45
3.2	Experimental	48
3.2.1	Chemicals	48
3.2.2	pK_a determinations	49
3.2.3	Photolysis experiments	49
3.2.4	HPLC analysis	51
3.2.5	Photoproduct identification	51
3.3	Results and Discussion	53
3.3.1	pK_a determinations	53
3.3.2	Photolysis kinetics	54
3.3.3	Product identification	58
3.3.4	Environmental implications	65

Chapter 4:

	Occurrence of Triclosan and Chlorinated Triclosan Derivatives in Wastewater Effluent Before and After Chlorine Disinfection	68
4.1	Introduction	69
4.2	Experimental	71
4.2.1	General	71
4.2.2	Wastewater sampling	71

4.2.3	Preliminary matrix reduction experiments	72
4.2.4	Trace analysis of wastewater samples	76
4.3	Results and Discussion	80
4.3.1	Preliminary matrix reduction experiments	80
4.3.2	Trace analytical method performance	82
4.3.3	Occurrence of triclosan and CTDs in wastewater	86

Chapter 5:

	Historical Record of Dioxin Photoproducts of Triclosan and its Chlorinated Derivatives in Riverine Sediment Cores	89
5.1	Introduction	90
5.2	Experimental	92
5.2.1	Chemicals	92
5.2.2	Sediment core collection	92
5.2.3	Triclosan analysis	94
5.2.4	Dioxin and furan analysis	96
5.3	Results and Discussion	98
5.3.1	Analytical method performance	98
5.3.2	Dioxin concentrations and temporal trends	99
5.3.3	Source of 2,8-DCDD, 2,3,7-TCDD, 1,2,8-TCDD, and 1,2,3,8-TeCDD	102
5.3.4	Contribution of triclosan-derived dioxins to total dioxin toxicity	105

References:

	Chapter 1	108
	Chapter 2	113
	Chapter 3	117
	Chapter 4	121
	Chapter 5	123

Appendix:

Synthesis and purification of chlorinated triclosan derivatives

126

List of Figures

Chapter 1

- | | | |
|-----|--|----|
| 1.1 | Spectral overlap of solar irradiance and absorbance of triclosan anion | 8 |
| 1.2 | Chemical structures of ranitidine and cimetidine | 11 |

Chapter 2

- | | | |
|------|---|----|
| 2.1 | Chemical structure of cimetidine | 17 |
| 2.2 | Stability of cimetidine and its chlorination products in the presence of ammonium chloride-quenched free chlorine | 24 |
| 2.3 | HPLC chromatograms of cimetidine and its chlorination products | 25 |
| 2.4 | Cimetidine chlorination in DI water and wastewater effluent | 26 |
| 2.5 | HPLC retention time match of cimetidine sulfoxide | 28 |
| 2.6 | ESI ⁺ mass spectrum of product 2 | 29 |
| 2.7 | ¹ H-NMR spectrum of product 2 | 29 |
| 2.8 | HPLC retention time match of 4-hydroxymethyl-5-methyl-1H-imidazole | 30 |
| 2.9 | ¹ H-NMR spectrum of product 1 | 30 |
| 2.10 | ESI ⁺ mass spectrum of product 1 | 31 |
| 2.11 | ESI ⁺ and ESI ⁻ mass spectra of product 3 | 32 |
| 2.12 | ¹ H/ ¹³ C heteronuclear multiple bond correlation NMR spectra of 1 and 3 | 33 |
| 2.13 | ESI ⁺ and ESI ⁻ mass spectra of product 4 in water | 34 |
| 2.14 | ESI ⁺ and chemical ionization mass spectra of product 4 in D ₂ O | 35 |
| 2.15 | ¹ H-NMR spectra of product 4 before and after deuterium exchange | 35 |
| 2.16 | Infrared spectrum of product 4 | 36 |
| 2.17 | Chlorination of products 3 and 4 | 38 |
| 2.18 | Chlorination of 4-hydroxymethyl-5-methyl-1H-imidazole | 39 |

Chapter 3

- | | | |
|-----|--|----|
| 3.1 | Spectrophotometric p <i>K</i> _a determinations of triclosan and chlorinated derivatives | 54 |
| 3.2 | Photochemical degradation of triclosan and chlorinated derivatives | 55 |

3.3	Relative photolysis rates vs. pH	56
3.4	Spectral overlap of substrate absorbance with solar irradiance	57
3.5	UV-visible absorbance spectra of dioxin photoproducts	60
3.6	Photochemical substrate degradation and concomitant dioxin growth	61

Chapter 4

4.1	UPLC-MS-Q ³ chromatograms of post-chlorination effluent extract	83
-----	--	----

Chapter 5

5.1	Map of Lake Pepin	93
5.2	Concentration profiles of 2,8-DCDD and triclosan for core I.3 and V.4	99
5.3	Concentration profiles of 2,3,7-TCDD, 1,2,8-TCDD, and 1,2,3,8-TeCDD for core I.3 and V.4	100
5.4	R ² values of linear correlations for 2,8-DCDD and OCDD trend types	102
5.5	PCDF and PCDD homologue profiles from core V.4, 1957-1968	103
5.6	Historical mass and toxicity contribution of triclosan-derived dioxins to total dioxin pool	106

List of Tables

Chapter 2

2.1	Predicted no-effect concentrations of cimetidine and its chlorination products	42
-----	--	----

Chapter 3

3.1	pK_a values, photolysis quantum yields, and dioxin yields for triclosan and chlorinated derivatives	53
3.2	Parent and fragmentation ions of dioxin photoproducts	61
3.3	Accurate mass measurements of dechlorination photoproducts	64

Chapter 4

4.1	Single reaction monitoring transitions for analyte quantification and identity confirmation	78
4.2	350 nm absorbance and triclosan % recovery in SPE wash solutions and extracts	80
4.3	350 nm absorbance of sequential SPE washes	81
4.4	Silica column recoveries of triclosan, 4-Cl-TCS, and 4,6-Cl-TCS	82
4.5	Triclosan and CTD wastewater concentrations and $^{13}C_{12}$ -triclosan recoveries	85

Chapter 5

5.1	Toxicity equivalence factors relative to 2,3,7,8-TeCDD	106
-----	--	-----

List of Schemes

Chapter 1

- | | | |
|-----|---|----|
| 1.1 | Generic direct photochemical reaction | 8 |
| 1.2 | Generic indirect photochemical reaction | 10 |

Chapter 2

- | | | |
|-----|----------------------------------|----|
| 2.1 | Cimetidine chlorination pathways | 28 |
|-----|----------------------------------|----|

Chapter 3

- | | | |
|-----|---|----|
| 3.1 | Dioxin production through triclosan chlorination and photolysis | 46 |
|-----|---|----|

Chapter 1:

Environmental Occurrence and Transformation Processes of Pharmaceutical and Personal Care Product Pollutants

1.1 Pharmaceuticals and Personal Care Products in the Environment

Concern has grown over the last decade regarding the presence of pharmaceuticals and personal care products (PPCPs) as micro-pollutants in natural waters.¹⁻⁴ As improved analytical methods have provided sufficient detection limits, PPCPs have been detected with increasing frequency in aquatic environments. In 2002, the U.S. Geological Survey reported the detection of organic wastewater contaminants including antibiotics, prescription drugs, steroids, and hormones, in 80% of waterways sampled throughout the U.S. that were impacted by urbanization or agriculture.⁵ Of the 95 selected analytes, 82 were observed in at least one of the 139 sampling locations.⁵ Many other studies have quantified a broad array of PPCPs of various classes in rivers, lakes, groundwater, and sediments throughout the world.⁶⁻¹⁴

There are several routes by which different classes of PPCPs may enter natural waters. The primary route for human-use compounds such as analgesics, antibiotics, hormones, and antibacterials is via wastewater treatment plants. Many pharmaceuticals are administered orally, incompletely metabolized, and excreted in urine or feces. Thus, these chemicals are flushed to wastewater treatment plants. Unused medications are often disposed of in a similar manner. Antibacterial chemicals in soap are washed down the drain along with many other chemicals in personal care products. Wastewater treatment plants have not traditionally been designed to eliminate low-level PPCP pollutants, and thus PPCPs may be incompletely removed during treatment and enter aquatic environments that receive treated wastewater effluent.^{12, 15-19} The removal of PPCPs from wastewater is currently a growing field of research because municipalities in arid regions such as the western U.S. and parts of Australia are exploring the reuse of

treated wastewater as a drinking water source. In addition to discharge with wastewater effluent, PPCPs may enter the environment through the land-application of sludge generated during the biological stage of treatment as fertilizer.² Sludge commonly contains hydrophobic PPCPs that are partially removed from the wastewater stream by sorption.^{2, 15, 17, 20} Finally, antibiotics and hormones are used on a large scale in commercial fisheries and in the production of livestock, and thus may enter natural waters directly or via runoff from agricultural fields to which manure is applied.^{2, 21, 22}

PPCPs are a potential threat to aquatic ecosystems and human health because they are specifically designed to elicit biological effects. One major concern is that antibiotics and antimicrobial compounds may result in the development of antibiotic resistance in aquatic organisms.^{1, 13, 22} Another concern is that estrogenic wastewater effluent impacted by PPCPs may cause reproductive disruption in aquatic organisms.²³⁻
²⁵ For example, estrogenic PPCPs have been implicated in the feminization of fish populations in water bodies that receive wastewater effluent.^{23, 24} There is also concern regarding the acute toxicity of individual PPCPs, and it is suspected that PPCPs, which individually may be present at no-effect levels in natural waters, may have additive or synergistic effects in mixtures with other PPCPs.¹ In 2008, the Associated Press reported that the drinking water supplies of 24 major U.S. metropolitan areas were contaminated with PPCPs.²⁶ Because drinking water treatment methods have proved unsuccessful in the complete elimination some PPCPs,²⁷⁻²⁹ human health could be impacted along with aquatic ecosystems. Assessing the ecotoxicological risks of PPCPs has proved a difficult challenge and requires further research.

1.2 Chemical Transformations of PPCP Pollutants

To fully assess the environmental impact of PPCP pollutants, their transport and fate during wastewater treatment and in aquatic environments must be taken into account. During wastewater treatment, PPCPs may be removed via physical mechanisms such as sorption to particles and settling during primary treatment or sorption to sludge during secondary activated sludge treatment. They may also be eliminated by biological degradation during activated sludge treatment, by chemical reactions with oxidants such as chlorine or ozone used in the final disinfection stage of wastewater treatment, or by photochemical degradation when UV light is used to disinfect wastewater effluent. In aquatic environments, PPCPs may sorb to particles and deposit in sediments, accumulate in biota, volatilize into the atmosphere, undergo biological degradation by microorganisms, or be photochemically transformed by solar irradiation. Chemical and photochemical transformations of PPCPs were investigated in this thesis, specifically the reactions of PPCPs with free chlorine during wastewater disinfection and the aquatic photochemistry of PPCPs in natural waters. While these processes may eliminate PPCPs from the aquatic environment via chemical degradation, it is crucial to study reaction products that may retain or possess enhanced levels of biological activity or toxicity.

1.2.1 Chlorine disinfection of wastewater

The practice of chlorinating treated wastewater before discharge to aquatic environments has gained prominence as a disinfection method. In addition to destroying pathogens and other potentially detrimental microorganisms natively present

in wastewater, chlorination also limits microorganisms used in modern activated sludge treatment from being discharged in the effluent. While wastewater chlorination preserves the health of aquatic ecosystems and humans who use wastewater-impacted water bodies as drinking water sources, there is widespread concern because it generates harmful disinfection byproducts. Dissolved organic matter present in wastewater effluent may be oxidized by chlorine to form halomethanes, haloacetic acids, and other regulated and unregulated products that are suspected carcinogens.³⁰

In wastewater chlorination, chlorine is typically applied as molecular chlorine gas ($\text{Cl}_{2(\text{g})}$) or as sodium hypochlorite ($\text{NaOCl}_{(\text{aq})}$) at a concentration of approximately 10 mg/L (0.14 mM) total Cl(I) for about 1 hour.³¹ In water, molecular chlorine rapidly hydrolyzes to form hypochlorous acid, according to Equation 1.1³²:



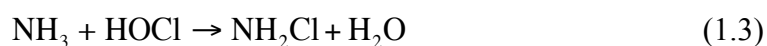
Sodium hypochlorite dissociates to hypochlorite ($\text{OCl}^-_{(\text{aq})}$). At circumneutral pH, hypochlorous acid and hypochlorite coexist in pH-dependent equilibrium³³ (Equation 1.2):



Molecular chlorine, hypochlorous acid, and hypochlorite are together referred to as free chlorine. Free chlorine is a non-specific oxidant that generally reacts with organic substrates with increasing rates as pH decreases due to the greater oxidizing strength of hypochlorous acid and molecular chlorine relative to hypochlorite.³⁴⁻³⁶ The reaction rates, however, also depend upon the speciation of the substrate. For example, phenolic compounds are increasingly activated towards chlorination with increasing pH.^{33, 35}

The competing speciation of the free chlorine oxidant and phenolic substrate results in a maximum rate near neutral pH.^{33, 35}

Whereas free chlorine is the primary disinfecting agent in wastewaters that have been treated with a nitrification step to oxidize inorganic nitrogen to nitrate, combined chlorine will be the primary chlorine oxidant in waters with high levels of ammonia or organic nitrogen.³¹ Combined chlorine refers to inorganic chloramines formed from the reaction of free chlorine with ammonia. At pHs relevant to wastewater disinfection, monochloramine is rapidly formed and is the dominant combined chlorine species (Equation 1.3),



though it may be further oxidized to di- and tri-chloramine to a small extent.³² While chloramines are active oxidants, they generally react with organic substrates several orders of magnitude slower than free chlorine.^{31, 36, 37} Wastewater disinfection via combined chlorine, known as chloramination, is preferred over free chlorination in some cases due to the reduction of hazardous disinfection byproducts.^{31, 32} Prior to discharge, chlorinated wastewater is commonly treated with a reductant such as bisulfite or sulfur dioxide gas to quench the active chlorine species (either free or combined chlorine) and to prevent its release to the receiving water.³¹

Because many PPCPs persist through biological wastewater treatment, they may be present to react with free chlorine or chloramines in the final disinfection stage. Even though PPCPs may be degraded by chlorination, their threat to aquatic environments may not be eliminated. Chlorination of PPCPs usually results in chlorinated, oxidized, or fragmented byproducts rather than complete mineralization.^{31,}

^{35, 36, 38-43} Several studies have reported the production of deleterious chlorination products with increased biological activity relative to the parent compounds.^{39, 43, 44} For example, the toxicants, 1,4-benzoquinone and *N*-acetyl-*p*-benzoquinone imine, were generated from the chlorination of acetaminophen,⁴³ and a chlorinated solution of bisphenol A exhibited a 24-fold increase in estrogenic binding affinity compared to the non-chlorinated solution.⁴⁴ In addition to studying the kinetics and pH-dependence of PPCP chlorination reactions, it is therefore crucial to identify the reaction products and consider their bioactivity/toxicity, because chlorination products may pose a greater environmental threat than parent PPCPs. Product identification often requires extensive characterization because authentic standards of PPCP chlorination products are often not commercially available. In addition to enabling a fuller assessment of the environmental impact of PPCP pollutants, the identification of chlorination products allows for the determination of reaction mechanisms, which may shed light on the likely chlorination pathways of PPCPs.

1.2.2 Environmental aquatic photochemistry

In surface waters, an organic chemical may be photochemically degraded by one of two mechanisms: direct or indirect photolysis. For a molecule to be photolyzed directly, it must contain a chromophore that absorbs light within the spectral region of solar irradiation. For example, the anion of triclosan exhibits spectral overlap with sunlight emission from between ~ 300-320 nm, allowing it to undergo direct photolysis (Figure 1.1).

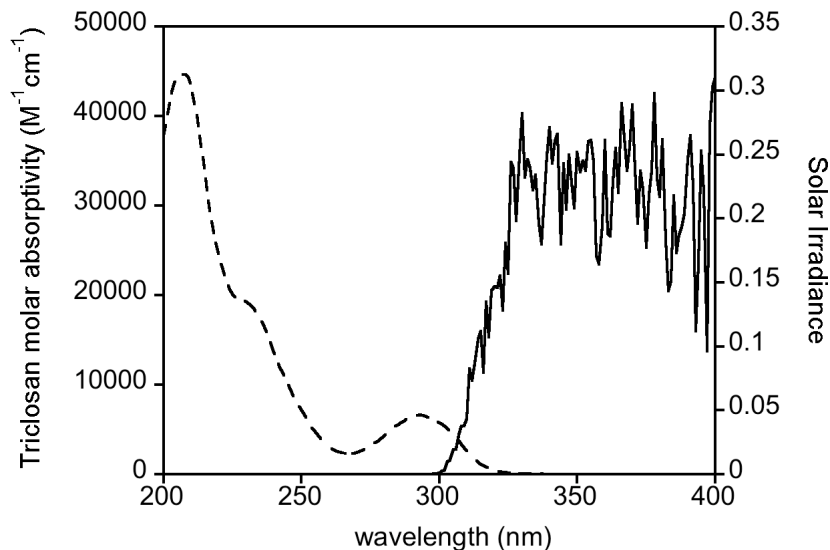
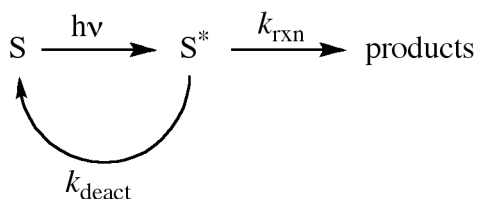


Figure 1.1. Spectral overlap of solar irradiance (—) and absorbance of triclosan anion (- - -). Solar irradiance was calculated using SMARTS for Minneapolis, MN (45° N) in June, 2008.

When a molecule absorbs a photon of light, it becomes electronically excited and the excited species may chemically degrade. The energy of the excited state may also be released by a variety of other mechanisms, including through collisional deactivation with solvent molecules or other constituents, returning the substrate to its ground state (Scheme 1.1).

Scheme 1.1. Generic direct photochemical reaction involving the excitation of substrate, S, to S^* , followed by chemical degradation with rate k_{rxn} or deactivation with rate k_{deact} .



The efficiency of a direct photoreaction is characterized by the quantum yield of substrate degradation (Φ_s), which is the fraction of photo-excited substrate molecules that chemically degrade. The Φ_s may be experimentally determined using a chemical

actinometer, a reference photochemical reaction for which the quantum yield, Φ_a , is known. The rate constant for the actinometer photoreaction, k_a , is calculated according to Equation 1.4:

$$k_a = 2.303 \sum_{\lambda_0}^n E_{\lambda} \epsilon_{a,\lambda} \Phi_{a,\lambda} \quad (1.4)$$

It depends upon the wavelength-dependent irradiance, E , molar absorptivity of the actinometer, ϵ_a , and Φ_a , summed over the range of wavelengths of spectral overlap between the actinometer and solar emission (λ_0 - n). The rate constant for the photochemical reaction of the substrate, k_s , is calculated in the same way (Equation 1.5):

$$k_s = 2.303 \sum_{\lambda_0}^n E_{\lambda} \epsilon_{s,\lambda} \Phi_{s,\lambda} \quad (1.5)$$

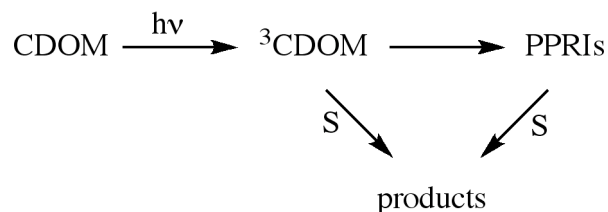
If the quantum yield of the substrate and actinometers are assumed to be wavelength-independent, then equations 3.4 and 3.5 may be combined to yield an expression for Φ_s (Equation 1.6):

$$\Phi_s = \frac{k_s}{k_a} \frac{\sum E_{\lambda} \epsilon_{a,\lambda}}{\sum E_{\lambda} \epsilon_{s,\lambda}} \Phi_{a,\lambda} \quad (1.6)$$

The ratio of k_s/k_a may be determined experimentally by irradiating the substrate and actinometer side-by-side. The solar emission spectrum may be obtained from literature sources or calculated using an atmospheric radiation modeling program (e.g., SMARTS^{45, 46}). The wavelength-dependent molar absorptivities may be determined in the laboratory using Beer's Law.

While direct photolysis is a significant photochemical loss process for some organic substrates, in other cases indirect photolysis may play a larger role. In an indirect photochemical reaction, the substrate in question does not absorb a photon. Rather, a different species acting as a sensitizer absorbs light, becomes electronically excited, and chemically reacts with the substrate. In natural waters, the primary sensitizing species is chromophoric dissolved organic matter (CDOM). It may be excited to form triplet CDOM ($^3\text{CDOM}$), which may react with a substrate, or go on to generate an array of other photochemically-produced reactive intermediates (PPRIs) such as singlet oxygen, hydroxyl radical, or peroxides which may degrade a substrate (Scheme 1.2).

Scheme 1.2. Generic indirect photochemical reaction where chromophoric dissolved organic matter (CDOM) absorbs light to generate $^3\text{CDOM}$, which may degrade a substrate (S) or generate other photochemically produced reactive intermediates (PPRIs) that may degrade the substrate.



It is possible for a substrate to be degraded in natural waters by both direct and indirect photolysis. The contribution of each process will be determined by their relative rates. For a given substrate, the rate of direct photolysis, a pseudo-first order reaction, is affected primarily by the substrate's ability to absorb light and the efficiency of the reaction. In contrast, indirect photolysis is a second order reaction whose rate will largely be affected by the level of CDOM and the steady-state concentrations of PPRIs in a given water body. Ranitidine (Figure 1.2, left) is an example of a substrate

capable of direct photodegradation or indirect photodegradation by singlet oxygen and hydroxyl radical, though the low steady-state concentrations of these PPRIs in natural waters make it difficult for indirect photolysis to compete with the rate of direct photolysis.⁴⁷

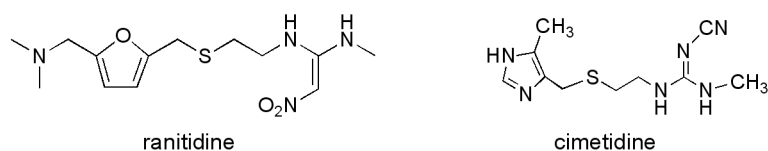


Figure 1.2. Chemical structures of ranitidine and cimetidine.

Cimetidine (Figure 1.2, right), on the other hand, contains no chromophore that absorbs solar irradiation, and thus is degraded completely by indirect photolysis via reaction with photochemically produced singlet oxygen.⁴⁷

Photochemistry has been shown to be a significant loss process for PPCPs in the aquatic environment.⁴⁷⁻⁵⁴ Wastewater effluent-derived PPCPs present in natural waters have persisted through intense biological treatment and are thus unlikely to undergo a substantial degree of further biotransformation.⁵⁰ Because hydrophobic organic pollutants are typically removed at a high rate via sorption to sludge during activated sludge treatment, PPCPs entering natural waters are likely to be relatively hydrophilic, and therefore will remain in the dissolved phase rather than volatilize or partition to particles and be removed by sedimentation. Many PPCPs are susceptible to photochemical degradation because they contain aromatic rings, heteroatoms, and other functional groups that either directly absorb sunlight or react with photoexcited sensitizers.⁵⁰ Diclofenac, an anti-inflammatory drug, resisted biodegradation and exhibited negligible sorption to sediment, but it degraded rapidly by photolysis ($t_{1/2} < 1$ hr), showing photodegradation to be the predominant loss process from a Swiss lake.⁶

Direct photodegradation accounted for 80% of the observed elimination of the antibacterial, triclosan, from the same lake during late summer/early autumn.⁵² An assortment of other compounds representing various pharmaceutical classes have been found to photodegrade by both direct and indirect processes at rates that suggest photochemistry will be their dominant elimination mechanism in aquatic environments.^{47-49, 51, 53, 54}

Photochemistry is important to study when assessing the environmental fate of PPCP pollutants, not only because it is a substantial loss process, but also because the photoproducts may retain or exhibit enhanced bioactivity or toxicity relative to the parent compounds. For example, the photoproduct of the calcium channel blocker drug, amlodipine, was found to exhibit greater long-term toxicity than amlodipine itself.⁵⁵ Similarly, other researchers showed that the aqueous photoproducts of tetracycline displayed increased toxicity to luminescent bacteria.⁵⁶ Thus, the identity of PPCP photoproducts must be determined and their bioactivity/toxicity characterized to fully evaluate the environmental risk of PPCP pollutants.

1.3 Environmental Analysis of PPCP Chlorination and Photolysis Products

Very few studies have analyzed for PPCP chlorination or photolysis products in the natural environment. One reason is that while many researchers have studied the degradation of PPCPs by chlorination reactions relevant to wastewater disinfection and by aqueous photolysis, only a fraction have identified the reaction byproducts. Even if PPCP transformation products are known, their analysis in natural waters is difficult due to low concentrations (often ng/L levels or less) and the lack of commercially

available authentic standards for calibration. In one case, the bio-methylated chlorination products of triclosan were detected in water in the outfall of a wastewater treatment plant and in carp in the receiving bay.⁵⁷ Such studies are important because they confirm that transformation processes that have been delineated under simulated conditions in the laboratory occur in natural water systems. Furthermore, the quantification of PPCPs and their transformation products helps to elucidate the relative contributions of various transformation processes.

The same analytical methods employed in the analysis of PPCP pollutants should prove suitable for the analysis of PPCP degradation products. Due to their relative hydrophilicity, PPCPs in natural waters are typically analyzed by liquid chromatography-tandem mass spectrometry (LC-MS/MS) with electrospray ionization (ESI) or atmospheric pressure chemical ionization (APCI).⁵⁸ In some cases, gas chromatography-tandem mass spectrometry (GC-MS/MS) is used, though GC-MS/MS often requires analyte derivatization. Triple quadrupole MS (MS-Q³) has been conventionally used for detection and quantification due to the low detection limits it provides. Quadrupole-time-of-flight MS (Qq-TOF-MS) also offers potential in the analysis of PPCPs due to the increased selectivity provided by the exact mass measurements (typical error < 2 mDa), though its sensitivity is less than that provided by MS-Q³.⁵⁹ The exact mass measurements provided by Qq-TOF-MS also offer promise in the structural characterization of PPCP degradation products.⁵⁹ Water samples are routinely prepared for analysis by filtration and concentration via solid-phase extraction. The isotope dilution method, in which samples are spiked with isotopically-labeled standards of the analytes at the beginning of the sample preparation

to account for analyte losses throughout the analysis, has gained prominence in the trace analysis of PPCPs and generally offers excellent relative recoveries.⁶⁰ LC-MS/MS analyses following solid-phase extraction using the isotope dilution method regularly achieve detection limits near or below the ng/L level.

1.4 Scope of Dissertation

This thesis investigates the fate of PPCP pollutants in the aquatic environment. The following two chapters examine the chemical transformation of PPCPs by wastewater chlorination and photolysis. Chapter 2 studies the aqueous free chlorination of the antacid drug, cimetidine, examining the kinetics, product identity and potential toxicity, and reaction pathways. In chapter 3, the aquatic photochemical reactions of triclosan and three previously identified chlorination products of triclosan are explored, with a focus on the formation of dioxin photoproducts. In chapters 4 and 5, wastewater and sediment samples are analyzed to investigate the chemical transformation of triclosan during chlorine disinfection of wastewater and subsequent aqueous photolysis. Chapter 4 describes the development of a method to analyze for triclosan and its chlorinated derivatives and initial results revealing the formation of chlorinated derivatives during wastewater disinfection. Finally, in chapter 5, the photochemical generation of dioxins from triclosan is confirmed through the analysis of a riverine sediment core downstream from a major wastewater discharge point.

Chapter 2:
Reaction Kinetics and Mechanisms of the Aqueous Chlorination
of Cimetidine¹

¹ A version of this chapter has been published as: Buth, J.M; Arnold, W.A.; McNeill, K. Unexpected products and reaction mechanisms of the aqueous chlorination of cimetidine. *Environ. Sci. Technol.* **2007**, *41*, 6228-6233.

2.1 Introduction

Recently, concern has grown regarding the presence of pharmaceuticals and personal care products (PPCPs) in aquatic systems.^{1, 2} Because these pollutants are specifically designed to elicit a biological response, it has been suggested that some can inflict biological harm even at trace concentrations, with possible synergistic effects.^{1, 2} It has been demonstrated that many PPCPs are not effectively removed by conventional wastewater treatment processes,³⁻⁵ thus passing the compounds to surface waters that receive wastewater effluent. Consequently, a wide range of PPCPs have been detected in rivers throughout the world.⁶⁻⁸ Their increasing production and use present a continuous source of these compounds to surface waters.

Because PPCPs often persist through wastewater treatment processes, they may be available to react with free chlorine or other oxidants used for disinfection. Free chlorine (HOCl/OCl⁻) is a non-specific oxidant used in wastewater disinfection that has been shown to degrade various PPCPs to chlorinated, oxidized, and fragmented byproducts.⁹⁻¹⁶ Concern exists that the reaction of free chlorine with PPCPs will generate products with increased toxicity or bioactivity relative to the parent compounds. For example, the toxicants, 1,4-benzoquinone and *N*-acetyl-*p*-benzoquinone imine, were generated from the chlorination of acetaminophen,¹³ and a chlorinated solution of bisphenol A exhibited a 24-fold increase in estrogenic binding affinity compared to the non-chlorinated solution.¹⁷ Because chlorination products may pose a greater threat than parent PPCPs, elucidation of product structures, formation kinetics, and toxicity are crucial for a complete assessment of environmental risk.

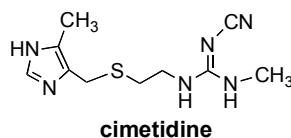


Figure 2.1. Chemical structure of cimetidine.

Cimetidine (structure shown in Figure 2.1), a non-prescription antacid sold as Tagamet[®], has an annual usage of 160,000 kg/year in the U.S.¹⁸ Accounting for 52% loss by human metabolism and an estimated removal efficiency of 70% for primary and secondary wastewater treatment yields an annual cimetidine load of 23,000 kg in U.S. wastewater effluent.¹⁸ Cimetidine, however, has only been detected in 10% of surveyed waterways throughout the U.S.⁶ Previously, the chlorination of cimetidine was studied along with other PPCPs and was reported to degrade completely by reaction with free chlorine to form a single unidentified product.¹² Thus, the disinfection of wastewater with free chlorine is an additional treatment step that may lead to reduction of the cimetidine load to the environment. Further questions regarding oxidation kinetics, product identification, reaction mechanisms, and pH dependence were beyond the scope of the prior survey.¹²

The goal of the present study is to thoroughly investigate the reaction of cimetidine with free chlorine. The kinetics of cimetidine degradation and product evolution over a broad pH range were monitored by high-pressure liquid chromatography (HPLC). Significant structural alterations in products required extensive product characterization including high-resolution mass spectrometry (HRMS), ¹H- and 2D-NMR spectroscopy, infrared (IR) spectroscopy, and HPLC retention time matching with authentic standards. Examining the evolution of cimetidine chlorination products and the reactivity of individual products with free

chlorine enabled the determination of the predominant reaction pathways. Additionally, the structure-activity model, ECOSAR,¹⁹ was used to estimate the toxicity of the reaction products.

2.2 Experimental

2.2.1 General

Cimetidine was purchased from Sigma. Sodium hypochlorite (NaOCl) was obtained from Aldrich ($\geq 4\%$) and Fisher (4-6%) and diluted to make aqueous stock solutions which were standardized by iodometric titration.²⁰ Ammonium chloride (NH_4Cl) and sodium sulfite (Na_2SO_3) were purchased from Mallinckrodt and 4-hydroxymethyl-5-methyl-1H-imidazole was purchased from TCI America. Deuterium oxide (D_2O) was obtained from Cambridge Isotope Labs. Cimetidine sulfoxide was prepared by oxidizing cimetidine with sodium periodate obtained from Aldrich as described by Kuzel et al.²¹ Water purified by a Milli-Q filtration system (Millipore) was used in all de-ionized (DI) water experiments and in the preparation of aqueous buffers.

2.2.2 Wastewater procurement and analysis

Wastewater effluent was obtained from a Twin Cities municipal wastewater treatment plant on November 9, 2006. A grab sample was collected at the point after secondary activated sludge treatment where chlorine disinfectant is typically applied, though the plant was not disinfecting at the time of year when the samples were obtained. The wastewater was filtered through Millipore 0.20 μm filters, adjusted to pH

2 with concentrated sulfuric acid for preservation, and stored at 4 °C until the experiments were performed. The original pH was 7.44. For wastewater experiments at pH 4, 7, and 10, the wastewater pH was adjusted with sulfuric acid and sodium hydroxide. Wastewater samples were analyzed on a Shimadzu TOC 5000A analyzer for dissolved organic carbon (DOC) following the procedures of Aiken et al.²² DOC was detected as non-purgeable organic carbon (NPOC) following acidification of the samples to pH 2.0 with concentrated sulfuric acid. Potassium hydrogen phthalate (KHP) was used to generate standard curves for the analysis. Samples were analyzed in triplicate and had a DOC content of 8.5 ± 0.9 mg/L C. Ammonia was measured colorimetrically by the Nessler method²³ using a Beckman DU 530 Life Science UV/Vis Spectrophotometer, analyzing at 420 nm. Nessler's Reagent was purchased from Hach Company. Samples were analyzed in triplicate and a result of 0.2 mg/L NH_4^+ -N was obtained.

2.2.3 Chlorination reactions

Chlorination reactions were initiated by spiking aliquots of an aqueous NaOCl stock solution to the substrate (cimetidine or one of its chlorination products). Substrate solutions were prepared by diluting aqueous stock solutions to 5 mL in 10 mM buffer (pH 4 acetate, pH 7 phosphate, or pH 10 carbonate) or wastewater adjusted to pH 4, 7, or 10. Solution pH was measured using a Thermo-Orion Ross Ultra Semi-micro pH probe. Reaction mixtures were stirred at ambient temperature in 20 mL glass vials covered in foil to prevent photoreactions. In the kinetic studies of cimetidine, cimetidine sulfoxide, and 4-hydroxymethyl-5-methyl-1H-imidazole, 100 μM substrate

solutions were reacted with a 10-fold molar excess of NaOCl in triplicate. This substrate concentration is orders of magnitude higher than what might be observed in wastewater to aid in the detection of substrates and products, and the chlorine concentration is consequently higher than practice to achieve a sufficient chlorine excess. Periodic sub-samples were removed, and the free chlorine was immediately quenched with greater than a 2-fold molar excess of NH₄Cl relative to the initial free chlorine concentration prior to HPLC analysis. Pseudo-first-order rate constants (k'_{obs}) were determined from the slopes of regression lines fitted to plots of $\ln([\text{substrate}]_t/[\text{substrate}]_0)$ vs. time. In addition to the kinetic experiments, larger scale reactions (> 100 mL) of 0.5–1.5 mM cimetidine with excess free chlorine were carried out in DI water and pH 7 phosphate buffer to generate a sufficient amount of products for isolation and characterization.

2.2.4 Ammonium chloride quenching control experiments

The use of NH₄Cl as an agent to quench free chlorine reactions has been demonstrated in the literature.⁹ NH₄Cl reacts rapidly with free chlorine, forming chloramines. Though chloramines are active oxidants, they generally react with organic substrates several orders of magnitude slower than free chlorine, effectively quenching a reaction over a suitable time window for analysis. Control experiments were performed to verify that the chlorination reactions in this work were effectively quenched with NH₄Cl by testing the stability of cimetidine and its chlorination products in NH₄Cl-quenched free chlorine solutions.

To test the stability of cimetidine and cimetidine sulfoxide in the presence of NH_4Cl -quenched free chlorine, solutions of 0.74 mM NaOCl in pH 4 acetate, pH 7 phosphate, and pH 10 carbonate were prepared. Each was quenched with a 2.5-fold molar excess of NH_4Cl relative to the initial NaOCl concentration ($[\text{NaOCl}_0]$). After the addition of NH_4Cl , an aliquot of cimetidine or cimetidine sulfoxide was added to achieve a $[\text{NaOCl}_0]:[\text{substrate}]$ ratio of 10:1. The reaction mixture was analyzed repeatedly by HPLC to monitor the stability of cimetidine or cimetidine sulfoxide in the presence of quenched free chlorine. To monitor the stability of the other cimetidine chlorination products in the presence of quenched free chlorine, 97 μM cimetidine solutions in pH 4 acetate, pH 7 phosphate, or pH 10 carbonate were reacted with a 8.7-fold molar excess of NaOCl to generate chlorination products. After 80 s, the reactions were quenched with a 2.5-fold molar excess of NH_4Cl relative to the initial NaOCl concentration and then analyzed repeatedly by HPLC to monitor the stability of chlorination products.

2.2.5 HPLC analysis

HPLC analyses were performed on a 1100 Series Hewlett-Packard HPLC equipped with UV-absorbance detection. Chromatograms to monitor substrate degradation and product evolution were obtained by injecting 10 μL samples on a Supelco Discovery RP-Amide C_{16} , 150×4.6 mm, 5 μm particle size column running a 5:10:85 methanol:acetonitrile:pH 3 phosphate buffer (v/v/v) mobile phase at a flow rate of 1.0 mL/min. The detection wavelength was 219 nm. Isolation of the cimetidine chlorination products was accomplished by preparative HPLC using a Supelco

Discovery RP-Amide C₁₆, 100 × 21.1 mm, 5 μm particle size column with a mobile phase of 15:85 methanol:water (v/v), a flow rate of 5.0 mL/min, 100 μL injections, and detection at 219 nm.

2.2.6 Product identification

Electrospray Ionization (ESI) mass spectra of products isolated from cimetidine chlorination reaction mixtures were acquired using a Bruker BioTOF II mass spectrometer in positive (ESI⁺) and negative (ESI⁻) mode. Polyethylene glycol was used as an internal calibrant for high-resolution mass spectra, which were obtained with ESI⁺. A Finnigan MAT 95 mass spectrometer was used to acquire spectra using chemical ionization (CI). ¹H-NMR spectra of isolates dissolved in D₂O were obtained with a Varian Unity 300 MHz NMR spectrometer. 2-D heteronuclear multiple bond correlation (HMBC) NMR experiments were conducted on a Varian Inova 500 or 600 MHz NMR spectrometer. IR spectra were recorded in transmission mode using a MIDAC Corp. M-Series FT-IR spectrometer.

2.2.7 ECOSAR analysis

Ecological Structure Activity Relationships (ECOSAR), a computer modeling program supplied by the U.S. Environmental Protection Agency (EPA), was used to estimate the toxicity of the chlorination products of cimetidine. ECOSAR predicts the toxicity of chemicals to various aquatic organisms based on toxicity data available for chemicals with similar structural moieties. According to the U.S. EPA's ECOSAR website, it is routinely used for chemicals being reviewed in response to Pre-

Manufacture Notices mandated by Section 5 of the Toxic Substances Control Act.²⁴ Following the method of Jones et al.,²⁵ predicted no-effect concentrations (PNECs) were determined by dividing the lowest acute toxicity value predicted by ECOSAR by a safety factor of 1,000.

2.3 Results and Discussion

2.3.1 Ammonium chloride quenching control experiments

Figure 2.2 shows plots of the cimetidine or cimetidine sulfoxide concentration normalized to its initial concentration vs. time at pH 4, 7, and 10 when exposed to free chlorine quenched with NH_4Cl . These results show that cimetidine is very reactive with the chloramines formed when free chlorine is quenched with NH_4Cl , degrading by at least 83 % within 3 min at each pH studied. However, because cimetidine reacts faster with free chlorine than chloramines, degrading completely by the first time point at 10 s in the free chlorine reactions, it is not important that it is unstable after NH_4Cl quenching. Cimetidine sulfoxide was found to be very stable in the presence of chloramines at pH 7 and 10, while it degraded slowly (20 % in 2.5 hr) at pH 4. Plots of the other cimetidine chlorination product concentrations normalized to their concentrations at the time of the first HPLC injection (~ 3 min after quenching) vs. time are also presented in Figure 2.2. These plots indicate that the cimetidine chlorination products are very stable at pH 4, 7, and 10 (< 6 % change from initial concentration) in the presence of NH_4Cl -quenched free chlorine, except the sultam product (< 18 % change from initial concentration). Overall, these control experiments show that NH_4Cl effectively quenches the free chlorine reactions described in this work.

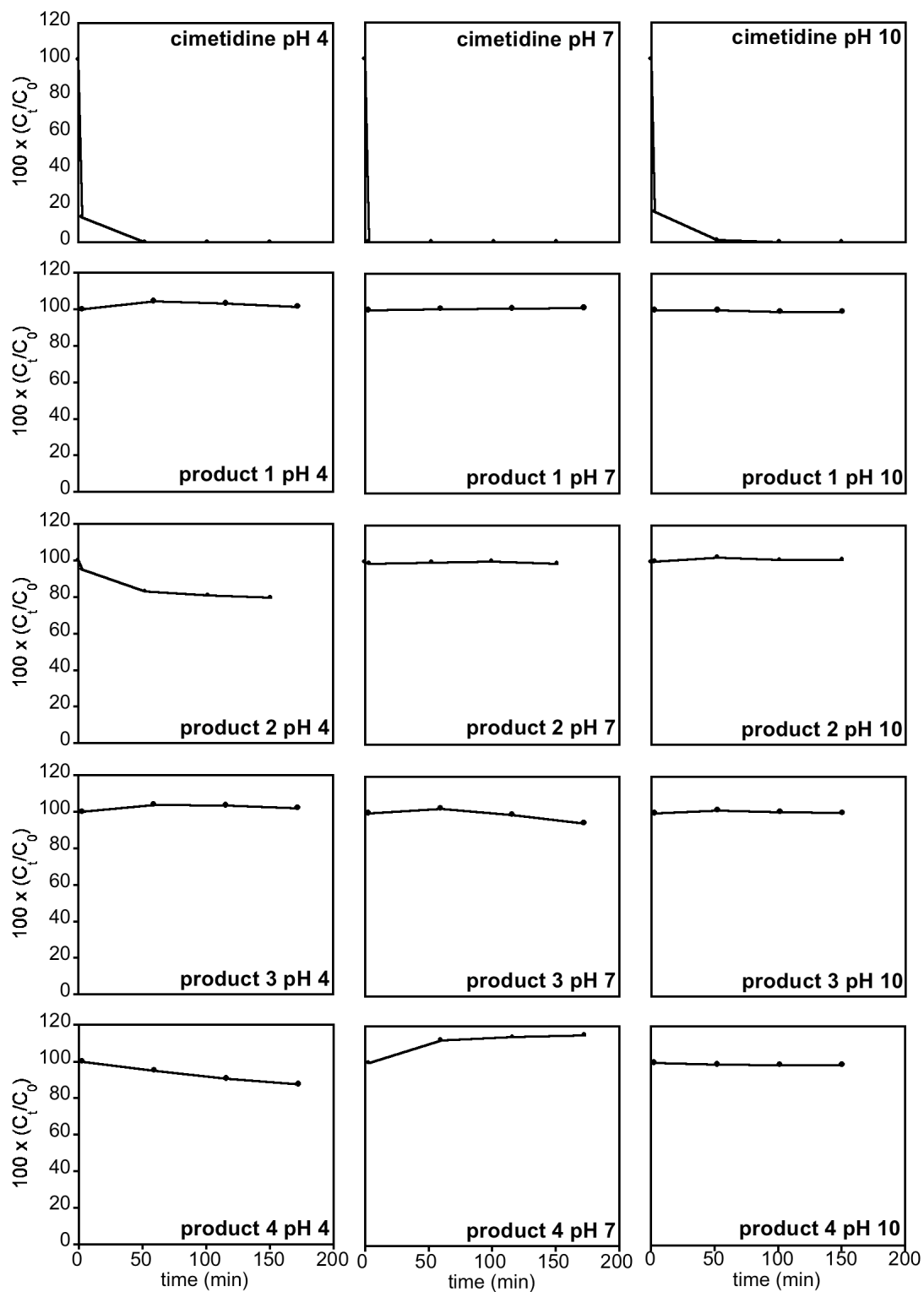


Figure 2.2. Stability of cimetidine and its chlorination products in the presence of excess free chlorine quenched with NH_4Cl at pH 4, 7, and 10.

2.3.2 Chlorination kinetics of cimetidine in DI water and wastewater

A representative chromatogram of a chlorinated cimetidine DI water solution quenched with NH_4Cl is displayed in Figure 2.3, showing four major product peaks, labeled **1 - 4**.

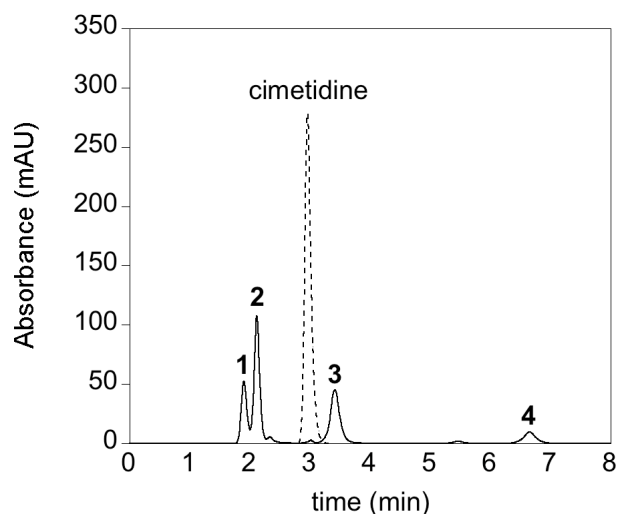


Figure 2.3. HPLC chromatograms of 200 μM cimetidine (····) reacted with a 3-fold molar excess of free chlorine for 3 hr in pH 7 phosphate buffer (—), revealing four new product peaks (**1 – 4**). Absorbance was measured at 219 nm.

As shown in Figure 2.4 A-C, cimetidine degraded rapidly in DI water, decaying completely within 10 s of contact time with a 10-fold molar excess of free chlorine at pH 4, 7, and 10. These results obtained using NH_4Cl to quench free chlorine were confirmed using Na_2SO_3 as a free chlorine quencher, since cimetidine was not stable after quenching with NH_4Cl (Figure 2.2). Reactions were monitored for 2 min. In parallel wastewater effluent reactions monitored for 5 min, cimetidine again degraded completely within 10 s to yield the same four major products at a similar distribution at pH 4, 7, and 10 (Figure 2.4 D-F).

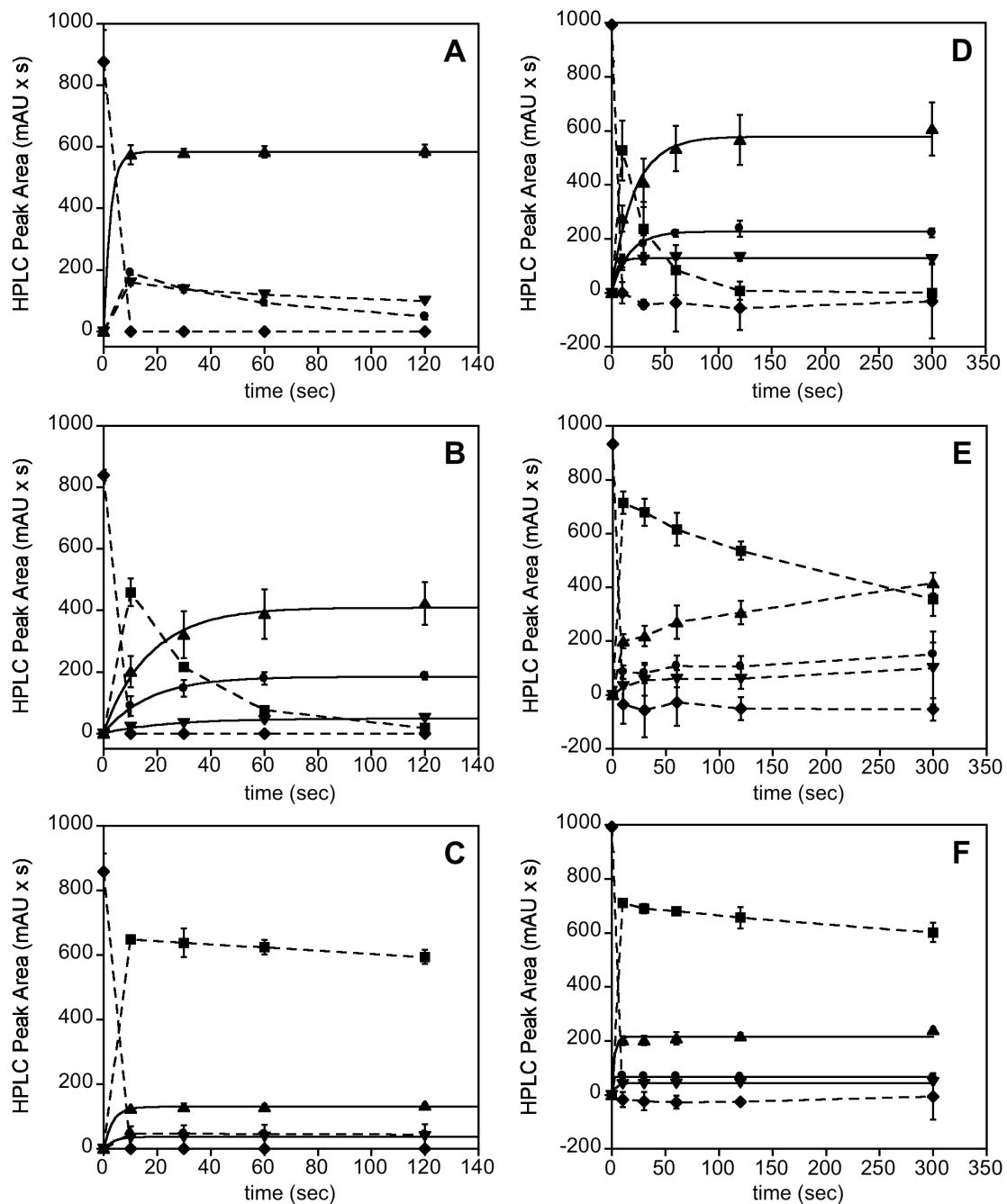


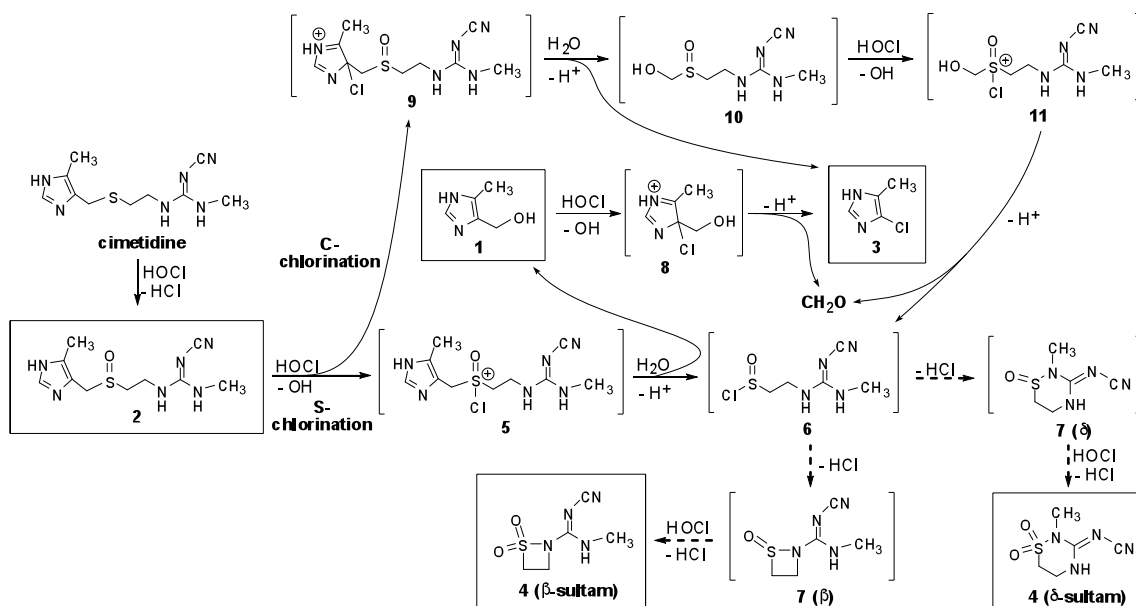
Figure 2.4. Degradation of 100 μM cimetidine (\blacklozenge) and evolution of its chlorination products **1** (\bullet), **2** (\blacksquare), **3** (\blacktriangle), and **4** (\blacktriangledown) upon the addition of a 10-fold molar excess of free chlorine in DI water at pH 4 (A), 7 (B), and 10 (C) and wastewater effluent at pH 4 (D), 7 (E), and 10 (F). In plots D-E, the cimetidine peak areas were corrected by subtracting the peak area of a co-eluting interferent in the wastewater. Solid lines represent fits to exponential growth equations ($R^2 > 0.99$). Dashed lines do not represent mathematical fits; they were added for the purpose of visualization. Error bars denote the 95% confidence interval for $n=3$.

However, the subsequent transformation of the four products was retarded by roughly an order of magnitude in the wastewater matrix, likely due to competition for free chlorine. In chlorine-absent controls, cimetidine was stable over the time course of the experiments in DI water and wastewater

2.3.3 Product identification

Given its structure, the chlorination of cimetidine may be expected to result in minor structural changes such as sulfur oxidation, electrophilic halogenation, and N-chlorination of one or more of its amino groups. Upon the addition of excess free chlorine at pH 7 and 10, product **2** formed most rapidly and then decayed as the concentration of the other products continued to rise (Figure 2.4 B-C). It was tentatively identified as cimetidine sulfoxide (Scheme 2.1) by a matching HPLC retention time (2.1 min) with that of an independently prepared authentic standard (Figure 2.5).

Scheme 2.1. Proposed reaction pathways for the reaction of cimetidine with free chlorine through the intermediacy of cimetidine sulfoxide.^{a,b,c}



^a Boxed structures represent observed products. ^b Bracketed structures represent probable reaction intermediates. ^c Dashed arrows represent pathways to form the two proposed structures for product 4, since the exact identity could not be determined.

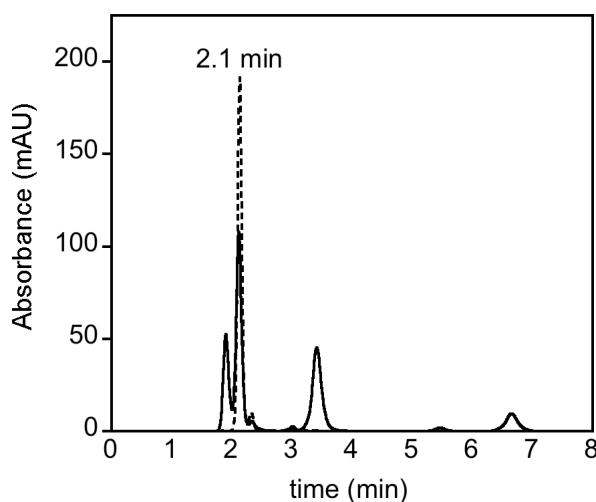


Figure 2.5. HPLC chromatograms comparing the retention times of authentic cimetidine sulfoxide (····) to those of the products formed by reacting 200 μM cimetidine with a 3-fold molar excess of free chlorine for 3 hr in DI water at pH 7 (—).

HRMS revealed one major peak at m/z 291.1012 ($M+Na$)⁺ (Figure 2.6), where M corresponds to a molecular formula of C₁₀H₁₆N₆SO (4.63 ppm error), the formula of cimetidine sulfoxide. Further evidence for the oxidation of the sulfide was provided by the ¹H-NMR spectrum of **2**, which matched the authentic material (Figure 2.7). The observed sulfur oxidation is consistent with results obtained by other researchers for the reaction of sulfides with free chlorine.^{26, 27}

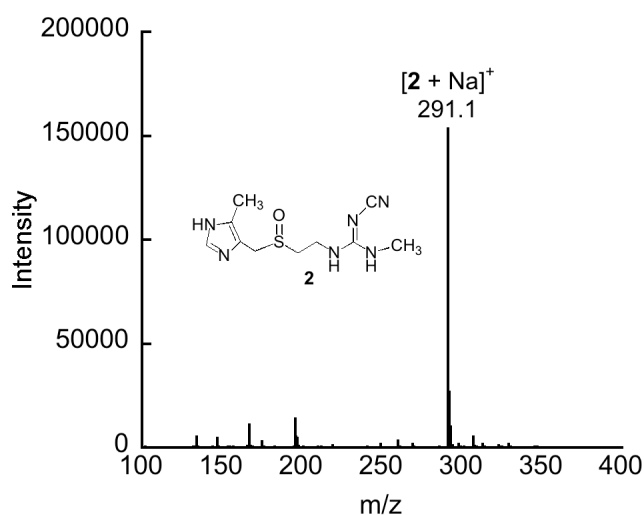


Figure 2.6. ESI⁺ mass spectrum of isolated product **2**, cimetidine sulfoxide.

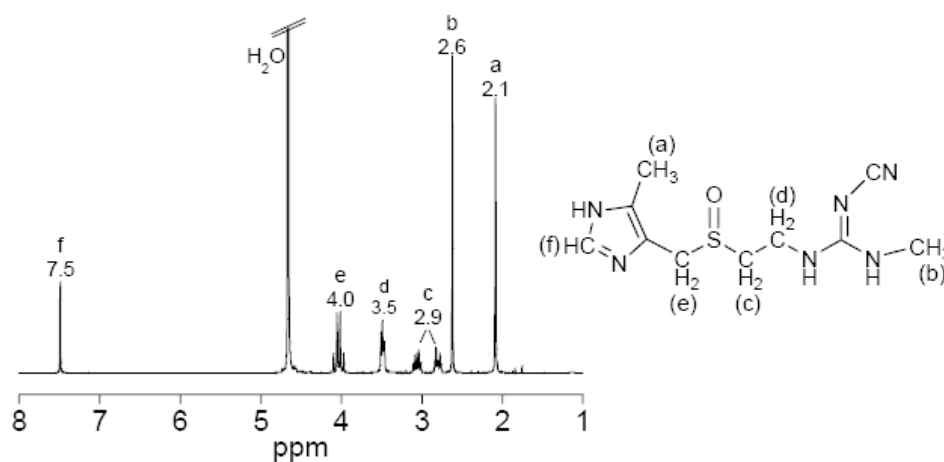


Figure 2.7. ¹H-NMR spectrum of product **2** (cimetidine sulfoxide) isolate in D₂O and its structure labeled with the corresponding ¹H-NMR peak assignments.

In addition to cimetidine sulfoxide, three unexpected products with more significant structural alterations were identified. Product **1** was preliminarily identified as 4-hydroxymethyl-5-methyl-1H-imidazole (Scheme 2.1) based on a matching HPLC retention time with an authentic standard (Figure 2.8) and confirmed by a matching ^1H -NMR spectrum (Figure 2.9).

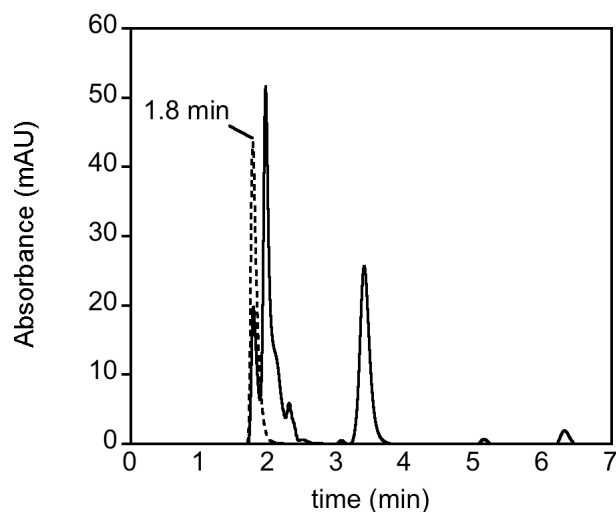


Figure 2.8. HPLC chromatograms comparing the retention times of authentic 4-hydroxymethyl-5-methyl-1H-imidazole (····) to those of the products formed by reacting 100 μM cimetidine with a 10-fold molar excess of free chlorine for 30 s in DI water at pH 7 (—).

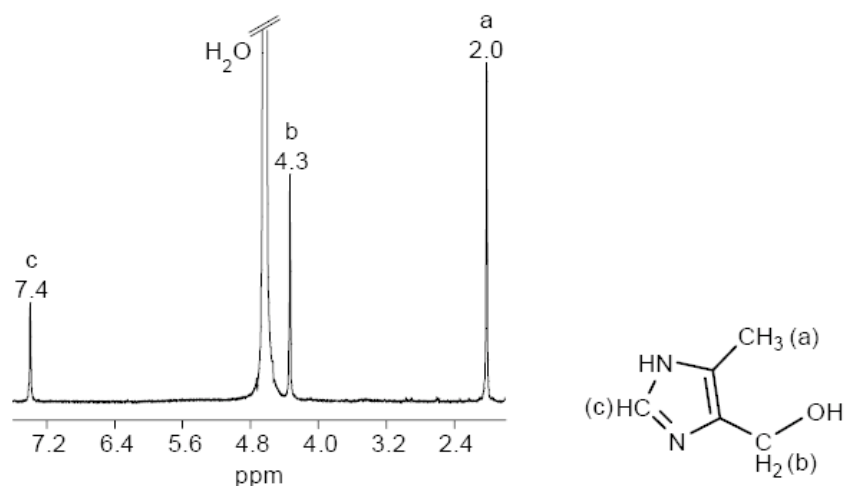


Figure 2.9. ^1H -NMR spectrum of product **1** (4-hydroxymethyl-5-methyl-1H-imidazole) isolate in D_2O and its structure labeled with the corresponding ^1H -NMR peak assignments.

The ESI⁺ mass spectrum revealed a peak at m/z 95.1 (Figure 2.10), which was below the calibration range for high-resolution measurement.

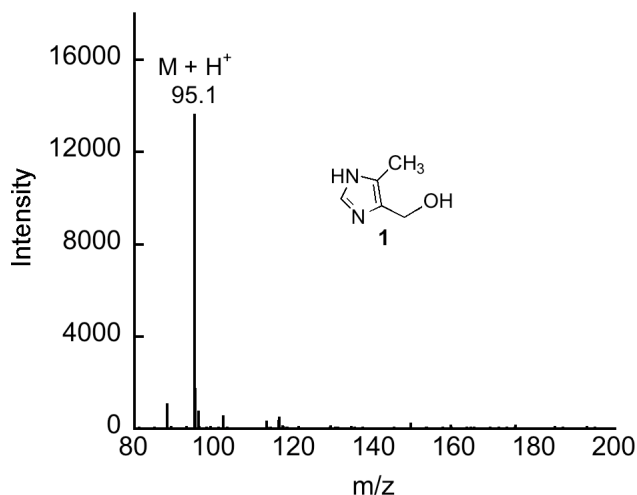
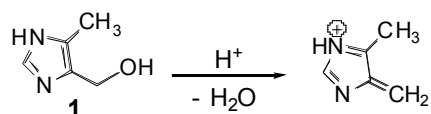


Figure 2.10. ESI⁺ mass spectrum of isolated product **1**, 4-hydroxymethyl-5-methyl-1H-imidazole.

The detected ion likely is 5-methyl-4-methylene-1H-imidazol-1-ium, resulting from the loss of water from **1**:



The same fragmentation was observed in the ESI⁺ mass spectrum of the authentic standard.

Product **3** was also identified as an imidazole-containing compound, 4-chloro-5-methyl-1H-imidazole (Scheme 2.1). ESI⁺ and ESI⁻ mass spectra revealed a single chlorine isotope pattern for the (M+H)⁺ and (M-H)⁻ ions, respectively (Figure 2.11).

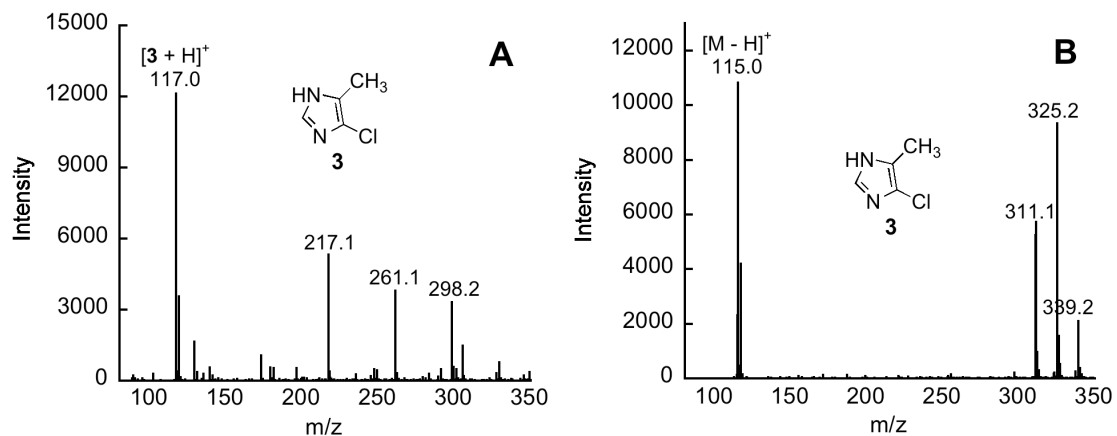


Figure 2.11. ESI mass spectrum of isolated product **3**, 4-chloro-5-methyl-1H-imidazole, in positive mode (A) and negative mode (B).

The exact mass of 117.0214 for the $(M+H)^+$ ion corresponds to a molecular formula of $C_4H_5N_2Cl$ for M (0.020 ppm error). Further confirmation for this identification came from a 2D-NMR HMBC experiment, which displayed 1H - ^{13}C correlations for product **3** in very similar positions as those for the methyl and 2-position protons seen in the HMBC spectrum of **1** (Figure 2.12). The notable difference is that the methylene signals of **1** at 4.3 ppm (1H shift) were missing from the spectrum of **3**, consistent with the replacement of the hydroxymethyl substituent with chlorine. The formation of product **3** was unexpected because it required the breaking of a C-C bond, a transformation not frequently observed in free chlorine reactions of PPCPs.

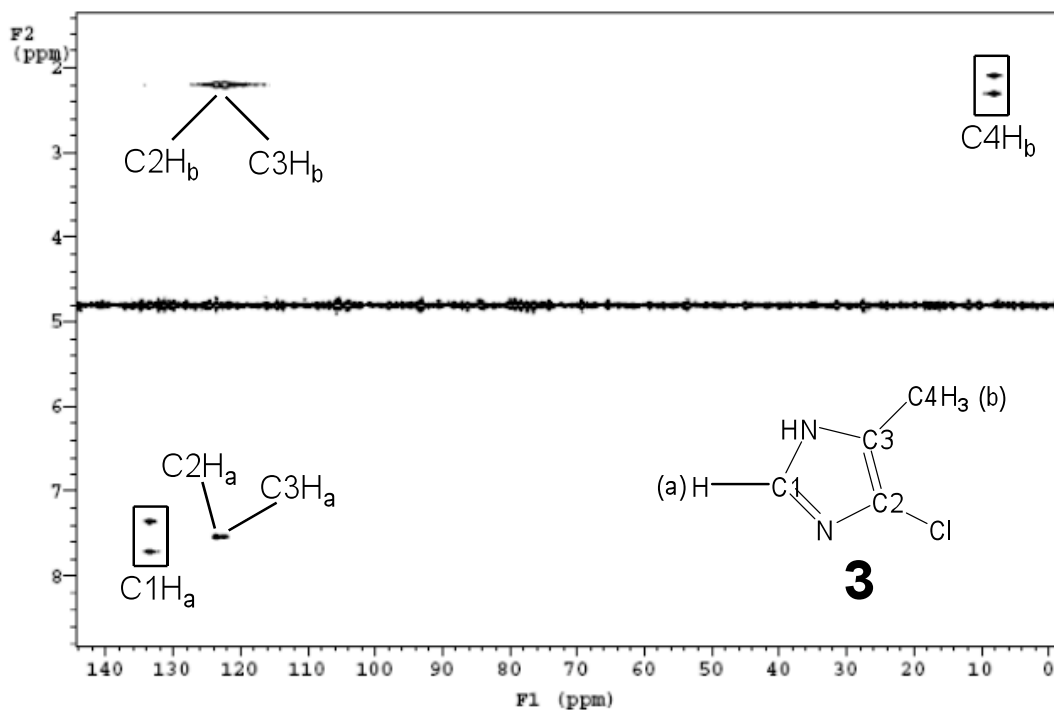
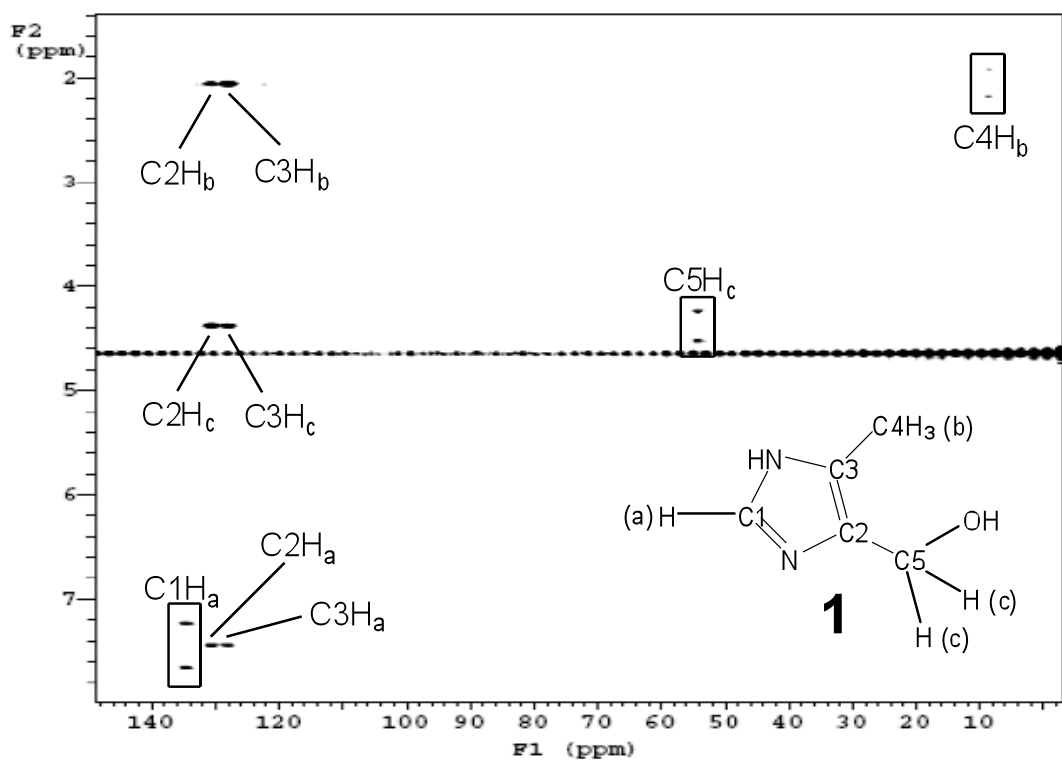


Figure 2.12. $^1\text{H}/^{13}\text{C}$ heteronuclear multiple bond correlation (HMBC) nuclear magnetic resonance spectra of isolates of **1** (top) and **3** (bottom) dissolved in D_2O with labeled structures. The ^{13}C chemical shift is displayed on the F1 axis while the ^1H chemical shift is displayed on the F2 axis.

Finally, either a β -sultam, N-cyano-N'-methyl-N''- β -sultamylguanidine, or a δ -sultam, N-(2-methyl-1,1-dioxide-1,2,4-thiadiazinan-3-ylidene)cyanamide, which could not be distinguished by the mass spectrometric or spectroscopic data, is proposed for the identity of product **4** (Scheme 2.1). The ESI⁺ mass spectrum (Figure 2.13 A) revealed an exact mass of 211.0244 (M+Na)⁺, where M represents the molecular formula C₅H₈N₄O₂S (7.66 ppm error), consistent with both proposed structures. A corresponding peak at *m/z* 187.0 (M-H)⁻ was obtained in the ESI⁻ spectrum (Figure 2.13 B).

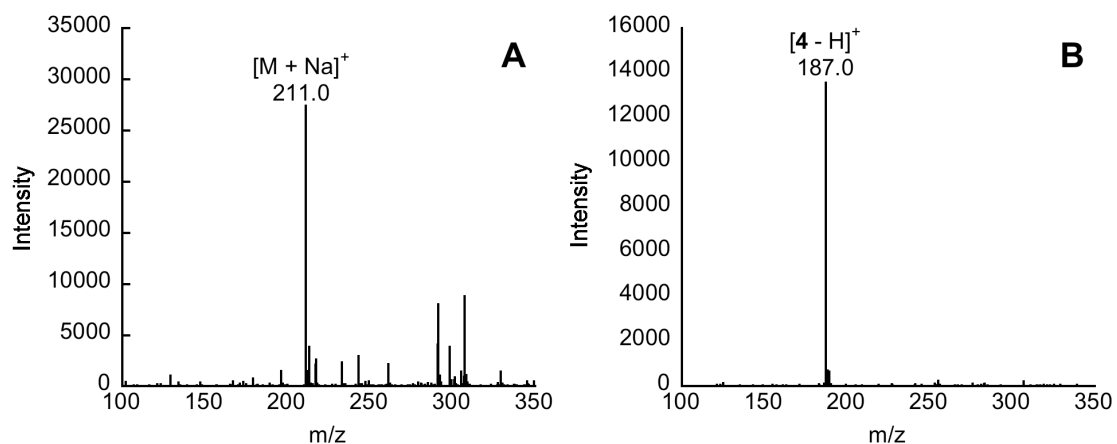


Figure 2.13. ESI positive mode (A) and ESI negative mode (B) mass spectra of isolated product **4** dissolved in water.

Exchanging the solvent from H₂O to D₂O for **4** showed a peak at *m/z* 214.0 in the ESI⁺ spectrum in place of the peak at *m/z* 211.0 observed in H₂O, indicating the exchange of 3 protons with deuterons to form **4-d₃** (Figure 2.14 A). The most acidic protons likely to exchange on the proposed structures are on the secondary amine and the carbon atom α to the sulfonamide functionality. Using chemical ionization, a harder ionization method than ESI, revealed a fragment ion peak 64 *m/z* units lower than the parent ion peak of **4-d₃**, attributable to the loss of SO₂ (Figure 2.14 B).

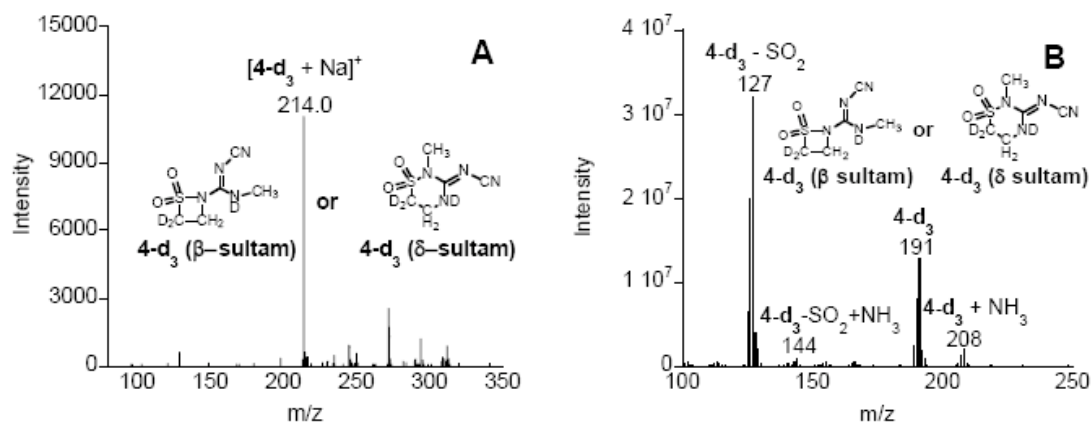


Figure 2.14. ESI positive mode (A) and chemical ionization (B) mass spectra of isolated product **4** dissolved in D₂O.

The mass spectrometric evidence did not enable the unequivocal identification of **4**, because both proposed isomers may exhibit the same proton-deuterium exchange pattern and fragmentation under CI.

Further evidence for the identity of **4** was provided by its ¹H-NMR spectrum (Figure 2.15).

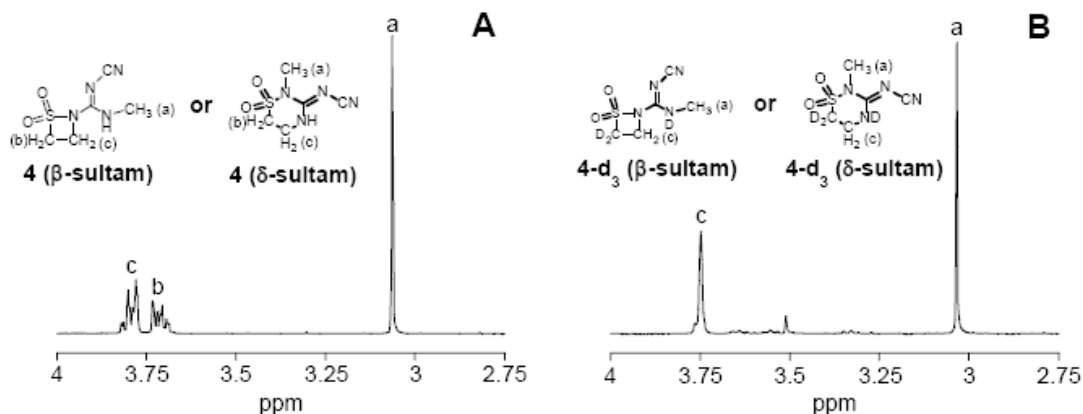


Figure 2.15. ¹H-NMR spectra of product **4** prior to deuterium exchange (A) and deuterated product **4** (**4-d₃**) (B) with ¹H-NMR peak assignments labeled on the structures.

Given sufficient time for deuterium exchange in D₂O, the methyl singlet (a) at 3.1 ppm shifted slightly to 3.0 ppm, while the two multiplet peaks at 3.7 and 3.8 ppm, integrating

to two protons each and likely arising from methylene protons b and c, were replaced by one singlet (b), integrating to two protons total. It is likely that the protons at site b, α to the sulfonamide group, have been exchanged with deuterium leaving only a singlet for the protons at site c (Figure 2.15), which are no longer coupled to protons at site b. This matches well with the deuterium exchange of three protons observed in the mass spectrometry solvent exchange experiment. The observed signals of the IR spectrum, including the characteristic imine, nitrile, and symmetric and asymmetric sulfone stretches, also support the identification of **4** as a sultam structure (Figure 2.16).

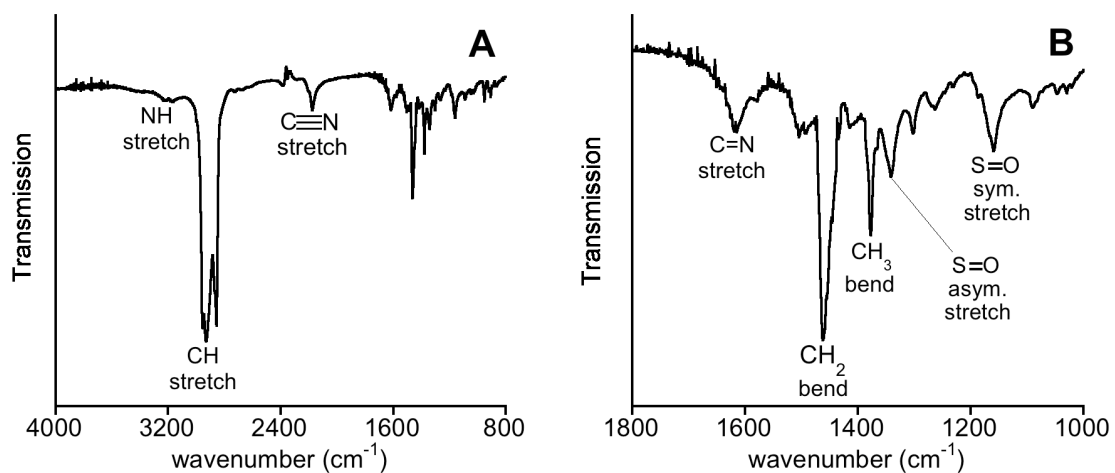


Figure 2.16. Infrared spectra of isolated product **4**: (A) full wavelength range and (B) zoom-in of low wavenumber region.

Both the NMR and IR signals could support either the β -sultam or the δ -sultam structure as the identity of **4**. Again, **4** represents an unexpected product, resulting from C-S cleavage, intramolecular nucleophilic substitution, and oxidation.

2.3.4 Intermediacy of chlorination products

During the fast degradation of cimetidine by a 10-fold molar excess of free chlorine at pH 7 in DI water, product **2** formed rapidly and then decayed almost completely within 2 min as the concentrations of the other three products increased (Figure 2.4 B). At pH 4, no product **2** was detected (Figure 2.4 A), presumably because it formed from cimetidine and degraded to the other products before the first time point was taken at 10 s. At pH 10, product **2** again formed rapidly from cimetidine but was slow to decay (Figure 2.4 C). Due to the observed pH dependence of the degradation of **2**, authentic cimetidine sulfoxide was chlorinated independently from cimetidine, yielding pseudo-first-order rate constants of 0.0436 s^{-1} and $5.04 \times 10^{-4}\text{ s}^{-1}$ at pH 7 and 10, respectively. The plots of $\ln([\text{substrate}]_t/[\text{substrate}]_0)$ vs. time from which the rate constants were obtained were found to be linear ($R^2 > 0.99$). At pH 4, complete degradation occurred before the first time point was taken at 5 s, so that a rate constant could not be determined. With a half-life of $<5\text{ s}$, the pseudo-first-order rate constant must be $> 0.14\text{ s}^{-1}$. The same three products formed at pH 4 during the chlorination of cimetidine sulfoxide as were observed from cimetidine at pH 4, confirming the intermediacy of **2** at this pH. Cimetidine sulfoxide was stable in the absence of free chlorine at the pH values studied, showing that transformations to all subsequent products required free chlorine to occur. The observed pH dependence can be explained by the greater oxidizing strength of HOCl compared to dissociated OCl⁻ ($\text{p}K_a = 7.54$)²⁸ that has been observed by other researchers.^{9, 11, 29}

To test if any products other than cimetidine sulfoxide acted as intermediates, authentic 4-hydroxymethyl-5-methyl-1H-imidazole (**1**), and isolates of **3** and **4** were

independently chlorinated with a ~10-fold molar excess of free chlorine at pH 7. Over the course of 60 min, **3** and **4** reacted minimally (<10% degradation) and did not produce any products matching in HPLC retention time with any other cimetidine chlorination products (Figure 2.17).

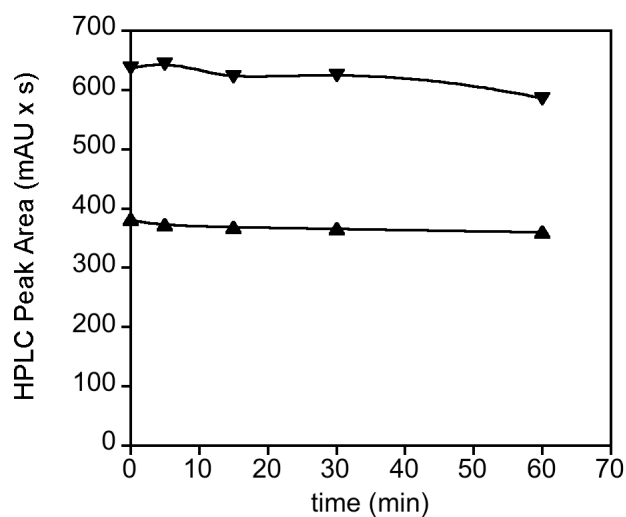


Figure 2.17. Degradation of products **3** (▲) and **4** (▼) in the presence of ~ 10-fold molar excess of free chlorine in pH 7 DI water, showing both products to be relatively unreactive.

By contrast, 4-hydroxymethyl-5-methyl-1H-imidazole degraded appreciably (55%) with concomitant formation of **3** (Figure 2.18), giving evidence for a pathway to **3** via the intermediacy of **1**.

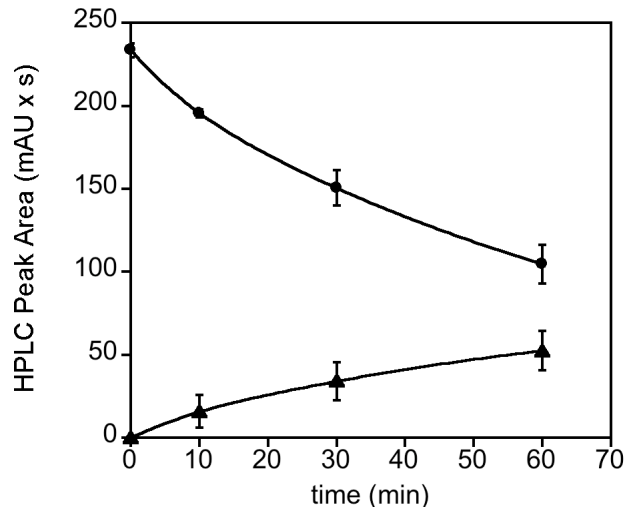


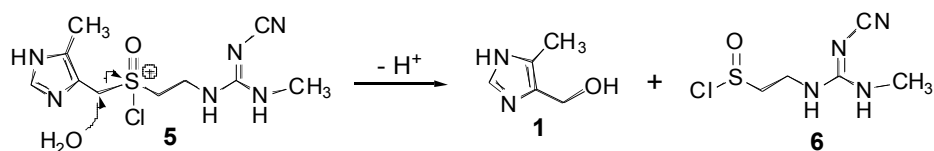
Figure 2.18. Degradation of authentic **1**, 4-hydroxymethyl-5-methyl-1H-imidazole (●), in the presence of a 10-fold molar excess of free chlorine in DI water (pH 7) and simultaneous growth of **3** (▲). Lines represent fits to exponential growth and decay equations ($R^2 > 0.99$). Error bars denote the 95% confidence interval for $n=3$.

2.3.5 Proposed reaction pathways and mechanisms

Postulated reaction pathways for the reaction of cimetidine with free chlorine proceeding through the intermediacy of cimetidine sulfoxide are shown in Scheme 2.1. These pathways appear to be operative at acidic and neutral pHs, while direct conversion of cimetidine to products **1**, **3**, and **4**, bypassing cimetidine sulfoxide, may occur under basic conditions. At pH 10, products **1**, **3**, and **4** initially form from cimetidine at a higher rate than cimetidine sulfoxide degrades (Figure 2.4 C). While the speciation of cimetidine ($pK_a = 7.1$)³⁰ may have an effect on the preferred reaction pathway, the same products are observed whether cimetidine is in its neutral or imidazole-protonated conjugate acid form.

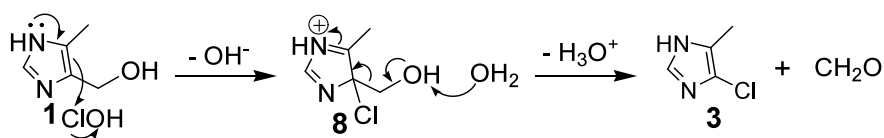
The reaction pathways in Scheme 2.1 begin with the fast oxidation of cimetidine to cimetidine sulfoxide (**2**) by free chlorine, followed by S-chlorination to form the

chlorosulfoxonium intermediate, **5**. This type of S-chlorination has been proposed for the free chlorination of dialkyl sulfoxides in the synthesis of α -chlorosulfoxides.^{31, 32} The next likely step is attack of water at the imidazole-substituted methylene of **5**, generating 4-hydroxymethyl-5-methyl-1H-imidazole (**1**) and the sulfinyl chloride, **6**:



This type of C-S fragmentation has been observed for chlorosulfoxonium ions bearing 2-trimethylsilylethyl groups.³³ The 2-silylethyl group was thought to stabilize the incipient carbocation formation on the S-bound carbon, as the imidazolymethyl group would in the present case. Sulfinyl chloride **6** may then undergo an intramolecular nucleophilic attack of either secondary amine at the electrophilic sulfur center to form either the β -sultone, **7** (β), or the δ -sultone, **7** (δ). Whichever sultone structure forms may be subsequently oxidized by free chlorine to form product **4**.

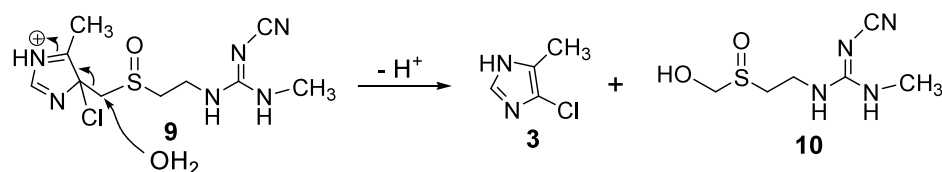
The transformation of **1** to **3** described above can be explained by electrophilic chlorination at the 4-position of the imidazole ring of **1** to yield the chloroimidazolium intermediate, **8**. The hydroxyl of **8** may be deprotonated, eliminating formaldehyde and forming 4-chloro-5-methyl-1H-imidazole (**3**):



Literature precedent for such chlorine substitution of hydroxymethyl imidazoles and benzyl alcohols by free chlorine supports such a mechanism.³⁴⁻³⁶ In the case of benzyl alcohols, an activating group *para* to the carbinol group to be replaced is important.³⁶

In the present study, the enamine of the imidazole ring may provide the necessary activation towards chlorination at the 4-position.

While this pathway accounts for the formation of all the observed products, it does not match the observed order of product formation. Namely, product **3** forms at a much faster initial rate during the chlorination of cimetidine at pH 7 than during the chlorination of 4-hydroxymethyl-5-methyl-1H-imidazole at pH 7 with the same free chlorine dose. Thus, it appears that a second parallel pathway is operative that produces **3** directly from cimetidine sulfoxide (**2**). This pathway is initiated by C-chlorination at the 4-position of the imidazole ring, giving the chloroimidazolium intermediate, **9**. Nucleophilic attack of water at the methylene bound to the 4-position may displace **3** from **9** and generate the hydroxymethylsulfoxide intermediate, **10**:



S-chlorination may then convert intermediate **10** to the chlorosulfoxonium intermediate, **11**, which may cleave to form sulfinyl chloride **6** and formaldehyde by a mechanism similar to that put forward for the cleavage of formaldehyde from **1** to form **3**. At this point, the C-chlorination pathway converges with the S-chlorination pathway and proceeds to yield product **4**. Products **3**, **4**, and formaldehyde are the terminal products of these parallel pathways.

2.3.6 Toxicity of products

The PNECs for cimetidine and its chlorination products predicted by the ECOSAR analysis are displayed in Table 2.1.

Table 2.1. Predicted no-effect concentrations (PNECs) of cimetidine and its chlorination products as well as several well-known aquatic pollutants.

Compound	PNEC ($\mu\text{g/L}$)	Species
Cimetidine	35 ^a	Daphnid
1	20 ^a	Daphnid
2	370 ^b	Green algae
3	6.5 ^a	Daphnid
4 (β -sultam)	630 ^b	Daphnid
4 (δ -sultam)	630 ^b	Daphnid
2,4-dichlorophenol	4.1 ^a	Daphnid
Atrazine	2.3 ^b	Daphnid
Dichlorvos	14 ^b	Green algae

^a PNEC derived from lethal concentration (LC50). ^b PNEC derived from effect concentration (EC50).

Products **1** and **3** are predicted to be more toxic than cimetidine. While **2** and **4** had relatively high PNECs on the order of 100 $\mu\text{g/L}$, **3** had a PNEC of 6.5 $\mu\text{g/L}$, a value on the same order of magnitude as aquatic pollutants such as 2,4-dichlorophenol and atrazine. These values suggest that cimetidine degradation by free chlorine does not eliminate an environmental threat, but rather increases it.

2.3.7 Environmental significance

Although the 1 mM free chlorine dose used in the experiments in this study exceeded typical wastewater disinfection levels (~ 0.14 mM),¹⁶ the reaction times (2 min for DI water and 5 min for wastewater) were much shorter than practice (typically ~ 1 hr), so that the total chlorine exposure in these experiments was less than practice. Because cimetidine was found to react rapidly with free chlorine, it is likely to be completely degraded during the disinfection of wastewater effluent in cases where a

chlorine residual exists. Results from the NH_4Cl quenching control experiments show that cimetidine also reacts rapidly (100% degradation in 3 min at pH 7) with a 10-fold molar excess of chloramines formed by the quenching of free chlorine with NH_4Cl . This indicates that cimetidine will likely be significantly transformed even in wastewaters with high ammonia and organic nitrogen content that will consume free chlorine. The fast reaction of cimetidine with free chlorine and chloramines may be why it has not been detected more frequently in natural waters receiving wastewater effluent. Analysis of terminal products **3** and **4** in natural waters may provide a more effective indicator of the cimetidine load than cimetidine itself. The enhanced toxicity of products **1** and **3** predicted by ECOSAR supports the results observed by other researchers that treatment of PPCPs with free chlorine may generate products of greater environmental concern than the parent compounds. The rapid chlorination rate observed, the unexpected products identified, and the toxicity increase predicted in this work indicate that further detailed studies will be necessary to fully evaluate the environmental impacts of PPCP pollutants.

Chapter 3:

Aquatic Photochemistry of Chlorinated Triclosan Derivatives: Potential Source Of Polychlorodibenzo-*p*-dioxins¹

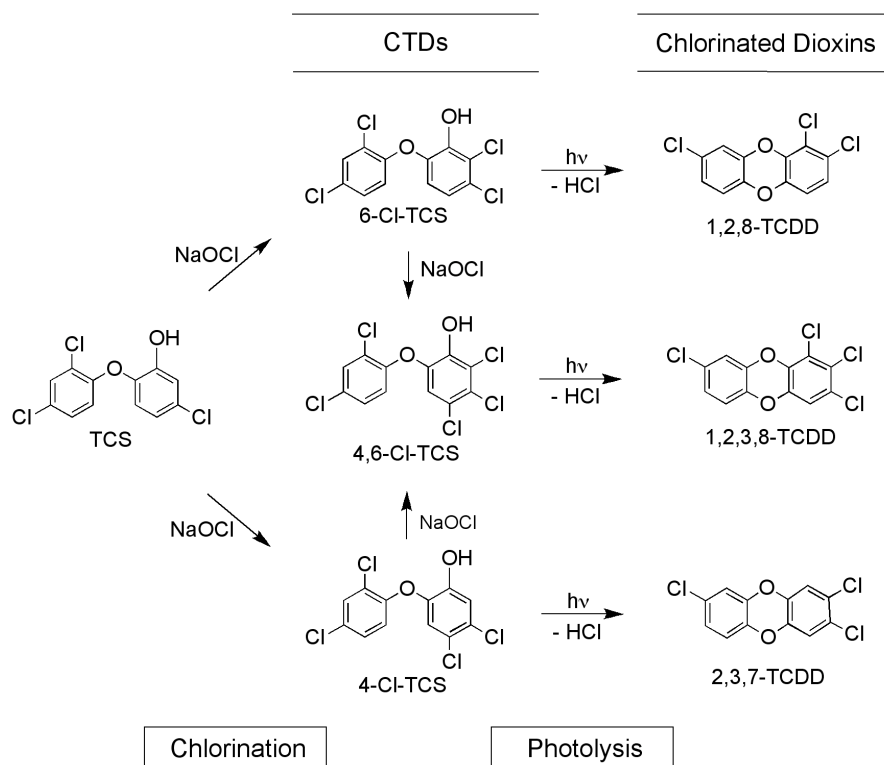
¹ A version of this chapter has been published as: Buth, J.M; Grandbois, M.; McNeill, K.; Arnold, W.A. Aquatic photochemistry of chlorinated triclosan derivatives: potential source of polychlorodibenzo-*p*-dioxins. *Environ. Toxicol. Chem.* In press.

3.1 Introduction

Concern has grown in the last decade regarding the presence of pharmaceutical and personal care product (PPCP) pollutants in aquatic environments due to their potential impact on the health of aquatic ecosystems and humans.^{1,2} Triclosan (TCS; 5-chloro-2-(2,4-dichlorophenoxy)phenol), a widely used antimicrobial agent, is a prominent PPCP pollutant in natural aquatic systems. It was detected in 58% of 85 sampled U.S. waterways at a median concentration of 0.14 $\mu\text{g/L}$ and a maximum concentration of 2.3 $\mu\text{g/L}$ in a recent survey.³ The prevalence of TCS in the environment is not surprising given its high use in many consumer products including liquid hand soap, toothpaste, and athletic clothing.

It has become evident that reactions with free chlorine during wastewater disinfection and solar photolysis play important roles in the fate of PPCPs and may increase the environmental hazard through the generation of deleterious byproducts.⁴⁻⁷ Triclosan has been shown to react with free chlorine to form the chlorinated triclosan derivatives (CTDs), 4,5-dichloro-2-(2,4-dichlorophenoxy)phenol (4-Cl-TCS), 5,6-dichloro-2-(2,4-dichlorophenoxy)phenol (6-Cl-TCS), and 4,5,6-trichloro-2-(2,4-dichlorophenoxy)phenol (4,6-Cl-TCS) (Scheme 3.1), as well as chlorophenols and chloroform.⁸⁻¹⁰ The CTDs have been detected in wastewater influent, effluent, a wastewater-impacted stream, and in carp of a wastewater-impacted bay.^{11, 12}

Scheme 3.1. Hypothesized pathway for the formation of 2,3,7-TCDD, 1,2,8-TCDD, and 1,2,3,8-TeCDD from the respective photolysis of 4-Cl-TCS, 6-Cl-TCS, and 4,6-Cl-TCS formed from the chlorination of triclosan (TCS).



Another process that plays a major role in the environmental fate of TCS is photolysis. When discharged into natural water bodies with wastewater effluent, TCS may absorb solar energy and photodegrade. Photolysis accounted for 80% of the total observed elimination of TCS from Lake Greifensee during late summer/early autumn.¹³ Photolysis half-lives on the order of one day were calculated during summer months for various water bodies.¹³ A major concern regarding the photochemical degradation of TCS is the potential formation of dioxin products. It has long been known that polychlorophenoxyphenols are photochemically converted to polychlorodibenzo-*p*-dioxins (PCDDs) via an intramolecular photochemical substitution reaction.^{14, 15} This type of reaction was found to generate 2,8-dichlorodibenzo-*p*-dioxin (2,8-DCDD) from

the irradiation of TCS in pure and natural water under artificial UV and solar irradiation.^{6, 16-18} While 2,8-DCDD was found to be essentially non-toxic to guinea pigs, chick embryos, and Japanese medaka embryos,¹⁹⁻²¹ the toxicity of dioxins increases with increasing chlorine substitution at the lateral positions.²² Several reports have shown that CTDs in the solid state and in aqueous solution are converted to higher-chlorinated PCDDs under UV lamp and sunlight irradiation, with 2,3,7-trichlorodibenzo-*p*-dioxin (2,3,7-TCDD), 1,2,8-trichlorodibenzo-*p*-dioxin (1,2,8-TCDD), and 1,2,3,8-tetrachlorodibenzo-*p*-dioxin (1,2,3,8-TeCDD) identified as the major respective PCDD photoproducts of 4-Cl-TCS, 6-Cl-TCS, and 4,6-Cl-TCS (Scheme 3.1).^{14, 16, 23, 24}

We hypothesize that a fraction of TCS entering wastewater streams will persist through wastewater treatment and may be chlorinated to form CTDs during disinfection with chlorine. A fraction of CTDs entering the wastewater treatment stream may persist as well. These CTDs would enter aquatic systems with wastewater effluent and potentially undergo an intramolecular photochemical substitution reaction to generate PCDDs. While the photochemistry of CTDs has been examined in part, further investigation is required to understand the photochemical fate of CTDs in natural aquatic systems.

The aim of the present study was to confirm the photochemical formation of PCDDs from 4-Cl-TCS, 6-Cl-TCS, and 4,6-Cl-TCS in aqueous solution, including natural waters. Relative rates were measured for CTD photolysis for both the phenol and phenolate forms, because the photoreaction was highly pH-dependent. Additionally, this work determined the photolysis quantum yields of CTDs, as well as

the quantum yields of PCDD formation. The influence of dissolved organic matter on the photochemistry was investigated by irradiating samples in Mississippi River and Lake Josephine waters. From the quantum yields obtained in the present study, the absorption spectra of the analytes, and the measured pK_a values, phototransformation half-lives may be calculated for any given set of environmental conditions. Finally, the total load of TCS- and CTD-derived PCDDs to U.S. surface waters was estimated.

3.2 Experimental

3.2.1 Chemicals

TCS (97 %) and pyridine (≥ 99 %) were purchased from Sigma Aldrich, and *p*-nitroacetophenone (PNAP; 97 %) and *p*-nitroanisole (PNA) were obtained from Acros Organics. Solutions of 2,8-DCDD and 2,3,7-TCDD in isooctane (50 $\mu\text{g/mL}$) were purchased from AccuStandard, and a 50 $\mu\text{g/mL}$ mixture of 1,2,3,7/1,2,3,8-TeCDD in *n*-nonane was purchased from Cerilliant. The CTDs (4-Cl-TCS, 6-Cl-TCS, and 4,6-Cl-TCS) were synthesized and purified as described in the Appendix. Grab samples of Mississippi River water (MRW; pH 8.2; dissolved organic carbon (DOC) = 15.3 mg/L) obtained at Minneapolis, MN, USA and Lake Josephine water (LJW; pH 8.1; DOC = 10.8 mg/L) obtained at Roseville, MN, USA were filtered (0.2 μm pore size) prior to use in photolysis experiments. A Thermo-Orion Ross Ultra Semi-Micro pH probe was used to measure pH, and a Sievers 900 Portable TOC Analyzer was used to make DOC measurements. Ultrapure water (18 $\text{M}\Omega$) was obtained from a Millipore Simplicity UV purification system. All other chemicals and solvents were used as received. All solvents were of chromatography grade.

3.2.2 pK_a determinations

Solutions of 35 μM TCS, 4-Cl-TCS, and 6-Cl-TCS in 90:10 water:methanol (v/v) and 4,6-Cl-TCS in 80:20 water:methanol (v/v) were adjusted to $\text{pH} < 4$ with HCl. The solutions were then titrated to basic pH with a minimal volume of NaOH, so as not to significantly alter the analyte concentration. At each pH value, UV-visible absorbance spectra were measured using an Ocean Optics USB2000 spectrophotometer. The absorbances at the λ_{max} of the phenolate species were plotted versus pH, and the resulting curves were fit using a non-linear regression (Kaleidograph v. 3.5) to determine the pK_a values.

3.2.3 Photolysis experiments

Photolysis solutions (10 μM) were prepared by diluting methanolic stock solutions of the substrates (TCS or CTDs) in buffered, pure water. Photolyses of the phenolate substrates were carried out in 10 mM borate buffer (pH 10.1), where each substrate was fully de-protonated ($> 99\%$). Photolyses of the fully protonated ($\geq 99\%$) substrates were carried out in 10 mM acetate buffer (pH 3.8) or 80:20 acetate buffer:methanol (v/v; adjusted to pH 3.9 with HCl). Photolyses were also performed in MRW (pH 8.2) and LJW (adjusted to pH 8.2 with HCl/NaOH), and 10 mM borate buffer (adjusted to pH 8.2 with HCl/NaOH) to assess the effect of dissolved organic matter on the photochemical reaction of each substrate.

In each experiment, 5 mL triplicate or duplicate samples were irradiated in quartz test tubes capped with cork stoppers with a dark control sample under natural sunlight in Minneapolis, MN, USA (45°N latitude) during late spring and summer. The

tubes were placed at a 45° angle to the incident sunlight. Triplicate or duplicate PNA (10.0 μM)/pyridine (20.0 mM) and PNAP (20.0 μM)/pyridine (29.9 mM) actinometer samples were irradiated alongside the basic and acidic substrate solutions, respectively, to determine the light intensity reaching the samples according to the method described by Leifer.²⁵ For kinetic analyses, 100 μL aliquots were sub-sampled periodically for high-pressure liquid chromatography (HPLC) analysis.

Quantum yields of substrate photolysis ($\Phi_{\text{substrate}}$) were calculated by comparing the rate constant for substrate loss (k_s) to the rate constant for the disappearance of PNA or PNAP (k_a), which are actinometers with known quantum yields.²⁶ The ratio, k_s/k_a , was determined from the slope of the plot of $\ln(C_{t,s}/C_{0,s})$ vs. $\ln(C_{t,a}/C_{0,a})$, where $C_{0,s}$ and $C_{t,s}$ are the concentrations of substrate initially and at any given time point, respectively, and $C_{0,a}$ and $C_{t,a}$ are the concentrations of PNA or PNAP at the corresponding time points. The spectral overlap integral for substrates and actinometers was calculated from their molar absorptivities (measured using an Ocean Optics USB2000 spectrophotometer with a 1 cm quartz cell) and the solar light intensity spectrum (obtained from the atmospheric radiation modeling program, SMARTS v. 2.9.5^{27, 28}).

By apportioning the substrate degradation into two pathways, dioxin formation and formation of other products, a set of differential equations was developed and numerically integrated to the kinetic data using MicroMath Scientist for Windows v. 2.02 to determine the rate of PCDD formation (k_{PCDD}). The ratio, k_{PCDD}/k_s , gave the molar yield of PCDD, from which the quantum yield of PCDD formation (Φ_{PCDD}) was determined. Quantum yield calculations for the natural water photolyses took into account the effect of acid-base speciation on the absorbance of each substrate and were

corrected for light screening of the matrices over the relevant spectral range as described by Schwarzenbach et al.²⁹

For product identification purposes, samples were irradiated at 250 W/m² with an Atlas Suntest CPS+ solar simulator, an artificial lamp that mimics the solar spectrum.

3.2.4 HPLC analysis

Kinetic analyses were performed on an 1100 Series Hewlett-Packard HPLC with UV-absorbance detection using a Supelco Discovery RP-Amide C₁₆, 150 × 4.6 mm, 5 μm particle size column. In the analysis of substrate photolysis solutions, 35 μL injections were made running a mobile phase of 82:18 acetonitrile:pH 5 acetate buffer (v/v) at a flow rate of 1.0 mL/min with detection at 230 nm. This method was also used to construct 5-point calibration curves for TCS, CTDs, 2,3,7-TCDD, 1,2,8-DCDD, and 1,2,3,7/1,2,3,8-TeCDD. Triclosan and CTD standards were prepared in water, and PCDD standards were prepared in isopropanol. All calibration curves were linear with R² values of ≥ 0.998. Actinometer solutions were analyzed for PNA or PNAP with 50 μL injections, a mobile phase of 55:45 acetonitrile:pH 3 phosphate buffer (v/v) run at 1.0 mL/min, and detection at 280 nm.

3.2.5 Photoproduct identification

To identify photoproducts of TCS and the CTDs, triplicate 5 mL samples (pH 10.1 borate buffer; 10 μM initial substrate concentration) were irradiated in the solar simulator. The photolysis solutions were combined, acidified with H₂SO₄, and

extracted into *n*-hexanes or cyclohexane. The extracts were then solvent exchanged into methanol and concentrated to minimal volume for instrumental analysis.

Retention times and UV-vis spectra of putative PCDD products in the concentrated photolysis extracts were compared to authentic PCDD standards by analyzing them on an Agilent 1200 Series HPLC equipped with photo-diode array detection, acquiring data from 210 to 400 nm at 2 nm intervals. The same column and method used to analyze the aqueous photolysis solutions were used.

Extracts of photolysis solutions were also analyzed by gas chromatography/mass spectrometry (GC/MS) on an Hewlett-Packard G1800A GCD Series gas chromatograph equipped with electron impact ionization. Splitless injections (1 μ L) were separated on a Restek Rtx-5 column (30 m \times 0.25 mm; 0.25 μ m film thickness) using helium as the carrier gas, an inlet temperature of 250°C, and a detector temperature of 280°C. The oven temperature was held at 60°C for 2 min, ramped to 210°C at 7°C/min, then ramped to 280°C at 15°C/min and held for 5 min. The MS was operated in either selective ion monitoring or scan mode. When using scan mode, extracted ion chromatograms were generated for the masses of parent and photoproduct compounds. To rule out the possibility of thermal cyclization of TCS or CTDs in the inlet or contamination of parent compounds with PCDDs, standards of TCS and CTDs were injected on the GC/MS. While a single PCDD was detected with each parent compound standard, corresponding to a ring-closing cyclization reaction, the amounts were insignificant compared to the amount of parent compound detected (\leq 1%).

Photolysis extracts were further analyzed by direct infusion on a Bruker BioTOF II electrospray ionization time-of-flight mass spectrometer (ESI-TOF-MS) in

negative mode. Exact mass measurements with less than 10 ppm error were made using polyethylene glycol as an internal mass calibrant.

3.3 Results and Discussion

3.3.1 pK_a determinations

Triclosan and the CTDs each possess a phenolic moiety that is subject to acid-base ionization. The spectrophotometrically determined pK_a values of triclosan and the CTDs are displayed in Table 3.1.

Table 3.1. Triclosan (TCS) and chlorinated triclosan derivative pK_a values, photolysis quantum yields of substrate degradation ($\Phi_{\text{substrate}}$) and polychlorodibenzo-*p*-dioxin (PCDD) formation (Φ_{PCDD}), and % PCDD yields.

		TCS	4-Cl-TCS	6-Cl-TCS	4,6-Cl-TCS
pK_a		7.6	7.1	6.3	5.9
Borate buffer (pH 10.1)	$\Phi_{\text{substrate}}$	0.39	0.29	0.066	0.051
	$\Phi_{\text{PCDD}} (\times 10^3)$	8.0	1.5	1.1	0.48
	% yield PCDD	2.0	0.5	1.7	0.96
Borate buffer (pH 8.2)	$\Phi_{\text{substrate}}$	0.40	0.22	0.056	0.071
	$\Phi_{\text{PCDD}} (\times 10^3)$	3.9	2.8	1.3	0.41
	% yield PCDD	0.97	1.3	2.3	0.58
Mississippi River water (pH 8.2)	$\Phi_{\text{substrate}}$	0.34	0.21	0.056	0.067
	$\Phi_{\text{PCDD}} (\times 10^3)$	3.3	2.7	0.89	0.54
	% yield PCDD	0.95	1.3	1.6	0.80
Lake Josephine water (pH 8.2)	$\Phi_{\text{substrate}}$	0.31	0.20	0.050	0.066
	$\Phi_{\text{PCDD}} (\times 10^3)$	3.0	2.5	1.2	0.49
	% yield PCDD	0.97	1.2	2.5	0.75

The pK_a titration plots from which the values were obtained are shown in Figure 3.1.

The pK_a values of the CTDs are lower than that of TCS, consistent with the electron withdrawing effect of the chlorine substituents.

3.3.2 Photolysis kinetics

The pH-dependent speciation of the CTDs was expected to influence their aquatic photochemistry given that their pK_a values fall within the pH range of most natural water systems (pH 6-9). Thus, the photolysis of both the phenol and phenolate forms was studied for each analyte, so that the rate could be predicted at any pH by taking into account the speciation.

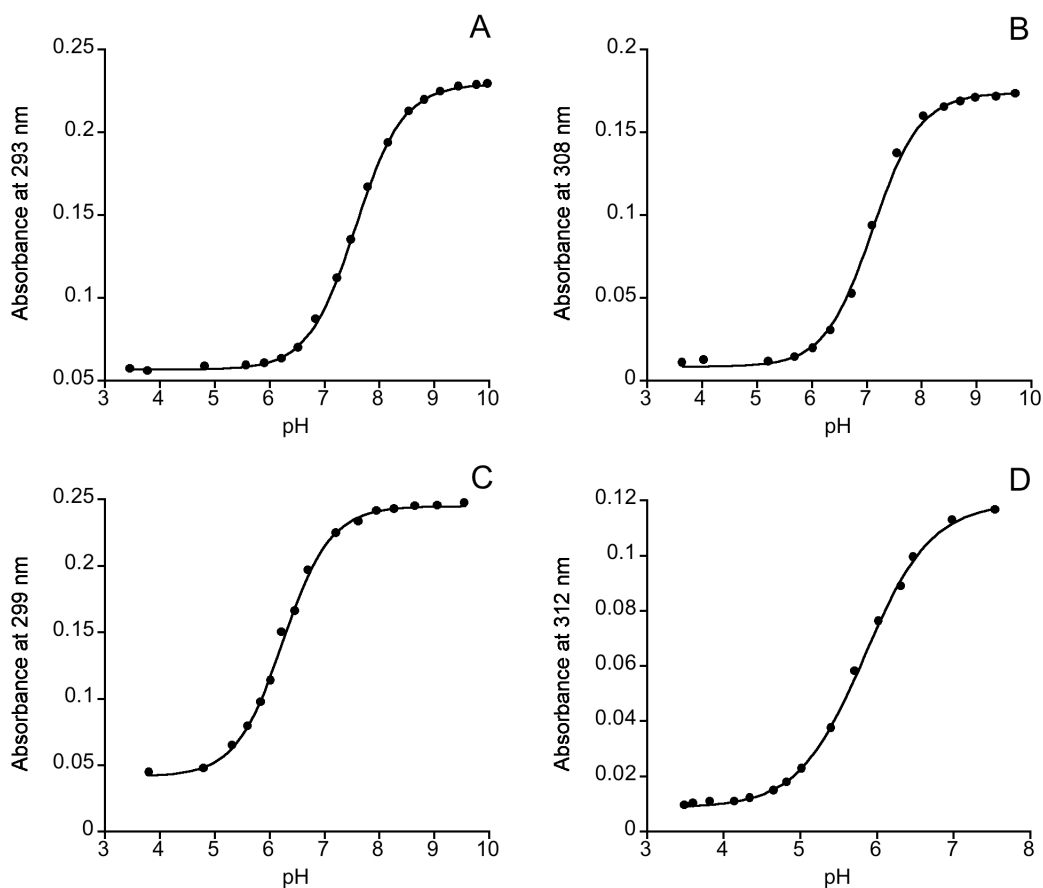


Figure 3.1. Plots of the spectrophotometric pH titrations of (A) triclosan, (B) 4-Cl-TCS, (C) 6-Cl-TCS, and (D) 4,6-Cl-TCS from which the pK_a values were obtained.

The photolysis rates measured at pH 10.1 for the phenolate forms of TCS and the CTDs were much higher ($t_{1/2} = 8-25$ min) than those measured in 80:20 acetate buffer:methanol (v/v; pH 3.9), where the phenol form predominates ($t_{1/2} > 1$ day).

Negligible substrate degradation was observed in the dark control experiments. The methanol co-solvent used at acidic pH was found to have little influence on photolysis rate; the rate of TCS photolysis was only 4% higher in pure acetate buffer (pH 3.8) than with 20% methanol. After normalizing for light intensity using a PNA/pyridine actinometer system, the following relative order of photolysis rates was obtained under basic conditions: 4-Cl-TCS > TCS > 4,6-Cl-TCS > 6-Cl-TCS (Figure 3.2 A).

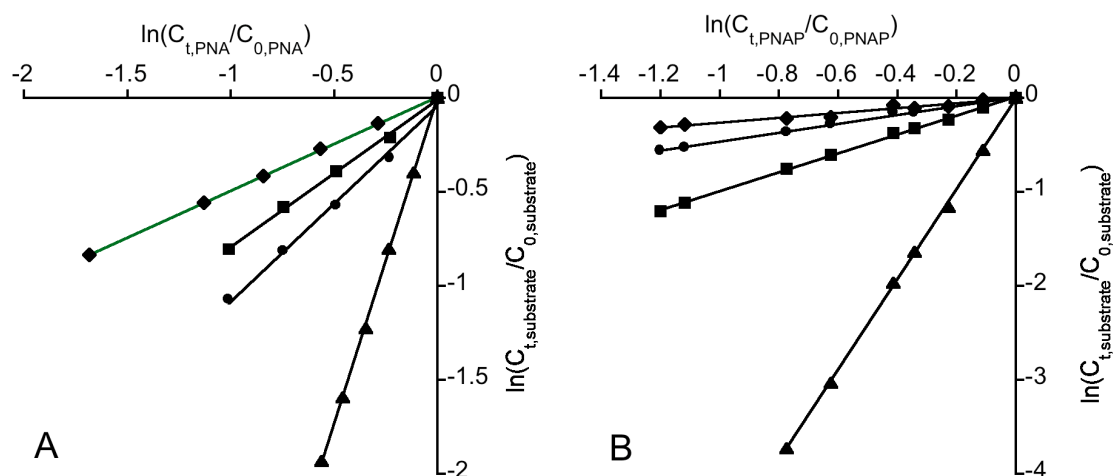


Figure 3.2. Degradation rate of triclosan (TCS) (●), 4-Cl-TCS (▲), 6-Cl-TCS (◆), and 4,6-Cl-TCS (■) at (A) pH 10.1 versus a PNA/pyridine actinometer and (B) pH 3.9 versus a PNAP/pyridine actinometer.

Under acidic conditions, the 4,6-Cl-TCS and TCS photolysis rates switched in the reactivity order (Figure 3.2 B). Relative photolysis rates of the four substrates normalized to the phenolic form of TCS (rate = 1) are plotted as a function of pH, taking into account their speciation based on the measured pK_a values (Figure 3.3).

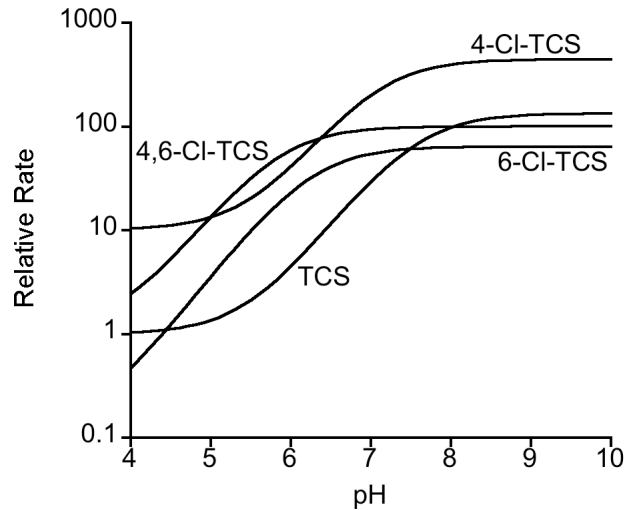


Figure 3.3. Relative photolysis rates as a function of pH of triclosan (TCS), 4-Cl-TCS, 6-Cl-TCS, and 4,6-Cl-TCS, normalized to the phenol form of TCS (rate = 1).

The enhanced photolysis rate at basic pH is largely due to the red-shifted absorbance of the phenolate anion compared to the phenol species. The four substrates' phenolic forms exhibit maximum absorbances at wavelengths ranging between 280-289 nm with little absorbance beyond 300 nm. The absorbance maxima of the phenolate anion species range between 293-312 nm with photon absorption beyond 320 nm, resulting in greater spectral overlap with sunlight irradiance, which increases drastically in intensity from 300 to 320 nm (Figure 3.4).

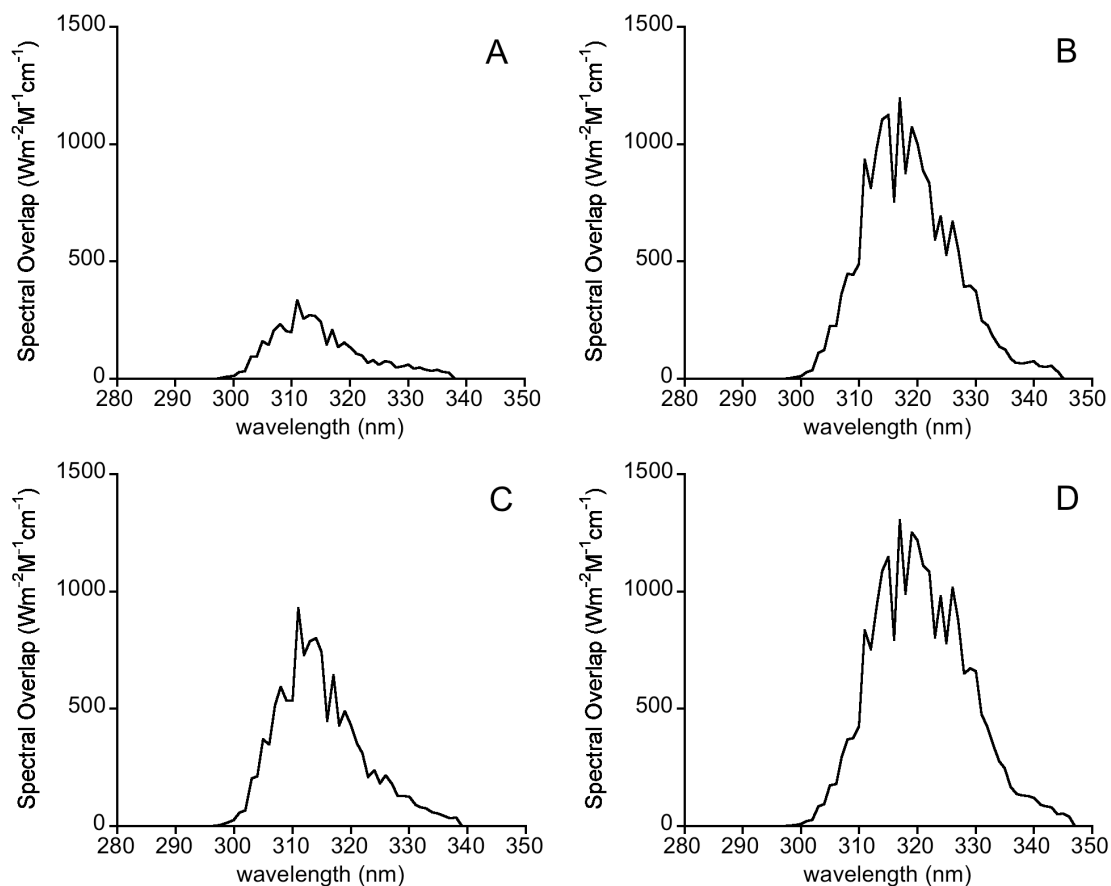


Figure 3.4. Solar irradiance spectral overlap with absorbance of (A) triclosan (TCS), (B) 4-Cl-TCS, (C) 6-Cl-TCS, and (D) 4,6-Cl-TCS at pH 10. Solar spectrum calculated by SMARTS for Minneapolis, MN, USA on June 13, 2008.

Because the phenolate forms of TCS and CTDs proved to be the dominant photoactive species, $\Phi_{\text{-substrate}}$ values were measured at pH 10.1 (Table 3.1). Photolysis quantum yields of the phenol forms of TCS and CTDs are not reported, because there were large errors associated with the light absorption rates due the very small absorbances of the protonated species in the sunlight spectral region, making the accurate determination of quantum yields difficult. At pH 10.1, the photolyses of TCS and 4-Cl-TCS are much more efficient than that of 6-Cl-TCS and 4,6-Cl-TCS. Chlorine substitution in the *ortho* position of the phenol ring hinders the efficiency of the photoreaction for the de-protonated substrates. This effect may be attributable to the

steric bulk of the *ortho*-chlorine that hinders solvation of the adjacent hydroxyl group. Benitez et al.³⁰ observed similar behavior, as the quantum yield of 4-chlorophenol was determined to be eight times higher than that of *ortho*-chlorinated 2,4-DCP under basic conditions.

When the photolyses were performed in MRW, LJW, and borate buffer at pH 8.2, differences in substrate photolysis quantum yields were minimal after correcting for matrix light screening (Table 3.1). This indicates that any indirect photoreactions, such as the reaction of substrates with singlet oxygen or hydroxyl radical produced via photosensitization of dissolved organic matter, are negligible compared to direct photolysis. This agrees with the results of Tixier et al.¹³ and Latch et al.,³¹ who determined that the steady-state concentrations of photoexcited reactive oxygen species in natural waters are too low for indirect photodegradation of TCS to compete with direct photolysis. Negligible substrate degradation was observed in dark control experiments in natural waters.

3.3.3 Product identification

Polychlorodibenzo-p-dioxin (PCDD) products. In the HPLC chromatograms of the aqueous photolysis solutions of TCS, 4-Cl-TCS, 6-Cl-TCS, and 4,6-Cl-TCS, a single peak of greater hydrophobicity relative to the parent substrate was observed. Retention times of authentic standards of 2,8-DCDD, 2,3,7-TCDD, and 1,2,3,8-TeCDD matched those of the hydrophobic product of TCS, 4-Cl-TCS, and 4,6-Cl-TCS, respectively, supporting the photochemical generation of these specific PCDDs from the parent compounds. UV-visible photodiode array detection of these photoproducts

afforded UV-visible spectra that matched with the authentic standards (Figure 3.5). A commercial standard of 1,2,8-TCDD, the putative photoproduct of 6-Cl-TCS, was not available, but the UV-visible spectrum closely resembled that of 2,3,7-TCDD, a TCDD with similar chlorine substitution.

Further confirmation of the identity of the PCDD photoproducts was provided by GC/MS analysis of methanol extracts of aqueous photolysis solutions. Chromatograms of TCS, 4-Cl-TCS, and 4,6-Cl-TCS photolysis extracts each yielded a peak whose GC/MS retention time matched that of authentic standards of 2,8-DCDD, 2,3,7-TCDD, and 1,2,3,8-TeCDD, respectively. The parent and fragmentation ions and the chlorine isotope pattern observed for each PCDD photoproduct (including 1,2,8-TCDD) confirmed the asserted identities (Table 3.2).

The degradation of parent TCS and CTDs and the concomitant growth of their respective PCDD photoproducts at pH 10.1 are displayed in Figure 3.6. From this kinetic data, the percent yield and quantum yield of PCDD formation from the phenolate forms of TCS and the CTDs were determined as described in the experimental section (Table 3.1). The magnitudes of the yields indicate that PCDD formation is a minor pathway in the phototransformation of TCS and CTDs. It is important to note that PCDDs are themselves photolabile in aqueous solution, yielding products including chlorinated dihydroxybiphenyls, dechlorinated dioxins, and chlorinated phenoxyphenols.^{6, 32, 33}

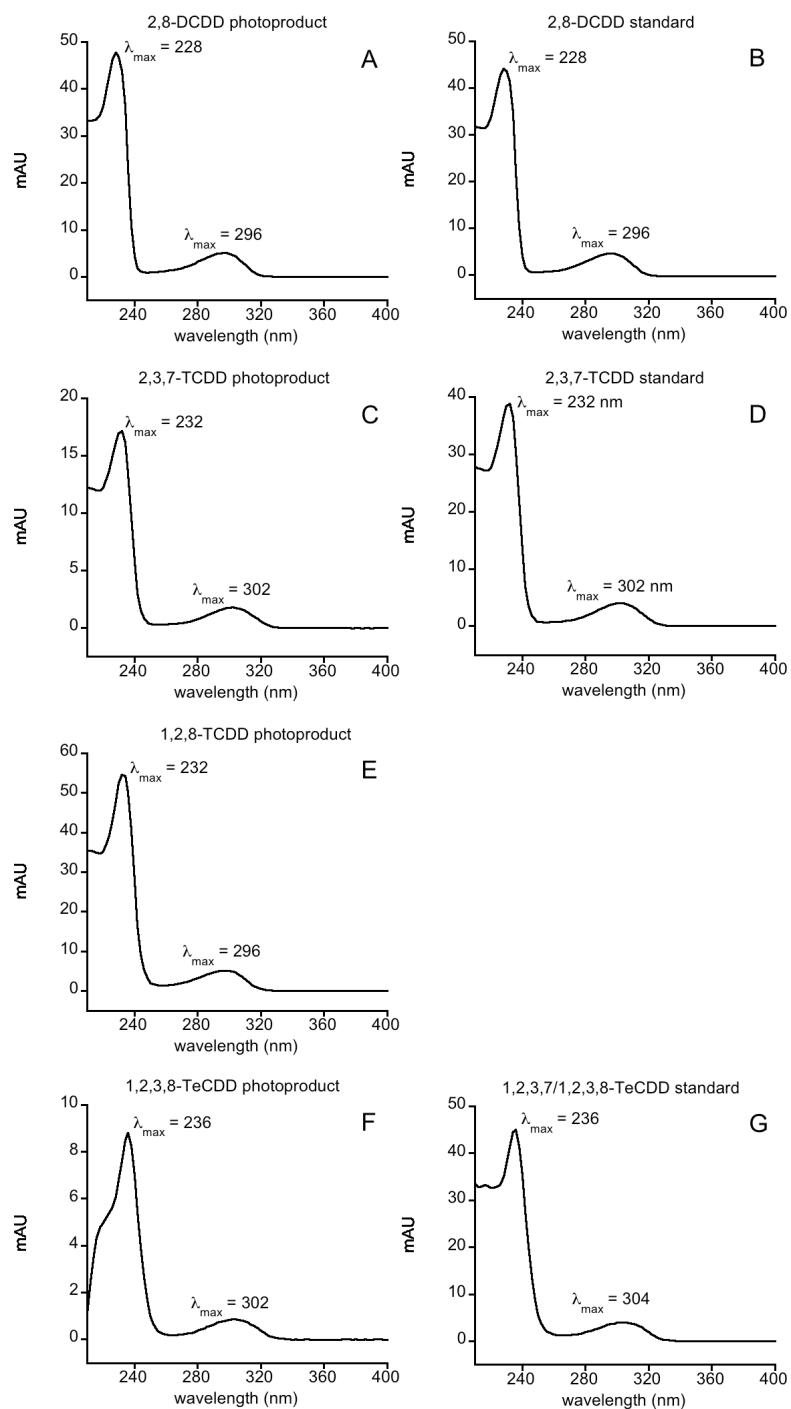


Figure 3.5. UV-visible absorbance spectra of the PCDD product of (A) triclosan (TCS), (C) 4-Cl-TCS, (F) 4,6-Cl-TCS, and of respective standards confirming their identity: (B) 2,8-DCDD, (D) 2,3,7-TCDD, and (G) 1,2,3,7/1,2,3,8-TeCDD. The UV-visible spectrum of the PCDD product of 6-Cl-TCS (1,2,8-TCDD) is shown in (E), though a standard was not commercially available.

Table 3.2. Parent and fragmentation ions of the mass spectra of 2,8-DCDD, 2,3,7-TCDD, 1,2,8-TCDD, and 1,2,3,8-TeCDD, the respective photoproducts of triclosan (TCS), 4-Cl-TCS, 6-Cl-TCS, and 4,6-Cl-TCS.

Parent Compound	Dioxin Photoproduct	Mass spectra		
		<i>m/z</i>	Cl isotope pattern	assignment
TCS	2,8-DCDD	252	Cl ₂	parent
		217 ^a		(-Cl)
		189	Cl	(-COCl)
		126 ^a		(-2COCl)
4-Cl-TCS	2,3,7-TCDD	286	Cl ₃	parent
		223 ^a		(-COCl)
6-Cl-TCS	1,2,8-TCDD	286	Cl ₃	parent
		223 ^a		(-COCl)
4,6-Cl-TCS	1,2,3,8- TeCDD	320	Cl ₄	parent

^a peak was of very low intensity so that an isotope pattern was not observed

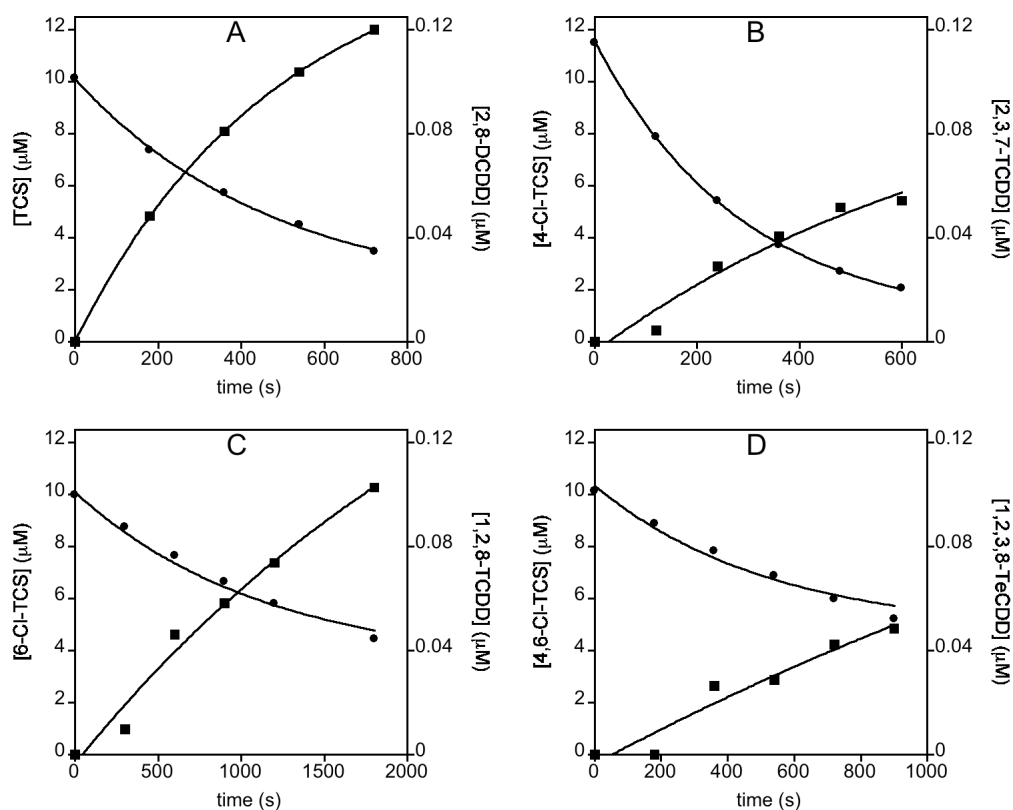


Figure 3.6. Solar photolysis of phenoxyphenol substrates (●) and concomitant dioxin formation (■) in 10 mM borate buffer (pH 10.1). A) triclosan (TCS) → 2,8-DCDD. B) 4-Cl-TCS → 2,3,7-TCDD. C) 6-Cl-TCS → 1,2,8-TCDD. D) 4,6-Cl-TCS → 1,2,3,8-TeCDD.

Latch, et al.⁶ reported photolysis quantum yields of 2,8-DCDD ranging from 2 to 20 times lower than its quantum yield of formation from TCS under various conditions. Photodegradation of PCDDs was not taken into account in the present determination of PCDD formation yields. Therefore, the reported values represent low-end approximations. The percent yield and quantum yield of PCDD formation in MRW, LJW and borate buffer at pH 8.2 exhibited little variability between the matrices, suggesting that the presence of DOM has a negligible effect on this reaction pathway. While the dioxin percent yields obtained for the different matrices at pH 8.2 vary from those determined at pH 10.1, an evaluation of the errors associated with the data fitting showed that these differences are not significant.

Concentrations of PCDDs were trace or non-detectable by HPLC in pH 3.9 kinetic experiments. The 2,8-DCDD, 2,3,7-TCDD, 1,2,8-TCDD, and 1,2,3,8-TeCDD products, however, were detected by GC/MS in concentrated methanol extracts of the acidic photolysis solutions of TCS, 4-Cl-TCS, 6-Cl-TCS, and 4,6-Cl-TCS, respectively, from the kinetic experiments. One explanation for why the PCDD levels were minimal in kinetic experiments at pH 3.9 is that PCDDs may photolyze much more quickly than the phenolic forms of TCS and CTDs, resulting in low steady-state concentrations. Alternatively, the PCDDs may not be produced from the degradation of the protonated substrates, but rather from the small fractions of TCS and CTDs that exist in the phenolate form at pH 3.9. Regardless, it is clear that because the phenolate forms photodegrade much faster than the phenol forms, they will be completely, or at least predominately, responsible for PCDD formation under environmental conditions.

2,4-dichlorophenol. A previously identified photoproduct of TCS was 2,4-dichlorophenol (2,4-DCP).³¹ Evidence suggests that 2,4-DCP may also be produced from the photolysis of CTDs. Analysis of a methanol extract of the aqueous photolysis solution of each substrate by ESI-TOF-MS revealed a product at m/z 161.0 (M-H⁺), where M represents the molecular formula of 2,4-DCP, C₆H₄Cl₂O (measured mass was outside the calibration range for high resolution measurement). While the mass does not provide confirmation of 2,4-DCP over other possible isomers, it is likely that 2,4-DCP is produced from the non-hydroxylated aromatic ring of each substrate via cleavage of the ether linkage. If chlorophenols were generated from the hydroxylated ring, varying degrees of chlorine substitution would be expected from the different substrates, which was not observed. The chromatographic method did not sufficiently retain 2,4-DCP to accurately determine its concentration. Its approximate yields (< 10%) indicate that 2,4-DCP is a minor product, and like the PCDDs, 2,4-DCP is photolabile.³¹

Dechlorination products. Reductive dechlorination photoproducts were observed by ESI-TOF-MS in concentrated extracts of photolysis solutions of each substrate. Table 3.3 displays the accurate mass measurements for the putative dechlorination products for each substrate, which are in good agreement with the theoretical masses of molecular formulas that correspond to the replacement of chlorine atoms with hydrogen. The masses and molecular formulas represent the phenolate anion species, because the extracts were analyzed in negative mode. A singly dechlorinated product was observed for each parent compound, while a doubly dechlorinated product was also observed for 6-Cl-TCS.

Table 3.3. Accurate mass measurements of reductive dechlorination photoproducts by ESI-TOF-MS.

Parent Compound	Accurate Mass Measurement (<i>m/z</i>)	Cl isotope pattern	Proposed Formula	Theoretical Mass (<i>m/z</i>)	Mass Error (ppm)
TCS	252.9812	Cl ₂	C ₁₂ H ₇ Cl ₂ O ₂	252.9829	6.7
4-Cl-TCS	286.9428	Cl ₃	C ₁₂ H ₆ Cl ₃ O ₂	286.9439	3.8
6-Cl-TCS	286.9432	Cl ₃	C ₁₂ H ₆ Cl ₃ O ₂	286.9439	2.4
6-Cl-TCS	252.9846	Cl ₂	C ₁₂ H ₇ Cl ₂ O ₂	252.9829	6.7
4,6-Cl-TCS	320.9026	Cl ₄	C ₁₂ H ₅ Cl ₄ O ₂	320.9049	7.2

Similar products attributable to reductive dechlorination have previously been observed in the photolysis of TCS.^{34, 35} The mass spectral data do not permit elucidation of the specific positions of dechlorination. In kinetic experiments, minor product peaks with shorter HPLC retention times than the parent compounds were observed for some substrates, which may represent dechlorination products. However, a lack of authentic standards prevented their identification and quantification.

Additional products. The PCDDs, 2,4-DCP, and dechlorination products observed in this study accounted for a small fraction of the photolysis product mass balance for TCS and the CTDs. While several unidentified products may be attributable to reductive dechlorination, additional minor pathways may include hydroxylation at positions of chlorine substitution, ring-closure to form hydroxylated furans, or formation of other chlorophenols.^{34, 35} Latch, et al.³¹ provided evidence that the photolysis of TCS may form polymeric products from the photocoupling of TCS with other TCS molecules or with dissolved organic matter in natural waters. This photopolymerization pathway likely contributed significantly to the photolysis product mass balance for the CTDs, as well.

3.3.4 Environmental implications

The observed formation of PCDDs during the solar irradiation of CTDs in natural waters indicate that this transformation is likely to take place in natural waters that receive wastewater effluent containing CTDs. This transformation raises increased environmental concern compared to the photogeneration of 2,8-DCDD directly from TCS. Dioxin toxicity generally increases with chlorine substitution in the lateral positions, and 2,3,7-TCDD and 1,2,3,8-TeCDD are both chlorinated in 3 of 4 possible lateral positions. Wisk and Cooper²¹ observed a dose dependent increase in visible lesions for 2,3,7-TCDD on Japanese medaka from 50-50,000 ng/L, while no effect was observed for 2,8-DCDD. Poland and Glover²⁰ found that 2,3,7-TCDD induces alanine synthetase and aryl hydrocarbon hydroxylase in chick embryos to a substantially higher degree than 2,8-DCDD.

Due to the enhanced toxicity of CTD-derived PCDDs, even the small conversion yields leading to their production found in the present study could result in an important source of dioxins to aquatic environments. To estimate the potential load of photochemically-generated PCDDs from TCS and CTDs in U.S. surface waters, the loading of the parent compounds must first be estimated. Assuming a wastewater influent mass of TCS of 3 mg/day per capita (the value measured for Columbus, OH in 1997 by McAvoy and co-workers,¹¹ who also found similar values for four nearby smaller communities (3 to 5 mg/day per capita)), the annual load of TCS is roughly estimated by multiplying the per capita release by the US population (300 million people) and the removal efficiency of wastewater treatment processes (approximately 75% of wastewater flow is treated by activated sludge treatment giving 96% removal

and 25% by other less efficient processes approximated at 85% removal¹¹). This estimate yields a TCS release of 22 metric tons/year into US surface waters. The sum of CTDs measured in wastewater influent was 25 times lower than that of triclosan.¹¹ Assuming the same removal efficiencies as for TCS, the load of CTDs would be 0.88 metric tons/year. This does not account for the CTDs that may be formed during chlorine disinfection. An alternative estimation is to use the average wastewater influent concentrations of 10 µg/L TCS and 0.4 µg/L total CTDs observed by McAvoy et al.¹¹ This TCS load falls within observed wastewater influent concentrations for TCS ranging from 0.24 to 37.8 µg/L.³⁶⁻³⁸ Assuming 150 L/day per capita of domestic water use, a population of 300 million, and the same removal rates above, a loading of 11 metric tons/year TCS and 0.44 metric tons/year CTDs is obtained.

To calculate the potential PCDD load, it is assumed that 10% of TCS and CTDs are lost from the water column due to photolysis. The value of 10% is arrived at via a box model for a river²⁹ that accounts for photolysis and sorption to/settling of particles as the major loss processes with corrections for pH and photic zone. This estimate is based on wastewater discharges to rivers, but it is likely higher than 10% for more transparent lakes or oceans. For example, Tixier et al.¹³ attributed 80% of triclosan loss in Lake Greifensee to photolysis. The dioxin yield is then taken as 3%. While this is higher than the values reported in Table 3.1, we did not consider the concurrent photolysis of the PCDDs when determining the yield, so 3% is a potential upper limit. This gives a loading of 33-66 kg/year of 2,8-DCDD and 1.3-2.6 kg/year of TCDDs and TeCDDs. Dioxin loadings, however, are usually reported in terms of toxicity equivalent units (TEQs) relative to 2,3,7,8-TeCDD. Toxicity factors for DCDDs,

TCDDs, and TeCDDs relative to 2,3,7,8-TeCDD are 0.001, 0.01, and 0.01, respectively.³⁹ Thus, the potential combined TCS- and CTD-derived dioxin TEQ is 46-92 g/year, and the CTD-derived dioxin toxicity represents a 40% increase over 2,8-DCDD toxicity, despite the small weight percentage. For comparison, the U.S. combined PCDD/polychlorodibenzofuran (PCDF) inventory for emissions to air is 2501 g TEQ/year.⁴⁰ Thus, the estimated PCDD load from TCS and CTDs is 1.8-3.7% of air emissions. While it is a comparatively small fraction, the load of TCS-derived PPCPs is noteworthy because it represents a direct discharge into the aquatic environment.

The present work confirms that solar photolysis of CTDs in buffered, pure water and natural waters produces PCDDs. The photolysis rates of CTDs were highly pH-dependent, with the phenolate species dominating their photochemistry. Minimal differences were observed in the photolysis of CTDs between pure and natural waters, indicating that direct photodegradation of CTDs out-competes any indirect photolysis processes. While the yields of PCDD photoproducts were low (0.5-2.5%), they may represent a substantial fraction of the total PCDD load to aquatic systems.

Chapter 4:

Occurrence of Triclosan and Chlorinated Triclosan Derivatives in Wastewater Effluent Before and After Chlorine Disinfection

4.1 Introduction

Triclosan is an antimicrobial chemical widely-used in liquid hand soaps, personal care products, and plastics. The use of triclosan-containing products results in it being rinsed down drains and entering wastewater treatment plants with municipal sewage. Although triclosan is typically removed at a high rate (> 90%) by modern secondary treatment facilities,¹⁻⁷ due to high influent concentrations reaching 10 µg/L,¹ a significant amount persists through treatment and enters aquatic environments that receive wastewater effluent. Triclosan concentrations on the order of 10 to 100 ng/L in wastewater effluent^{1, 2, 4} and 10 ng/L in surface waters^{2, 8, 9} are regularly observed. The presence of triclosan in natural waters is of concern because it is known to photolyze to form 2,8-dichlorodibenzo-*p*-dioxin (2,8-DCDD) under natural sunlight.¹⁰⁻¹³

Because a fraction of triclosan may persist through water treatment, it may be present in the effluent during the final disinfection stage, where free chlorine is commonly used in the U.S. as a disinfecting oxidant. Several researchers have identified three chlorinated triclosan derivative (CTD) products from the aqueous reaction of triclosan with free chlorine: 4,5-dichloro-2-(2,4-dichlorophenoxy)phenol (4-Cl-TCS), 5,6-dichloro-2-(2,4-dichlorophenoxy)phenol (6-Cl-TCS), and 4,5,6-trichloro-2-(2,4-dichlorophenoxy)phenol (4,6-Cl-TCS) (Scheme 3.1), as well as additional products such as chlorophenols and chloroform.¹⁴⁻¹⁶ Rule et al.¹⁵ showed that this reaction reaches a maximum rate near neutral pH, so that triclosan may be chlorinated under chlorine disinfection conditions for nitrified/de-nitrified effluent. The same CTDs are also formed upon the chloramination of triclosan, but the rate was depressed by several orders of magnitude compared to free chlorination.¹⁷ Thus, it is unlikely that

CTDs would form to an appreciable extent in the disinfection of non-nitrified wastewater. Chlorinated triclosan derivatives may also potentially form by reaction of triclosan with residual chlorine in tap water during transport to wastewater treatment plants. This possibility is supported by the results of McAvoy et al.,¹ who detected CTDs in the influent of wastewater treatment plants at concentrations as high as 1.06 µg/L (total CTDs). Leiker et al.¹⁸ detected bio-methylated analogues of the CTDs in a stream receiving wastewater effluent and in carp from a wastewater-impacted bay. The CTDs are of environmental concern, because, like triclosan, they have the potential to photochemically form chlorinated dioxins,^{11, 19-21} as demonstrated in Chapter 3 of this thesis.

In the present study, an analytical method was developed for triclosan, 4-Cl-TCS, 6-Cl-TCS, and 4,6-Cl-TCS in wastewater secondary influent and pre- and post-chlorination effluent. The larger goal was to investigate their transformation during wastewater treatment, specifically the potential formation of CTDs from triclosan during the chlorination step. While one study previously measured triclosan and CTD concentrations at various points throughout the wastewater treatment process,¹ the effect of chlorination was not investigated. Preliminary method development experiments were conducted to minimize the amount of interfering matrix dissolved organic matter (DOM). The developed method included solid-phase extraction (SPE) for cleanup and analyte concentration followed by a silica column cleanup step to prepare samples for ultra performance liquid chromatography-triple quadrupole mass spectrometry analysis (UPLC-MS-Q³).

4.2 Experimental

4.2.1 General

Chemicals. Triclosan (5-chloro-2-(2,4-dichlorophenoxy)phenol; 97%) was purchased from Sigma Aldrich. A methanolic solution of $^{13}\text{C}_{12}$ -triclosan (> 99% chemical purity; $\geq 99\%$ isotopic purity) was obtained from Wellington Laboratories. Three CTDs, 4-Cl-TCS, 6-Cl-TCS, and 4,6-Cl-TCS, were synthesized and purified as described in the Appendix. Sulfuric acid (H_2SO_4) and sodium hydroxide (NaOH) were obtained from Mallinckrodt. Humic acid sodium salt was purchased from Aldrich. Ultrapure water (18.2 M Ω) was obtained from a Millipore Simplicity UV purification system. All solvents used were of chromatography grade, except for methyl *t*-butyl ether (MTBE) that was obtained from Sigma-Aldrich at 99+% purity.

Washing of glassware. For all trace analyses, all sampling vessels and glassware were pre-washed with triclosan-free soap, then rinsed three times consecutively with tap water, deionized water, methanol, and either MTBE or ethyl acetate. Disposable glassware was assumed to be free of contamination and was not pre-washed. All syringes were flushed five times consecutively with acetone, methanol, and acetonitrile prior to each transfer.

4.2.2 Wastewater sampling

Secondary wastewater influent (collected after primary settling and prior to activated sludge treatment) and pre- and post-chlorination wastewater effluent samples were collected from the Metropolitan Wastewater Treatment Plant in St. Paul, MN in pre-washed glass bottles. This activated sludge facility, one of the largest in the U.S.,

serves a population of 1.8 million at a maximum capacity of 251 million gallons/day and discharges into the Mississippi River. The plant employs a nitrification treatment step by which inorganic nitrogen is oxidized to nitrate. Disinfection is performed with NaOCl at a dosage of 1.25 $\mu\text{g/L}$ Cl as Cl_2 for > 30 min, aiming for a residual of 0.20 $\mu\text{g/L}$ Cl as Cl_2 , followed by de-chlorination with sodium bisulfite at 0.95 $\mu\text{g/L}$. Chlorination/de-chlorination is carried out from April through October, but not during the winter months. Each sample was collected over a 24 hour period, representing an integrated record to diminish the influence of any spikes throughout the course of a day. The pre-chlorination effluent was collected at a 6 hour offset delay from the secondary influent, and the post-chlorination effluent was collected with a 30 min offset delay from the pre-chlorination effluent, so that the samples represented the same wastewater stream. After collection, the samples were transported to the laboratory within 1 hour and stored at 4 °C in the dark until processing, which was carried out within 72 hours. In the early development of the method, samples were processed by filtration through 0.2 μm Millipore nylon filters and adjustment to pH 2 with H_2SO_4 for preservation and then stored at 4 °C until further sample preparation was carried out. Later, samples were processed by filtration through 0.7 μm glass fiber filters (Fisher Scientific) and then immediately prepared for analysis. After filtration, the pH of the samples was recorded using a Thermo-Orion Ross Ultra Semi-Micro pH probe.

4.2.3 Preliminary matrix reduction experiments

Several experiments were conducted in the preliminary development of the method to reduce the level of interfering dissolved organic matter (DOM) present in the

wastewater matrices. In these experiments, wastewater samples were fortified with mg/L concentrations of triclosan and CTDs, far above their native ng/L levels, and analyzed by high pressure liquid chromatography (HPLC) equipped with UV-detection rather than the more sensitive UPLC-MS-Q³ system described below. Using a 1100 series Hewlett-Packard HPLC, injections of 5, 10, or 35 μ L were made on a Supelco Discovery RP-Amide C₁₆, 150 \times 4.6 mm, 5 μ m particle size column running an 82:18 acetonitrile:pH 5 acetate buffer (v/v) mobile phase at a flow rate of 1.0 mL/min. The detection wavelength was 230 nm.

Optimization of sample pH. In the first matrix reduction experiment, the pH of a wastewater sample was varied to determine whether the sample pH affected the retention of DOM on the SPE sorbent. DOM contains many phenolic and acidic functional groups that become protonated under acidic conditions, which was expected to promote DOM retention. Similarly, the phenolic analytes were expected to retain more strongly at acidic pH in their protonated, neutral form. The goal was to minimize the retention of DOM while sufficiently protonating the analytes for maximal retention. Pre-chlorination wastewater effluent used in this experiment was collected on December 6, 2007, processed by filtration through 0.2 μ m nylon filters and adjustment to pH 2 with H₂SO₄, and stored at 4 °C. Triplicate 240 mL samples augmented with 0.7 to 0.9 mg/L of triclosan, 4-Cl-TCS, 6-Cl-TCS, and 4,6-Cl-TCS were prepared at pH 3, 4, and 5 by adjusting with H₂SO₄ and NaOH. Samples were solid-phase extracted on Oasis HLB cartridges pre-conditioned with consecutive 5 mL aliquots of acetonitrile, methanol, and pH 2 water. After washing the cartridges with 5 mL of pH 2 water and drying under vacuum for 30 min, they were eluted with two 6.5 mL aliquots of

acetonitrile. The relative amount of DOM in the extracts was determined visually by the intensity of the observed yellow color. The analyte recoveries were measured as the ratio of the signal of the final acetonitrile extract to that of the original wastewater sample, with the signal of the extract normalized by its concentration factor.

Optimization of SPE cartridge wash step. The solvent used to wash the SPE cartridges after running a sample but prior to cartridge drying and elution was varied to determine whether DOM could be washed off the cartridge prior to the analyte elution step. Ten 100 mL samples spiked with 1.4 mg/L triclosan were prepared from the pre-chlorination effluent described above after adjustment to pH 4.2 with NaOH/H₂SO₄. They were solid-phase extracted as described above, using 5 different solvents for the 5 mL wash step, providing duplicate samples for each solvent. The washing solvents used were pH 2.5 water, un-adjusted water, 10:90 methanol:water (v/v), 20:80 methanol:water (v/v), and 50:50 methanol:water (v/v). The two 6.5 mL aliquots used to elute the analytes were collected in separate vessels and analyzed separately. Subsamples of the 5 mL wash aliquots and of the final acetonitrile extracts were analyzed by HPLC for triclosan. Triclosan recoveries were calculated as described above. The absorbance of the wash aliquots and final acetonitrile extracts at 350 nm was also measured using an Ocean Optics USB2000 UV-visible spectrophotometer. Because DOM contains many chromophoric functionalities with tailing absorption into the visible range and triclosan does not absorb beyond 340 nm, the absorbance at 350 nm was used as a proxy for DOM concentration.

After 50:50 methanol:water (v/v) was determined to be the optimal wash solvent, an experiment was conducted to test the effectiveness of multiple washes. Triplicate

250 mL samples of the same pre-chlorination effluent at pH 2 were spiked with 1.4 mg/L triclosan and solid-phase extracted as described above. After the wastewater samples were passed through the cartridges, the cartridges were washed with four sequential 5 mL aliquots of 50:50 methanol:water (v/v), collecting each 5 mL aliquot separately for analysis. The cartridges were then dried and eluted. Wash solutions and final acetonitrile extracts were analyzed by HPLC for triclosan and for absorbance at 350 nm. Triclosan recoveries were calculated as described above.

Silica column cleanup. A silica column cleanup step was developed to remove matrix impurities such as DOM from the SPE extracts. Silica columns were prepared by packing 6 cc disposable syringes with a plug of glass wool, a thin layer of sand, 2.00 g of silica gel (Sorbent Technologies Premium Rf, 60 Å, 40-75 µm) in a slurry of ethyl acetate, and a thin upper layer of sand. The columns were then rinsed with ethyl acetate to remove any analyte contamination. As a surrogate for a wastewater extract, a 3 to 4 mg/L methanolic solution of triclosan, 4-Cl-TCS, and 4,6-Cl-TCS was saturated with Aldrich humic acid via sonication for 1 hour and then filtered through a Gelman GHP Acrodisc (0.45 µm) filter syringe. Aliquots of this solution (1.00 mL) were quantitatively loaded onto triplicate silica columns and eluted by gravity with 10 mL of ethyl acetate. The ethyl acetate eluants were solvent exchanged into methanol and analyzed by HPLC along with aliquots of the original wastewater surrogate solution to determine analyte recoveries. The HPLC analysis was carried out using a 1100 series Hewlett-Packard HPLC, with 10 µL injections on a YMC ODS-AQ, 150 × 2.0 mm, 5 µm particle size column running an 82:18 methanol:pH 3 phosphate buffer (v/v) mobile phase at a flow rate of 0.3 mL/min. The detection wavelength was 230 nm.

4.2.4 Trace analysis of wastewater samples

Each wastewater sample was adjusted to pH 4.0 with H₂SO₄ and NaOH, spiked with 100 ng/L ¹³C₁₂-triclosan as an isotopic surrogate, and sub-divided into replicate 250 or 500 mL samples. For each group of replicate samples, a corresponding single sample was also spiked with 100 ng/L ¹³C₁₂-triclosan, as well as 500 ng/L un-labeled triclosan and 50 ng/L 4-Cl-TCS, 6-Cl-TCS and 4,6-Cl-TCS. By subtracting the determined mean analyte concentration for the un-spiked replicates from the determined concentration for the spiked sample and dividing by the nominal spiked concentration, the analyte recoveries were calculated to verify the method accuracy. After spiking, the samples were sonicated for 10 min, manually inverted 20 times for mixing, and stored at room temperature in the dark overnight to allow for analyte equilibration with the wastewater matrix. For each group of replicate samples, a method blank was prepared by adjusting ultrapure water to pH 4.0 with H₂SO₄/NaOH to test for analyte contamination during sample processing and analysis.

SPE and silica column cleanup. SPE was carried out according to a modified version of the method described by Vanderford and Snyder.⁸ Waters Oasis HLB 6 cc/200 mg cartridges were used on a Restek 12-port vacuum manifold. The cartridges were pre-conditioned with sequential 5 mL aliquots of MTBE, methanol, and water. The transfer lines between the sample reservoirs and cartridges were rinsed sequentially with ~ 10 mL MTBE, methanol, and water prior to each use. Wastewater samples were loaded onto the cartridges and run under vacuum at ~ 15 mL/min. The volume of each sample was determined as the difference in mass of the sample vessel before and after the extraction. After the samples were run, the cartridges were then washed with three

consecutive 5 mL aliquots of 50:50 methanol:water (v/v), dried under vacuum for 25 min, and eluted into graduated glass centrifuge tubes with 5 mL of methanol followed by 5 mL of 90:10 MTBE:methanol (v/v). If the extracts were not further processed by silica column cleanup, they were concentrated under nitrogen and solvent exchanged into a final volume of ~ 100 μ L of 50:50 acetonitrile:water (v/v). The SPE extracts that underwent silica column cleanup were concentrated under nitrogen to < 500 μ L and quantitatively loaded onto silica columns prepared and run as described above. The ethyl acetate eluants were concentrated under nitrogen and solvent exchanged into 50:50 acetonitrile:water (v/v). The cleaned up effluent samples were concentrated to a final volume of ~ 30-40 μ L, and the influent samples were concentrated to ~ 100 μ L.

LC-MS-Q³ analysis. Analysis of processed samples was carried out using a Waters NanoAcquity UPLC equipped with a Finnigan TSQ Quantum Ultra MS-Q³ detector or an Agilent 1100 series capillary HPLC equipped with a Finnigan TSQ Quantum Discovery MAX MS-Q³ detector. With either LC-MS-Q³ system, sample injections of 8 μ L were made onto a Phenomenex Synergi MAX-RP column (150 \times 0.5 mm, 4 μ m, 80 Å) using a binary gradient of 15 mM ammonium acetate buffer (A) and acetonitrile (B) at a constant flow rate of 10 μ L/min. The gradient began at 50% B, ramped up linearly to 100% B at 20 min, ramped linearly down to 50 % B at 23 min, and held at 50% B until 35 min to allow for re-equilibration. The LC effluent was diverted to waste during the first 10 min and last 10 min of the run when analytes were not eluting to prevent contamination of the ionization source. The analytes were ionized using negative mode electrospray ionization (ESI), due to the ease with which their phenolic moieties de-protonated.

A fragmentation experiment was conducted for triclosan to determine its most intense product ion in order to use single reaction monitoring (SRM) for the analysis to reduce noise and improve sensitivity. A solution of 290 µg/L triclosan solution in 80:20 water:acetonitrile (v/v) was directly infused into the ESI source and its precursor ion, $[M - H]^+$ (m/z 287), was selected by the first quadrupole. The collision energy of the second quadrupole was varied while a full scan was obtained with the third quadrupole to identify the major product ions. Chloride ion ($^{35}\text{Cl}^-$; m/z 35) was the dominant product ion at an optimal collision voltage of 12 V, and thus, the 287 to 35 SRM transition was selected for quantification. Due to the structural similarity of the CTD analytes to triclosan, the same collision voltage and analogous precursor ion to chloride SRM transition were used for quantification of each CTD. For identity confirmation, a second SRM transition from the isotopomer 2 mass units above quantification precursor ion to $^{37}\text{Cl}^-$ (m/z 37) was also monitored for each analyte. The specific SRM transitions selected are listed in Table 4.1.

Table 4.1. Single reaction monitoring transitions for analyte quantification and identity confirmation.

Analyte	Precursor ion m/z	Product ion m/z	Purpose
Triclosan	287	35	quantification
	289	37	confirmation
4-Cl-TCS	321	35	quantification
	323	37	confirmation
6-Cl-TCS	321	35	quantification
	323	37	confirmation
4,6-Cl-TCS	355	35	quantification
	357	37	confirmation
$^{13}\text{C}_{12}$ -triclosan	299	35	quantification

ESI-MS-Q³ parameters were set as follows: spray voltage 3,500 V, nitrogen sheath gas pressure 40, capillary temperature 250 °C, capillary offset -35 V, argon collision gas

pressure 1.0 mTorr, tube lens 140 V, dwell time 150 ms per SRM transition. Prior to each analysis, the ESI⁻ source and mass spectrometer were tuned by directly infusing a solution of ~ 2 mg/L of ¹³C₁₂-triclosan in 50:50 acetonitrile:water (v/v).

Calibration, limit of quantification, and quality control. Calibration standards were prepared in 50:50 acetonitrile:water (v/v) with varying triclosan and CTD concentrations (2.50 to 2,500 µg/L triclosan; 0.250 to 250 µg/L CTDs) and a constant concentration of ¹³C₁₂-triclosan internal standard (125 µg/L). Seven- or eight-point calibration curves were constructed by plotting the ratio of analyte signal to internal standard signal versus the analyte concentration. From the calibration curve for each analyte, a response factor was obtained from which the concentration of the analyte in the wastewater samples was determined by multiplying the response factor by the ratio of analyte signal to internal standard signal. The limit of quantification (LOQ) for each analyte was defined as the lowest calibration point that gave a signal-to-noise ratio > 10 within the wastewater matrix. Instrument blanks of 50:50 acetonitrile:water (v/v) were analyzed during LC-MS-Q³ runs, typically every 8-10 samples, to test for analyte carry-over between LC injections. The analytical signal for every sample was required to be > 10 times the signal in the method and instrument blanks. A 2.4 mg/L solution of ¹³C₁₂-triclosan was analyzed to determine whether it contained any trace impurity of unlabeled-triclosan. The absolute recovery of the spiked ¹³C₁₂-triclosan was calculated for every sample as the ratio of its peak area in the wastewater matrix compared to that in the standard, normalizing for the different spike levels and the concentration factor of the wastewater sample. While the effects of sample size and analyte concentration on absolute recovery were not investigated, the isotope dilution methodology should have

provided accurate results regardless of the absolute recoveries.

4.3 Results and Discussion

4.3.1 Preliminary matrix reduction experiments

Optimization of sample pH. By increasing the initial pH of the wastewater effluent from 3 to 5, the intensity of the yellow color of the SPE extracts was diminished, indicating a reduction of matrix DOM adsorption onto the SPE cartridge. There was no statistically significant decrease in the recovery of triclosan, 4-Cl-TCS, 6-Cl-TCS, or 4,6-Cl-TCS within one standard deviation with the increase in pH. A sample pH of 4.0 was chosen for the method to balance the reduction of DOM adsorption while keeping $\geq 99\%$ of each analyte in its neutral phenol form, as the lowest pK_a of the analytes is 5.9 for 4,6-Cl-TCS (Table 3.1).

Optimization of SPE cartridge wash step. By varying the solvent used to wash the SPE cartridges after running the wastewater sample and prior to drying and elution, it was found that an increase in the wash solution pH and methanol content greatly enhanced the 350 nm absorption of the wash solution (Table 4.2).

Table 4.2. Absorbance at 350 nm (\pm standard deviation, n=2) of SPE cartridge wash solutions and of the first 6.5 mL acetonitrile extract and triclosan % recovery (\pm standard deviation, n=2) in the SPE cartridge wash solutions and in the combined 13 mL acetonitrile extracts.

Wash solvent	Absorbance at 350 nm		Triclosan % recovery	
	Wash solution	Extract	Wash solution	Extract
pH 2 water	0.005 \pm 0.001	0.212 \pm 0.012	0	87 \pm 1
water	0.045 \pm 0.011	0.167 \pm 0.040	0	94 \pm 3
10:90 methanol:water	0.065 \pm 0.004	0.132 \pm 0.001	0	90 \pm 2
20:80 methanol:water	0.106 \pm 0.006	0.136 \pm 0.004	0	92 \pm 2
50:50 methanol:water	0.320 \pm 0.020	0.020 \pm 0.027	0	94 \pm 1

Inversely, the 350 nm absorbance of the first 6.5 mL acetonitrile extract decreased with an increase in wash solvent pH and methanol content (Table 4.2). These results indicate that matrix DOM is increasingly removed during the wash step with methanol addition to the wash solvent and is thus present in reduced amounts in the acetonitrile extract. It is likely that the addition of methanol aids in the dissolution of the more hydrophobic functional groups of the DOM. While the increase in methanol effectively removed DOM during the wash step, it was not found to elute the analytes, as no triclosan was detected in any of the wash solutions (Table 4.2). The measured triclosan % recoveries in the final acetonitrile extract also remained steady (Table 4.2). A 50:50 methanol:water (v/v) mixture was chosen as the wash solvent because it effectively removed matrix DOM without prematurely eluting the analytes.

Multiple wash steps with 5 mL of 50:50 methanol:water (v/v) were tested to determine the degree of DOM removal with further washing. Using the absorbance at 350 nm as a proxy for DOM, it was found that the most DOM was removed with the first 5 mL aliquot, with diminished removal with each additional aliquot (Table 4.3).

Table 4.3. Absorbance at 350 nm (\pm standard deviation, n=3) of sequential 5 mL 50:50 methanol:water (v/v) SPE cartridge washes.

Wash number	Absorbance at 350 nm
1	0.817 \pm 0.013
2	0.190 \pm 0.009
3	0.093 \pm 0.005
4	0.061 \pm 0.001

The additional wash steps were not found to decrease triclosan recovery. A total of three 5 mL washes with 50:50 methanol:water (v/v) was chosen for the cartridge wash step because it removed DOM with a high efficiency and did not prematurely elute

triclosan.

Silica column cleanup. The preliminary silica column cleanup recovery experiment showed that triclosan, 4-Cl-TCS, and 4,6-Cl-TCS were recovered at a high rate ($\geq 75\%$; Table 4.4) while the intensity of the brown color of the DOM was greatly reduced. Therefore, this cleanup step was implemented in the sample preparation of some of the wastewater samples.

Table 4.4. Silica column percent recoveries (\pm standard deviation, n=3) of triclosan, 4-Cl-TCS, and 4,6-Cl-TCS.

Analyte	% Recovery
triclosan	77 ± 7
4-Cl-TCS	76 ± 3
4,6-Cl-TCS	75 ± 3

4.3.2 Trace analytical method performance

The UPLC method effectively separated the analytes, providing satisfactory peak shape after the chromatograms were processed with 15-point Gaussian peak fitting, as seen in the sample chromatograms of a post-chlorination wastewater effluent extract shown in Figure 4.1. The mono-chlorinated isomers of triclosan, 6-Cl-TCS and 4-Cl-TCS, were monitored in the same chromatographic traces due to their identical precursor ion masses, and eluted at 14.7 and 15.3 min, respectively. An unknown compound in the matrix with the same SRM transitions eluted at 12.0 min.

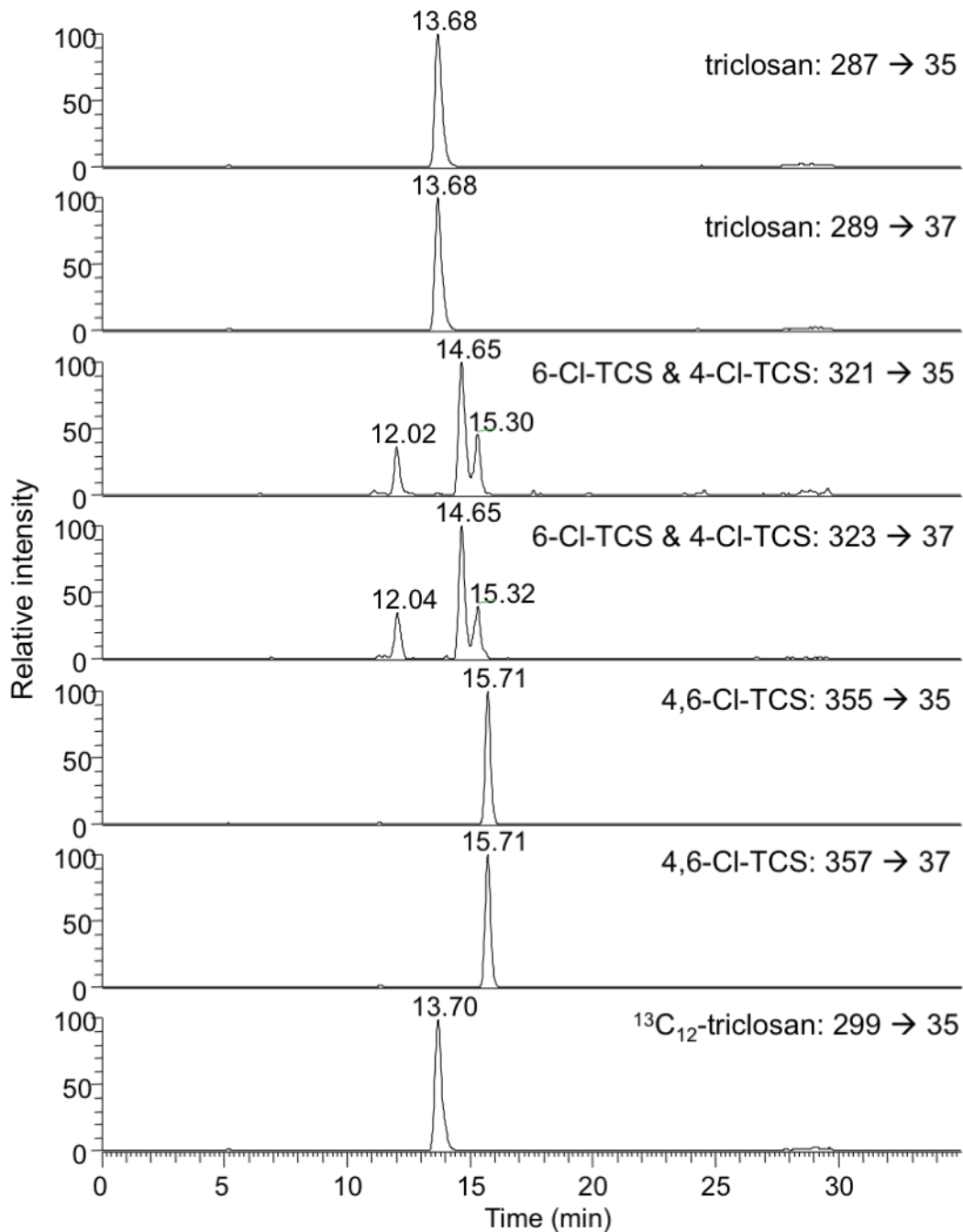


Figure 4.1. UPLC-MS-Q³ chromatograms of each single reaction monitoring transition of a post-chlorination effluent extract collected June 2, 2009. Retention times (min) are displayed above each peak. 6-Cl-TCS and 4-Cl-TCS eluted at 14.7 and 15.3 min, respectively, with an unknown matrix constituent eluting at 12.0 min in their chromatographic traces.

Calibration curves of the ratio of analyte signal to $^{13}\text{C}_{12}$ -triclosan signal versus analyte concentration generally resulted in a linear fit with an R^2 value of ≥ 0.99 . For each analyte, a LOQ of 2.5 ng/L was achieved. The analyte signals were below the LOQ for every instrument blank sample and most method blank samples. The analyte signals in every method blank sample were always $< 1\%$ of that for each quantified analyte. No unlabeled-triclosan or CTDs were detected in the $^{13}\text{C}_{12}$ -triclosan used in the analysis.

To compare the performance of 0.2 μm nylon filters versus 0.7 μm glass fiber filters, secondary influent and pre- and post-chlorination effluent samples collected on April 21, 2009 were filtered through both types of filter. Due to the heavy matrix of the secondary influent, the glass fiber filters were exchanged every $\sim 85\text{-}90$ mL to avoid substantial clogging. The matrix of the effluent samples was lighter and required exchange of the filters every ~ 750 mL. The finer 0.2 μm nylon filter required pre-filtration of the secondary influent with 0.7 μm glass fiber filters, or the sample would not pass through. For the effluent samples, the nylon filters were exchanged every ~ 200 to 250 mL, at which point the accumulating filter cake severely reduced the flow rate. After filtration, 250 mL subsamples were processed and analyzed according to the trace analytical procedure. Silica column cleanup was performed on the influent samples, but not on the effluent samples. Analyte concentrations determined from the 0.2 μm nylon filtered samples were much lower than those determined from the 0.7 μm glass fiber filtered samples (Table 4.5).

Table 4.5. Triclosan and CTD concentrations (\pm standard deviation) and % recoveries (\pm standard deviation) of $^{13}\text{C}_{12}$ -triclosan for wastewater samples collected on April 21, 2009 and June 2, 2009.

Sample Type	Collection Date	Original pH	Sample vol. (mL)	Filter type	Silica cleanup	Concentration \pm standard deviation (ng/L)				$^{13}\text{C}_{12}$ -triclosan % recovery
						triclosan	4-Cl-TCS	6-Cl-TCS	4,6-Cl-TCS	
Secondary influent (n=4)	4/21/09	7.57	250	0.2 μm nylon	Y	42 \pm 7	< LOQ	< LOQ	< LOQ	11 \pm 13
Pre-chlorination Effluent (n=4)	4/21/09	7.31	250	0.2 μm nylon	N	< LOQ	< LOQ	< LOQ	< LOQ	40 \pm 6
Post-chlorination Effluent (n=4)	4/21/09	7.51	250	0.2 μm nylon	N	< LOQ	< LOQ	< LOQ	< LOQ	43 \pm 4
Secondary Influent (n=2)	4/21/09	7.57	250	0.7 μm GF	Y	813 \pm 34	< LOQ	14 \pm 7	3 \pm 2	19 \pm 5
Pre-chlorination Effluent (n=2)	4/21/09	7.31	250	0.7 μm GF	N	128 \pm 7	< LOQ	< LOQ	< LOQ	25 \pm 1
Post-chlorination Effluent (n=2)	4/21/09	7.51	250	0.7 μm GF	N	49.9 \pm 0.1	< LOQ	< LOQ	< LOQ	28 \pm 2
Secondary influent (n=2)	6/2/09	7.57	250	0.7 μm GF	Y	2,840 \pm 20	8 \pm 3	24 \pm 1	14 \pm 15	20 \pm 3
Pre-chlorination effluent (n=4)	6/2/09	7.59	500	0.7 μm GF	Y	212 \pm 8	< LOQ	3 \pm 2	3 \pm 2	57 \pm 12
Post-chlorination effluent (n=3)	6/2/09	7.60	500	0.7 μm GF	Y	183 \pm 5	4 \pm 1	6 \pm 4	21 \pm 8	61 \pm 11

It is likely that the hydrophobic analytes adsorbed strongly to both the nylon filters and the layer of caked particulate matter that accumulated on the nylon filters. The glass fiber filters, on the other hand, are much less likely to adsorb hydrophobic compounds, while they also accumulated much less adsorptive particulate matter. The absolute recoveries of $^{13}\text{C}_{12}$ -triclosan, which was spiked in after filtration, were generally higher for the nylon filters compared to the glass fiber filters (Table 4.5). This was likely due to a higher removal rate of matrix DOM by the nylon filters that resulted in less ionization suppression during the mass spectrometry analysis.

4.3.3 Occurrence of triclosan and CTDs in wastewater

Using glass fiber filtration, along with larger sample volumes (500 mL) and silica column cleanup for the pre- and post-chlorination effluent, greater concentration factors and absolute recoveries were obtained, providing signals above the detection limit for most analytes in all three types of wastewater collected on June 2, 2009 (Table 4.5). The silica column cleanup step for the effluent samples improved the recovery by a factor of approximately two compared to the effluent samples collected on April 21, 2009 that were processed with glass fiber filtration but did not undergo silica column cleanup. This improved recovery is attributed to a decrease in ion suppression due to the removal of interfering DOM by the silica cleanup. The reduction of matrix DOM also allowed the final extracts to be concentrated to ~ 30 to $40 \mu\text{L}$ instead of $\sim 100 \mu\text{L}$ like previously processed samples. The smaller volume of the final extract coupled with the doubled sample size provided a 6-fold increase in concentration factor.

The results for the wastewater samples collected on June 2, 2009 revealed a high

level of triclosan (2,840 ng/L) in the secondary influent, consistent with concentrations reported by other researchers.^{1, 3-6, 8} CTDs were also quantified in the secondary influent at much lower levels (8 to 24 ng/L), suggesting that triclosan was chlorinated by residual chlorine in tap water during transport to the water treatment plant. This scenario is consistent with the results of McAvoy et al.,¹ who also detected similar CTDs levels in various wastewater influents. Triclosan was eliminated from the wastewater stream by 93% between the secondary influent and the pre-chlorination effluent, in line with removal rates previously observed for other secondary treatment facilities.¹⁻⁷ The CTDs were also removed at a high rate, as would be expected by their increased hydrophobicity relative to triclosan, and hence, higher capacity to sorb to sludge during the biological treatment stage.

While the aforementioned results were previously observed by other researchers, this is the first study that has quantified the levels of triclosan and its chlorinated derivatives before and after the chlorine disinfection step. The results from the samples collected on June 2, 2009 show that triclosan was degraded to a small degree (14%) during chlorination, while the level of all three chlorinated derivatives substantially increased, from a total of 6 to 31 ng/L (Table 4.5). While 29 ng/L triclosan was removed during the disinfection stage, a total of 25 ng/L of CTDs was generated. On a molar basis, the CTDs contributed 72% to the product mass balance, revealing 4-Cl-TCS, 6-Cl-TCS, and 4,6-Cl-TCS as the major chlorination products of triclosan.

This work shows that the chlorination of triclosan may play a significant role in its environmental impact. While CTDs were detected in the influent, likely formed by the reaction of triclosan with residual chlorine in tap water in transport to the treatment

plant, they were eliminated at a high rate. The CTDs present in the final effluent are therefore predominantly the products of triclosan from chlorine disinfection. The level of CTDs formed during chlorine disinfection relative to the levels of triclosan in the final effluent are of concern because the toxicity of their dioxin photoproducts is estimated to be 10 times higher than the toxicity of 2,8-DCDD, the photoproduct of triclosan.²² The formation of CTDs from triclosan during chlorine disinfection of nitrified wastewater, therefore, must be considered in the evaluation of the environmental impact of triclosan.

Chapter 5:

Historical Record of Dioxin Photoproducts of Triclosan and its Chlorinated Derivatives in Riverine Sediment Cores

5.1 Introduction

The use of triclosan, a topical antimicrobial, has increased dramatically over the last half century as it has been incorporated into a growing number of products, resulting in widespread contamination of surface waters throughout the world.¹⁻⁴ Triclosan was first patented in 1964⁵ and added to medical supplies, soaps, shampoos, and deodorants. In the U.S., it was added to liquid hand soap in 1987, and in 2001, 76% of commercial liquid hand soap contained triclosan.⁶ In 1997, the U.S. Food and Drug Administration approved triclosan for use in toothpaste.⁷ Triclosan also has been embedded in plastics as Microban[®] for use in athletic clothing, children's toys, and other products. As 96% of the uses of triclosan are in consumer products disposed of in residential drains,⁸ large loads are routinely measured in wastewater treatment plant influents.⁹⁻¹¹ Despite typical removal efficiencies of greater than 90% by conventional activated sludge wastewater treatment, triclosan has been detected frequently in wastewater effluents and wastewater-impacted waterways.^{3, 9-11} In a national reconnaissance, the U.S. Geological Survey detected triclosan in 58% of sampled urban- and agriculturally-impacted waterways throughout the U.S. at a median concentration of 0.14 µg/L.¹ Evidence for increased triclosan use since the 1960s was captured in the upward-trending vertical concentration profile of triclosan in a sediment core from Lake Greifensee in Switzerland.²

The presence of triclosan in surface waters is of concern because it is known to undergo solar photochemical transformation in water to form a chlorinated dioxin, 2,8-dichlorodibenzo-*p*-dioxin (2,8-DCDD).¹²⁻¹⁴ Photolysis has been shown to be a major elimination process for triclosan in aquatic environments, contributing to 80% of its loss

in a small, eutrophic Swiss lake.¹⁵ In addition to photolysis, triclosan may also be transformed by chlorination at the *ortho*- and *para*- positions of its phenol ring to form three chlorinated triclosan derivatives (CTDs), 4,5-dichloro-2-(2,4-dichlorophenoxy)phenol (4-Cl-TCS), 5,6-dichloro-2-(2,4-dichlorophenoxy)phenol (6-Cl-TCS), and 4,5,6-trichloro-2-(2,4-dichlorophenoxy)phenol (4,6-Cl-TCS), upon exposure to sodium hypochlorite, the common wastewater and drinking water disinfectant (Scheme 3.1).^{16, 17} The CTDs have been detected in wastewater influent, effluent, and as their bio-transformed methylated analogues in water from a wastewater treatment plant drainage outlet and in carp in its receiving bay.^{9, 18} CTDs are likely formed by the reaction of triclosan with residual chlorine in tap water in transport to wastewater treatment facilities, and as shown in Chapter 4 of this thesis, during final chlorine disinfection of wastewater. Analogous to triclosan, 4-Cl-TCS, 6-Cl-TCS, and 4,6-Cl-TCS photolyze to form 2,3,7-TCDD, 1,2,8-TCDD, and 1,2,3,8-TeCDD, respectively, under solar irradiation in water as shown in Chapter 3 of this thesis (Scheme 3.1).¹² These dioxin products are of greater concern than 2,8-DCDD formed directly from triclosan, because dioxin toxicity increases with chlorine substitution in the lateral positions,¹⁹ and two of the three CTD dioxin photoproducts are substituted in three of the four possible lateral positions.

Based on the results of these studies, we hypothesized that the chlorination and subsequent photolysis of triclosan will generate a distinct pattern of four triclosan-derived dioxin congeners in aquatic environments at concentrations that reflect the increase in triclosan use over the last fifty years. To investigate this hypothesis, two sediment cores were collected from a depositional zone of the Mississippi River

downstream of several wastewater treatment plant outfalls. The cores were sectioned, dated, and analyzed for triclosan, its purported dioxin photoproducts, and a suite of polychlorodibenzo-*p*-dioxin and polychlorodibenzofuran (PCDD/F) homologues.

5.2 Experimental

5.2.1 Chemicals

Triclosan (5-chloro-2-(2,4-dichlorophenoxy)phenol; 97%) was purchased from Sigma Aldrich. A methanolic solution of $^{13}\text{C}_{12}$ -triclosan (> 99% chemical purity; $\geq 99\%$ isotopic purity) was obtained from Wellington Laboratories. Sulfuric acid (H_2SO_4) and sodium hydroxide (NaOH) were obtained from Mallinckrodt. Ultrapure water (18.2 M Ω) was obtained from a Millipore Simplicity UV purification system. All solvents used were of chromatography grade, except for methyl *t*-butyl ether (MTBE), which was obtained from Sigma-Aldrich at 99+% purity.

5.2.2 Sediment core collection

To assess the historical inputs of triclosan and potentially triclosan-derived dioxins into an aquatic system, two sediment cores were obtained from Lake Pepin (Minnesota, USA) in June, 2008. Due to their hydrophobicity, triclosan and dioxins were expected to associate with particles and deposit in sediment. Lake Pepin is a 34 km-long depositional zone of the Mississippi River 35 km downstream from the Metropolitan Wastewater Treatment Plant that serves the Minneapolis/St. Paul metropolitan area and discharges its wastewater to the Mississippi River (Figure 5.1).

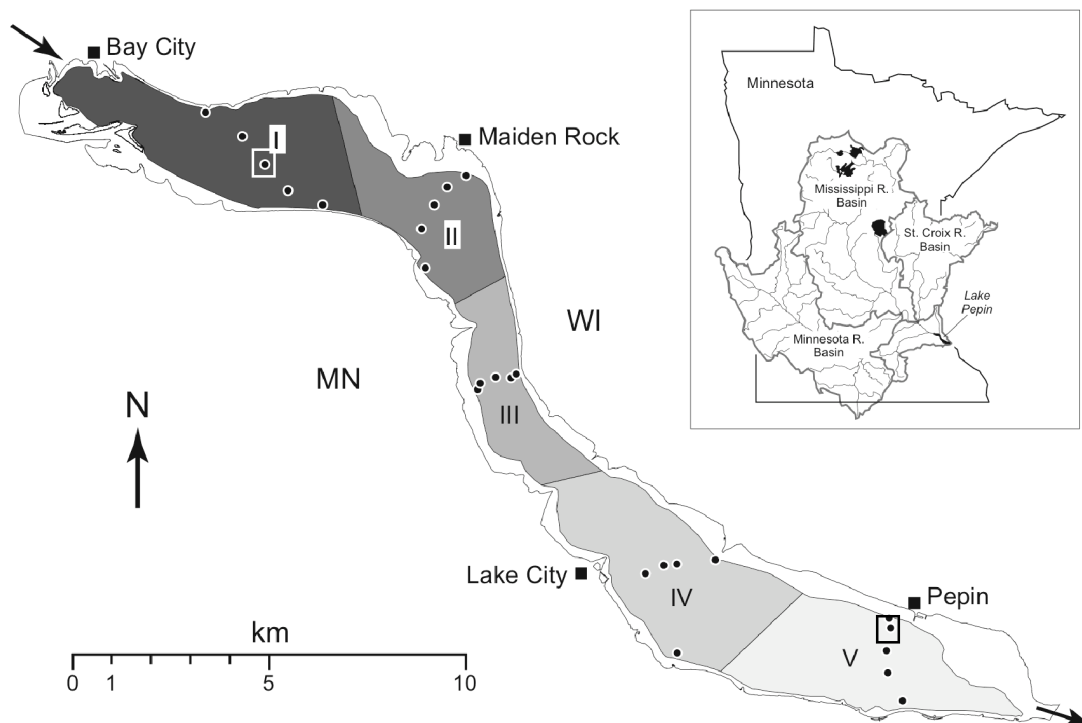


Figure 5.1. Map of Lake Pepin and its placement within Minnesota watersheds (inset). Sediment cores were collected at I.3 and V.4 (boxed).

Several other smaller wastewater treatment plants also discharge their effluent upstream of Lake Pepin. Lake Pepin has a watershed population of 4.2 million.²⁰ The first core (I.3; 80 cm depth) was collected 6 km from the inflow of Lake Pepin (44°33'18.391"N, 92°22'56.082"W) and was dated by magnetic susceptibility to 1986. The second core (V.4; 76 cm depth) was collected 4 km from its outflow (44°26'04.267"N, 92°09'30.685"W) and dated to 1940. Core I.3 was sectioned into 10 slices of 4 to 10 cm depth, and core V.4 was divided into 9 slices of 8 to 10 cm depth. Each section was homogenized and the moisture content was determined gravimetrically after drying a subsample in an oven at 110 °C until constant weight was achieved.

5.2.3 *Triclosan analysis*

Wet samples with a mass corresponding to approximately 10 g dry weight (based on the measured moisture content) from each core section were spiked with 500 ng of $^{13}\text{C}_{12}$ -triclosan as an isotope dilution internal standard for the analysis of triclosan. A single un-spiked blank sample of clean sand was processed and analyzed to ensure that there was no triclosan contamination. The samples were Soxhlet extracted into methanol. The extracts were concentrated to ~ 5 mL and centrifuged for 10 min at 5,000 rev/min to remove particulate matter. The supernatant was then transferred to a new vial by gas-tight syringe and its exact volume was recorded. From each supernatant, 1.00 mL was dissolved in 25 mL of pH 4 water adjusted with $\text{H}_2\text{SO}_4/\text{NaOH}$ via sonication for 10 min. These solutions were then solid-phase extracted according to a modified version of the method described by Vanderford and Snyder.²¹ Waters Oasis HLB 6 cc/200 mg cartridges were used on a Restek 12-port vacuum manifold. The cartridges were pre-conditioned with sequential 5 mL aliquots of MTBE, methanol, and water, and the samples were loaded and run under vacuum at ~ 2 mL/min. After the samples were run, the cartridges were washed with three consecutive 5 mL aliquots of 50:50 methanol:water (v/v), dried under vacuum for 25 min, and eluted into graduated glass centrifuge tubes with 5 mL of methanol followed by 5 mL of 90:10 MTBE:methanol (v/v). The SPE extracts were concentrated under nitrogen to < 500 μL and quantitatively loaded onto silica columns conditioned with ethyl acetate for further cleanup. Silica columns were prepared by packing 6 cc disposable syringes with a plug of glass wool, a thin layer of sand, 2.00 g of silica gel (Sorbent Technologies Premium Rf, 60 Å, 40-75 μm or Sorbent Technologies Standard

grade, 60 Å, 32-63 µm) in a slurry of ethyl acetate, and a thin upper layer of sand. The columns were eluted by gravity with 10 mL of ethyl acetate. The eluants were concentrated under nitrogen and solvent exchanged to a final volume of ~ 100 µL in 50:50 acetonitrile:water (v/v).

Calibration standards were prepared in 50:50 acetonitrile:water (v/v) with triclosan concentrations ranging from 2.50 to 2,500 µg/L and a constant concentration of ¹³C₁₂-triclosan internal standard (125 µg/L). An eight-point calibration curve was constructed by plotting the ratio of analyte signal to internal standard signal versus the analyte concentration. From the calibration curve, a response factor was obtained from which the triclosan concentration in the sediment samples was determined by multiplying the response factor by the ratio of analyte signal to internal standard signal.

Triclosan analysis of processed samples and calibration standards was carried out using a Waters NanoAcquity ultra performance liquid chromatograph (UPLC) equipped with a Finnigan TSQ Quantum Ultra triple quadrupole mass spectrometer (MS-Q³). Sample injections of 8 µL were made onto a Phenomenex Synergi MAX-RP column (150 × 0.5 mm, 4 µm, 80 Å) using a binary gradient of 15 mM ammonium acetate buffer (A) and acetonitrile (B) at a constant flow rate of 10 µL/min. The gradient began at 50% B, ramped up linearly to 100% B at 20 min, ramped linearly down to 50 % B at 23 min, and held at 50% B until 35 min to allow for re-equilibration. The LC effluent was diverted to waste during the first 10 min and last 10 min of the run when triclosan was not eluting to prevent contamination of the ionization source. Negative mode electrospray ionization (ESI) was used, due to the ease with which the phenolic moiety of triclosan de-protonated. Single reaction monitoring (SRM) of the

precursor ion (m/z 287) to chloride ($^{35}\text{Cl}^-$; m/z 35) transition was carried out for triclosan quantification at a collision voltage of 12 V. For identity confirmation, a second SRM transition from 289 to $^{37}\text{Cl}^-$ (m/z 37) was also monitored. The SRM transition from 299 to $^{35}\text{Cl}^-$ (m/z 35) was used for the quantification of the isotope dilution standard, $^{13}\text{C}_{12}$ -triclosan. ESI-MS-Q³ parameters were set as follows: spray voltage 3,500 V, nitrogen sheath gas pressure 40, capillary temperature 250 °C, capillary offset -35 V, argon collision gas pressure 1.0 mTorr, tube lens 140 V, dwell time 150 ms per SRM transition.

5.2.4 Dioxin and furan analysis

An approximately 10 g dry weight sample of each homogenized core section was spiked with nineteen $^{13}\text{C}_{12}$ -labeled di- through octa-CDD/F isomers as isotope dilution internal standards and analyzed following a version of U.S. EPA Method 1613B,²² expanded to analyze for di- and tri-CDD/Fs, as outlined below. Method blank and laboratory spike samples were prepared with the extraction batch to demonstrate freedom from laboratory contamination and to provide precision and accuracy information for the analysis. Each sample was extracted with toluene for 16-18 hours using a Soxhlet/Dean Stark apparatus. The extracts were spiked with $^{37}\text{Cl}_4$ -2,3,7,8-TeCDD as a cleanup standard, concentrated, and washed by shaking with concentrated sulfuric acid. Each extract was then eluted through a multi-layer silica column (2 grams neutral silica, 4 grams acidic silica, and 2 grams basic silica) with hexane. Each eluate was added to a 4 gram activated aluminum oxide column (Ecochrom Super 1) and eluted with 60:40 dichloromethane:hexane (v/v). Each eluate was then solvent

exchanged into hexane and added to a column containing approximately 0.5 gram of 18% activated carbon on Celite. Potentially interfering compounds were washed through each column in the forward direction and then the analytes were eluted off the column with 20 mL of toluene in the reverse direction. The toluene was then concentrated, spiked with $^{13}\text{C}_{12}$ -labeled PCDD/F recovery standards, and concentrated to a final volume of 40 μL .

In addition to the U.S. EPA Method 1613 calibration set, a secondary calibration standard set was prepared from individual di- and tri-CDD/Fs at the same levels as the tetra-chlorinated standards from the Method 1613 calibration set. Aliquots of these two calibration standard sets were combined to prepare a five-point calibration set containing di- through octa-CDD/Fs at concentrations ranging from 0.25 to 1000 $\text{pg}/\mu\text{L}$.

High-resolution gas chromatography-mass spectrometry (HRGC-MS) analysis was performed on a Waters Autospec Ultima high resolution mass spectrometer operated in selected ion recording mode (positive electron impact, > 10,000 resolution, 32 eV, 280°C). The acquisition windows were set to include all tetra- through octa-CDD/F isomers and selected di- and tri-CDD/F isomers. The concentrations reported for the total di- and tri-CDD/F homologues, therefore, should be considered as estimates because some di- and tri-CDD/F isomers may have eluted outside the acquisition windows. Selected sample extracts, however, were analyzed using expanded acquisition windows, and it was verified that other non-target di- and tri-CDD/F isomers were not present at significant levels.

5.3 Results and Discussion

5.3.1 Analytical method performance

For the triclosan analysis, a trace amount of triclosan was detected in the method blank sample, below the reporting limit. The triclosan signal for every sediment sample was at least 10 times greater than the triclosan signal in the method blank, and in most cases, several orders of magnitude greater. Due to the heavy matrix and high amount of ion suppression in the mass spectrometry analysis, low absolute recoveries of $^{13}\text{C}_{12}$ -triclosan were obtained ($13 \pm 8\%$, $n=17$). However, the isotope dilution method should have corrected for this loss. Higher and more precise recoveries could be obtained by further sample cleanup to reduce ion suppression by matrix constituents.

For the dioxin and furan analysis, the absolute recoveries of the isotopically-labeled PCDD/F internal standards in the sample extracts ranged from 23-114%. All of the labeled standard recoveries obtained were within the target ranges specified in U.S. EPA Method 1613. Because the quantification of the native analytes was based on isotope dilution methodology, the data were automatically corrected for variation in recovery. Laboratory samples fortified with native standards exhibited relative recoveries of 92-123% with a relative percent difference of 1.0 to 12.0% ($n=2$) after isotope dilution-correction, confirming the accuracy and precision of the method. No di- through tetra-CDD/F isomers were detected in the laboratory method blank. Some penta- through octa-CDD/F isomers were detected in the blank at levels well below the calibration range. Every reported concentration is at least 10 times higher than the level detected in the blank.

5.3.2 Dioxin concentrations and temporal trends

The concentration profile of 2,8-DCDD, the known photoproduct of triclosan, revealed a substantial increase from 1940-2008 in sediment core V.4 (Figure 5.2 A), corresponding with an increase in triclosan level over the same period (Figure 5.2 B).

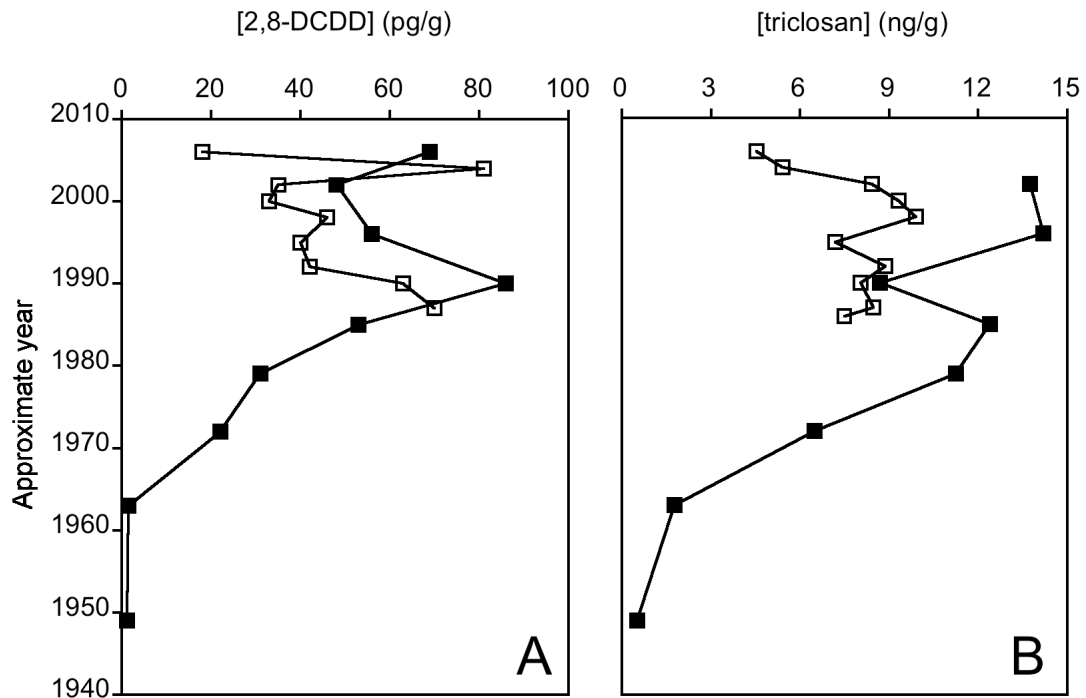


Figure 5.2. Concentration profiles of 2,8-DCDD (A) and triclosan (B) for core I.3 (open squares) and V.4 (closed squares). Approximate dates represent the mid-point of each core.

Similar levels of 2,8-DCDD and triclosan were also observed for core I.3, though no major temporal trend was observed, as this core did not date back as far as V.4. Concentrations of 2,3,7-TCDD, 1,2,8-TCDD, and 1,2,3,8-TeCDD, the known photoproducts of the chlorinated derivatives of triclosan, also increased over time in core V.4 with similar levels in I.3 (Figure 5.3).

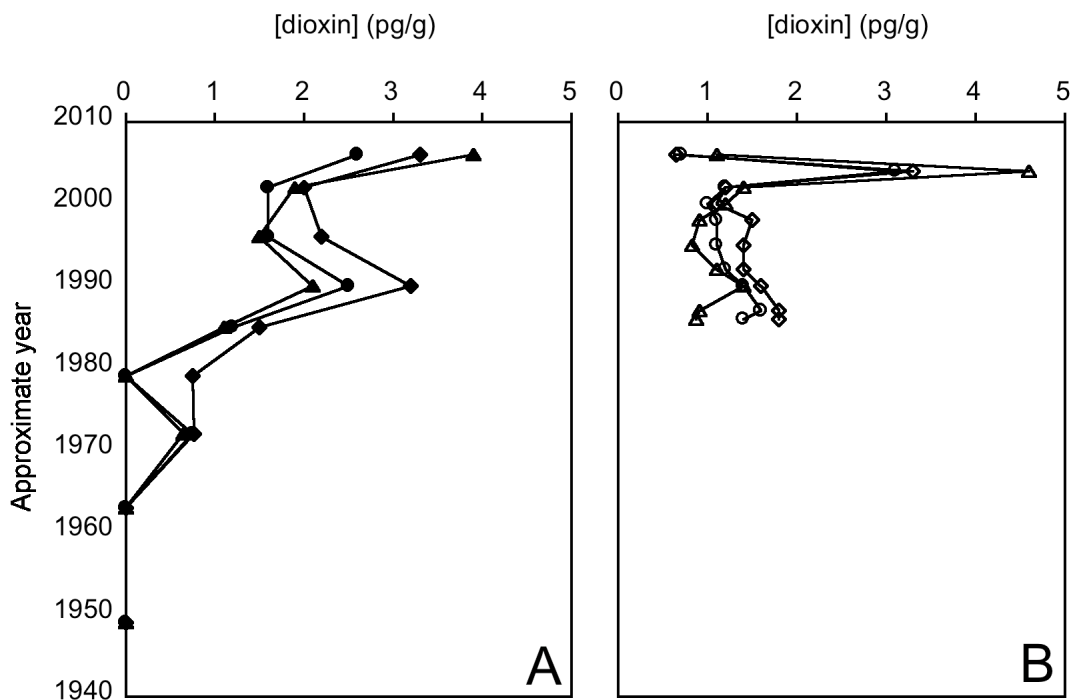


Figure 5.3. Concentration profiles of 2,3,7-TCDD (diamonds), 1,2,8-TCDD (circles), and 1,2,3,8-TeCDD (triangles) for core V.4 (A) and I.3 (B). Approximate dates represent the mid-point of each core.

Prior to advent of triclosan use in the mid-1960s, the 2,8-DCDD, 2,3,7-TCDD, 1,2,8-TCDD, and 1,2,3,8-TeCDD congeners were detected at very low levels, if at all, but were found at increasing levels in more recently deposited sediment, consistent with increased triclosan use. In core V.4, a peak in the concentration of these congeners was observed in the section dated from 1988-1993 followed by a dip in the 1990s. This dip was observed for all dioxin and furan homologues, and thus, is unlikely to reflect specific source or loss processes of these specific congeners. In core I.3, a peak in the concentrations of these congeners was observed in the section dated from 2003-2005 followed by a large decrease in the subsequent section. Again, this same pattern was observed for each dioxin and furan homologue, and likely does not reflect specific source or loss processes.

In all sections of cores I.3 and V.4, 2,8-DCDD comprised at least 90% of the sum of the concentration of all DCDD congeners (Σ [DCDD]), and in most core sections, 2,8-DCDD was the only DCDD congener detected. Likewise, 2,3,7-TCDD and 1,2,8-TCDD together made up at least 90% of Σ [TCDD], and in most sections were the only TCDD congeners detected. 1,2,3,8-TeCDD was not detected in the deepest core sections of V.4, but comprised an increasing fraction of Σ [TeCDD], reaching 37% and 35% of Σ [TeCDD] in the uppermost sections of core I.3 and V.4, respectively. The ratio of Σ [(2,3,7-TCDD), (1,2,8-TCDD), (1,2,3,8-TeCDD)]:[2,8-DCDD] in core sections of I.3 and V.4 ranged from 0.02-0.14. This ratio is comparable to the ratio of their putative photochemical precursors, Σ [chlorinated triclosans]:[triclosan], observed in several previous analyses of wastewater treatment plant effluents (0.01, 0.16, 0.07)⁹, measured in the effluent of the major plant that discharges into the Mississippi River upstream of Lake Pepin (0.17) (Table 4.5), and found as methylated analogues in carp of a wastewater treatment plant drainage outlet (0.03).¹⁸

Two contrasting temporal trend types were observed for PCDD/F concentrations in sediment core V.4. The first was best represented by 2,8-DCDD and was characterized by extremely low levels in the earliest core sections and an increase until a peak in the 1988-1993 section. This trend was shared by only three other dioxin congeners: 2,3,7-TCDD, 1,2,8-TCDD, and 1,2,3,8-TeCDD. Their concentrations profiles positively correlated with 2,8-DCDD with R^2 values of 0.93, 0.85, and 0.64, respectively (Figure 5.4 A).

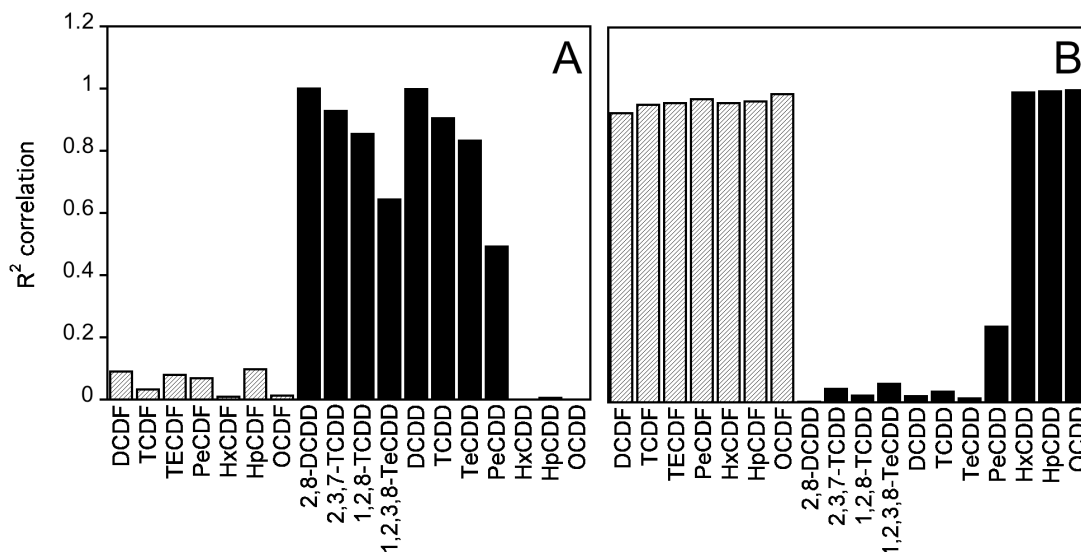


Figure 5.4. R^2 values of linear correlations for various dioxin congeners and dioxin and furan homologues with 2,8-DCDD (A) and OCDD (B).

The second trend type was exemplified by OCDD, the most abundant dioxin congener in all V.4 sections, and was characterized by a dramatic increase from 1940 until a peak in the early 1970s, followed by a decline over the subsequent decades while the 2,8-DCDD profile was increasing. This trend type was shared by the hexa-, and hepta-CDD homologues, and all PCDF homologues (positive linear correlations with R^2 values ≥ 0.93 ; Figure 5.4 B). The PeCDD homologue did not correlate well with either the 2,8-DCDD profile ($R^2 = 0.49$) or the OCDD profile ($R^2 = 0.24$). There was no correlation between the putative triclosan-derived dioxin congeners with the OCDD trend type ($R^2 \leq 0.06$).

5.3.3 Source of 2,8-DCDD, 2,3,7-TCDD, 1,2,8-TCDD, and 1,2,3,8-TeCDD

The two disparate trend profiles observed in sediment core V.4 indicate a distinct source for 2,8-DCDD, 2,3,7-TCDD, 1,2,8-TCDD, and 1,2,3,8-TeCDD from the other PCDD/F homologues, likely the photochemical transformation of triclosan and its

chlorinated derivatives. The OCDD trend profile discussed above is characteristic of PCDD/F atmospheric deposition in industrialized areas of the U.S. and Europe predominantly from incineration sources.²³ It usually coincides with PCDD/F homologue patterns dominated by PCDDs, especially the most-highly chlorinated homologues.²³ An example of this homologue pattern is presented in Figure 5.5 from the core V.4 section dated from 1957 to 1968. Excluding the triclosan-derived dioxin contribution, this homologue pattern was observed in all core I.3 and V.4 sections.

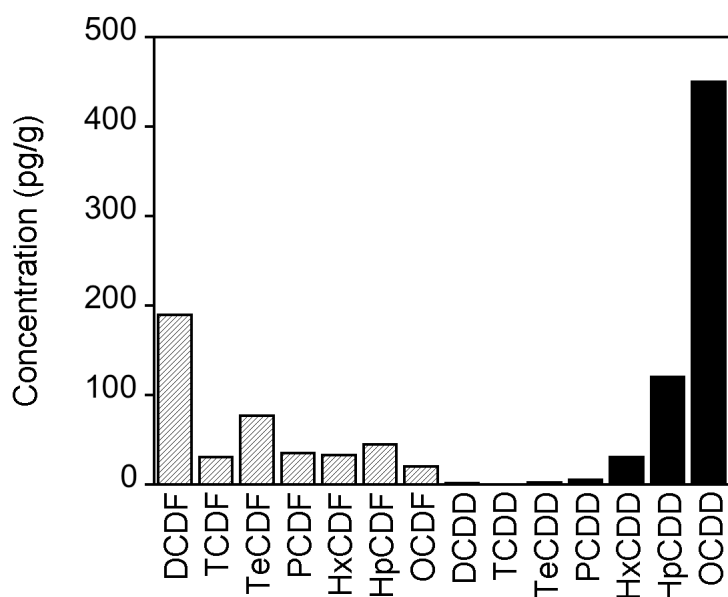


Figure 5.5. PCDF and PCDD homologue profiles from a core V.4 section (1957-1968).

In contrast to the more highly-chlorinated dioxins, 2,8-DCDD, 2,3,7-TCDD, 1,2,8-TCDD, and 1,2,3,8-TeCDD appear to originate from triclosan, as their temporal trend profiles match historical triclosan use. Furthermore, their identity, relative distribution, and predominance among di-, tri-, and tetra-CDD homologues are fully consistent with the transformation of triclosan by chlorine disinfection and the subsequent photochemical transformation of triclosan and its chlorinated derivatives. Greene et al.²³ observed a 4-fold increase in di-CDDs since 1955 in Esthwaite Water, a small

English lake, suggested to be the result of microbial de-chlorination of higher-chlorinated dioxins. While specific DCDD congeners were not quantified, it is quite possible that an increase in 2,8-DCDD photochemically produced from triclosan explains this result, as the lake receives treated domestic sewage.

In assigning photochemistry of triclosan and its chlorinated derivatives as the source of 2,8-DCDD, 2,3,7-TCDD, 1,2,8-TCDD, and 1,2,3,8-TeCDD in Lake Pepin, it is important to account for other potential sources of these specific congeners. An alternative source for these congeners that also derives from triclosan could be their presence as trace impurities in formulations of triclosan used in consumer products. 2,8-DCDD has been detected in triclosan formulations at concentrations on the order of 10 ng/g, along with other di- and tri-CDD/Fs at the ng/g level,²⁴ and several 2,3,7,8-substituted dioxin congeners at the low pg/g level.^{25, 26} Triclosan was detected along with an un-specified DCDD congener and several other structurally similar products attributed to the synthesis of triclosan in the wastewater of a specialty chemicals manufacturing plant and its receiving river, though the DCDD was not quantified.^{27, 28} In the present case, it is unlikely that any PCDD impurities in triclosan formulations would persist through activated sludge wastewater treatment to accumulate at detectable levels in Lake Pepin. Triclosan is generally removed by greater than 90% during activated sludge wastewater treatment largely via sorption to sludge due to its hydrophobicity ($\log K_{ow} = 4.2$),^{10, 29} even though a significant percentage may be in the more hydrophilic ionized form. PCDD/Fs, which do not ionize in aqueous solution, are much more hydrophobic ($\log K_{ow}$ values ranging from 5 to 8)³⁰ and are likely to be completely removed via sorption. Furthermore, it is unlikely that 2,8-DCDD, 2,3,7-

TCDD, 1,2,8-TCDD, and 1,2,3,8-TeCDD, the predominant di- and tri-CDDs detected in Lake Pepin, would represent the only PCDD/F synthetic impurities of triclosan.

A different potential source of these specific di- and tri-CDD congeners, not derived from triclosan, is the anaerobic biological reduction of higher chlorinated dioxins within the sediment.²³ This source is unlikely for Lake Pepin because the levels of 2,8-DCDD, 2,3,7-TCDD, 1,2,8-TCDD, and 1,2,3,8-TeCDD were lowest in the older core sections that had the highest levels of the potential higher-chlorinated precursors and the longest exposure time for anaerobic bio-transformation. Conversely, the levels of these di- and tri-chlorinated congeners were highest in more recent core sections that had lower levels of higher-chlorinated dioxins and less time available for bio-transformation. Furthermore, the bio-reduction of higher-chlorinated dioxins would be expected to yield a broader suite of di- and tri-chlorinated congeners than the three predominantly detected in this study. Considering the potential sources of 2,8-DCDD, 2,3,7-TCDD, 1,2,8-TCDD, and 1,2,3,8-TeCDD in Lake Pepin, it appears that the photolysis of triclosan and its chlorinated derivatives is the most likely.

5.3.4 Contribution of triclosan-derived dioxins to total dioxin toxicity

The levels of triclosan-derived dioxins observed in Lake Pepin show that the photochemical reactions of triclosan and its chlorinated derivatives contribute a substantial amount of mass to the total PCDD pool. As the level of triclosan-derived dioxins has increased over time while the level of higher-chlorinated dioxins has decreased, the mass contribution of triclosan-derived dioxins rose as high as 29% of the total dioxin pool in core I.3 and 31% in core V.4 (Figure 5.6).

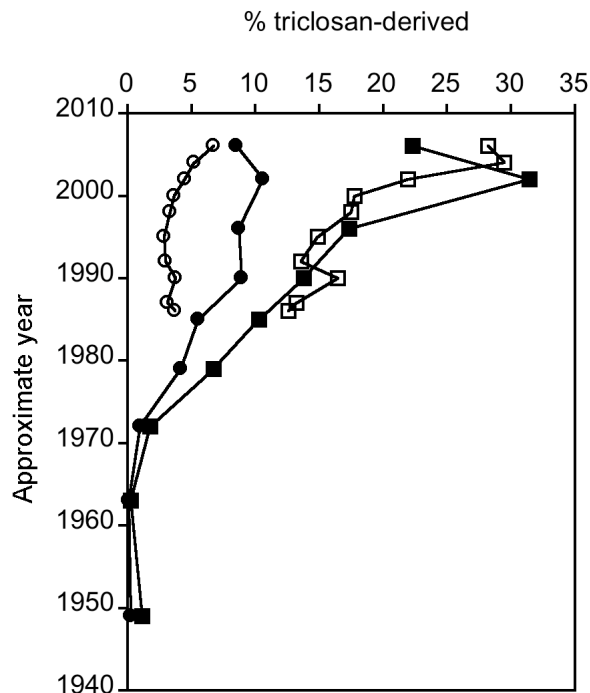


Figure 5.6. Percent contribution of triclosan-derived dioxins to the total dioxin pool in terms of mass (squares) and toxic equivalents (circles) for core I.3 (open symbols) and V.4 (closed symbols). Approximate dates represent the mid-point of each core.

To estimate the contribution of triclosan-derived dioxins to the total dioxin toxicity for Lake Pepin, the toxicity equivalence factors listed in Table 5.1 were applied.

Table 5.1. Toxicity equivalence factors for various dioxin congeners and homologues relative to 2,3,7,8-TeCDD.

Dioxin congener/homologue	Toxicity equivalence factor
DCDD	0.001 ³¹
TCDD	0.01 ³¹
2,3,7,8-TeCDD	1 ³²
other TeCDDs	0.01 ³¹
1,2,3,7,8-PeCDD	1 ³²
other PeCDDs	0.1 ³¹
HxCDD	0.1 ³¹
HpCDD	0.01 ³¹
OCDD	0.0001 ³¹

The factors normalize the toxicity of specific dioxin congeners and homologues to the toxicity of the most toxic congener, 2,3,7,8-TeCDD in units of toxic equivalents

(TEQs). The values in Table 5.1 represent a worst-case scenario, as more recent estimations of TEQ have deemed the toxicity of DCDDs or TCDDs to be negligible compared 2,3,7,8-TeCDD.³² The contribution of triclosan-derived dioxin toxicity to the total dioxin pool rose as high as 7% for core I.3 and 11% for core V.4 (Figure 5.6). The chlorination of triclosan appeared to play a significant role in increasing the toxic impact of triclosan-derived dioxins. While the concentrations of 2,3,7-TCDD, 1,2,8-TCDD, and 1,2,3,8-TeCDD, which are photochemically formed from chlorinated derivatives of triclosan, were much lower than that of 2,8-DCDD, which forms photochemically from triclosan, the total TEQ contribution of 2,3,7-TCDD, 1,2,8-TCDD, and 1,2,3,8-TeCDD was on approximately the same level as that of 2,8-DCDD for core I.3, and ranged as high as 5 times greater for core V.4. These results support the conclusions of Chapters 3 and 4 of this thesis that triclosan chlorination during wastewater disinfection and subsequent photolysis may contribute substantially to dioxin toxicity level in aquatic environments.

Chapter 1 References

1. Daughton, C. G.; Ternes, T. A., Pharmaceuticals and personal care products in the environment: Agents of subtle change? *Environ. Health Perspect.* **1999**, *107* (6), 907-938.
2. Halling-Sorensen, B.; Nors Nielsen, S.; Lanzky, P. F.; Ingerslev, F.; Holten Luthoft, H. C.; Jorgensen, S. E., Occurrence, fate and effects of pharmaceutical substances in the environment--A review. *Chemosphere* **1998**, *36* (2), 357-393.
3. Jones, O. A. H.; Voulvoulis, N.; Lester, J. N., Human pharmaceuticals in the aquatic environment a review. *Environ. Technol.* **2001**, *22* (12), 1383-1394.
4. Khetan, S. K.; Collins, T. J., Human pharmaceuticals in the aquatic environment: A challenge to green chemistry. *Chem. Rev.* **2007**, *107* (6), 2319-2364.
5. Kolpin, D. W.; Furlong, E. T.; Meyer, M. T.; Thurman, E. M.; Zaugg, S. D.; Barber, L. B.; Buxton, H. T., Pharmaceuticals, hormones, and other organic wastewater contaminants in U.S. streams, 1999-2000: A national reconnaissance. *Environ. Sci. Technol.* **2002**, *36* (6), 1202-1211.
6. Buser, H. R.; Muller, M. D.; Theobald, N., Occurrence of the pharmaceutical drug clofibric acid and the herbicide mecoprop in various swiss lakes and in the North Sea. *Environ. Sci. Technol.* **1998**, *32* (1), 188-192.
7. Ying, G.-G.; Kookana, R. S.; Ru, Y.-J., Occurrence and fate of hormone steroids in the environment. *Environ. Int.* **2002**, *28* (6), 545-551.
8. Glassmeyer, S. T.; Furlong, E. T.; Kolpin, D. W.; Cahill, J. D.; Zaugg, S. D.; Werner, S. L.; Meyer, M. T.; Kryak, D. D., Transport of chemical and microbial compounds from known wastewater discharges: Potential for use as indicators of human fecal contamination. *Environ. Sci. Technol.* **2005**, *39* (14), 5157-5169.
9. Managaki, S.; Murata, A.; Takada, H.; Tuyen, B. C.; Chiem, N. H., Distribution of macrolides, sulfonamides, and trimethoprim in tropical waters: Ubiquitous occurrence of veterinary antibiotics in the Mekong Delta. *Environ. Sci. Technol.* **2007**, *41* (23), 8004-8010.
10. Ternes, T. A., Occurrence of drugs in German sewage treatment plants and rivers. *Water Res.* **1998**, *32* (11), 3245-3260.
11. Stumpf, M.; Ternes, T. A.; Wilken, R.-D.; Silvana Vianna, R.; Baumann, W., Polar drug residues in sewage and natural waters in the state of Rio de Janeiro, Brazil. *Sci. Total Environ.* **1999**, *225* (1-2), 135-141.

12. Heberer, T., Occurrence, fate, and removal of pharmaceutical residues in the aquatic environment: A review of recent research data. *Toxicol. Lett.* **2002**, *131* (1-2), 5-17.
13. Singer, H.; Mueller, S.; Tixier, C.; Pillonel, L., Triclosan: occurrence and fate of a widely used biocide in the aquatic environment: Field measurements in wastewater treatment plants, surface waters, and lake sediments. *Environ. Sci. Technol.* **2002**, *36* (23), 4998-5004.
14. Miller, T. R.; Heidler, J.; Chillrud, S. N.; DeLaquil, A.; Ritchie, J. C.; Mihalic, J. N.; Bopp, R.; Halden, R. U., Fate of triclosan and evidence for reductive dechlorination of triclocarban in estuarine sediments. *Environ. Sci. Technol.* **2008**, *42* (12), 4570-4576.
15. Miao, X.-S.; Yang, J.-J.; Metcalfe, C. D., Carbamazepine and its metabolites in wastewater and in biosolids in a municipal wastewater treatment plant. *Environ. Sci. Technol.* **2005**, *39* (19), 7469-7475.
16. Castiglioni, S.; Bagnati, R.; Fanelli, R.; Pomati, F.; Calamari, D.; Zuccato, E., Removal of pharmaceuticals in sewage treatment plants in Italy. *Environ. Sci. Technol.* **2006**, *40* (1), 357-363.
17. McAvoy, D. C.; Schatowitz, B.; Jacob, M.; Hauk, A.; Eckhoff, W. S., Measurement of triclosan in wastewater treatment systems. *Environ. Toxicol. Chem.* **2002**, *21* (7), 1323-1329.
18. Soulet, B.; Tauxe, A.; Tarradellas, J., Analysis of acidic drugs in Swiss wastewaters. *Int. J. Environ. Anal. Chem.* **2002**, *82* (10), 659-667.
19. Androozzi, R.; Raffaele, M.; Nicklas, P., Pharmaceuticals in STP effluents and their solar photodegradation in aquatic environment. *Chemosphere* **2003**, *50* (10), 1319-1330.
20. Chenxi, W.; Spongberg, A. L.; Witter, J. D., Determination of the persistence of pharmaceuticals in biosolids using liquid-chromatography tandem mass spectrometry. *Chemosphere* **2008**, *73* (4), 511-518.
21. Stoob, K.; Singer, H. P.; Mueller, S. R.; Schwarzenbach, R. P.; Stamm, C. H., Dissipation and transport of veterinary sulfonamide antibiotics after manure application to grassland in a small catchment. *Environ. Sci. Technol.* **2007**, *41* (21), 7349-7355.
22. Hirsch, R.; Ternes, T.; Haberer, K.; Kratz, K.-L., Occurrence of antibiotics in the aquatic environment. *Sci. Total Environ.* **1999**, *225* (1-2), 109-118.
23. Kidd, K. A.; Blanchfield, P. J.; Mills, K. H.; Palace, V. P.; Evans, R. E.; Lazorchak, J. M.; Flick, R. W., Collapse of a fish population after exposure to a synthetic estrogen. *Proc. Natl. Acad. Sci.* **2007**, *104* (21), 8897-8901.

24. Vajda, A. M.; Barber, L. B.; Gray, J. L.; Lopez, E. M.; Woodling, J. D.; Norris, D. O., Reproductive disruption in fish downstream from an estrogenic wastewater effluent. *Environ. Sci. Technol.* **2008**, *42* (9), 3407-3414.
25. Thorpe, K. L.; Maack, G.; Benstead, R.; Tyler, C. R., Estrogenic wastewater treatment works effluents reduce egg production in fish. *Environ. Sci. Technol.* **2009**, *43* (8), 2976-2982.
26. Donn, J.; Mendoza, M.; Pritchard, J., AP: Drugs found in drinking water. *USA Today* [Online], **2008**. http://www.usatoday.com/news/nation/2008-03-10-drugs-tap-water_N.htm (accessed 7/8/09).
27. Adams, C.; Wang, Y.; Loftin, K.; Meyer, M., Removal of antibiotics from surface and distilled water in conventional water treatment processes. *J. Environ. Eng.* **2002**, *128* (3), 253-260.
28. Stackelberg, P. E.; Furlong, E. T.; Meyer, M. T.; Zaugg, S. D.; Henderson, A. K.; Reissman, D. B., Persistence of pharmaceutical compounds and other organic wastewater contaminants in a conventional drinking-water-treatment plant. *Sci. Total Environ.* **2004**, *329* (1-3), 99-113.
29. Westerhoff, P.; Yoon, Y.; Snyder, S.; Wert, E., Fate of endocrine-disruptor, pharmaceutical, and personal care product chemicals during simulated drinking water treatment processes. *Environ. Sci. Technol.* **2005**, *39* (17), 6649-6663.
30. Baird, C., The Purification of Polluted Water. *Environmental Chemistry*. 2nd ed.; W. H. Freeman and Company: New York, 1999.
31. Pinkston, K. E.; Sedlak, D. L., Transformation of aromatic ether- and amine-containing pharmaceuticals during chlorine disinfection. *Environ. Sci. Technol.* **2004**, *38* (14), 4019-4025.
32. Stumm, W.; Morgan, J. J., Kinetics of Redox Processes. *Aquatic Chemistry: Chemical Equilibria and Rates in Natural Waters*. 3rd ed.; John Wiley & Sons, Inc.: New York, 1996.
33. Gallard, H.; von Gunten, U., Chlorination of phenols: kinetics and formation of chloroform. *Environ. Sci. Technol.* **2002**, *36* (5), 884-890.
34. Rebenne, L. M.; Gonzalez, A. C.; Olson, T. M., Aqueous chlorination kinetics and mechanism of substituted dihydroxybenzenes. *Environ. Sci. Technol.* **1996**, *30* (7), 2235-2242.
35. Rule, K. L.; Ebbett, V. R.; Vikesland, P. J., Formation of chloroform and chlorinated organics by free-chlorine-mediated oxidation of triclosan. *Environ. Sci. Technol.* **2005**, *39* (9), 3176-3185.

36. Dodd, M. C.; Huang, C.-H., Transformation of the antibacterial agent sulfamethoxazole in reactions with chlorine: Kinetics, mechanisms, and pathways. *Environ. Sci. Technol.* **2004**, *38* (21), 5607-5615.
37. Greyshock, A. E.; Vikesland, P. J., Triclosan reactivity in chloraminated waters. *Environ. Sci. Technol.* **2006**, *40* (8), 2615-2622.
38. Bedner, M.; MacCrehan, W. A., Reactions of the amine-containing drugs fluoxetine and metoprolol during chlorination and dechlorination processes used in wastewater treatment. *Chemosphere* **2006**, *65* (11), 2130-2137.
39. DellaGreca, M.; Iesce, M. R.; Pistillo, P.; Previtera, L.; Temussi, F., Unusual products of the aqueous chlorination of atenolol. *Chemosphere* **2009**, *74* (5), 730-734.
40. Shah, A. D.; Kim, J.-H.; Huang, C.-H., Reaction kinetics and transformation of carbadox and structurally related compounds with aqueous chlorine. *Environ. Sci. Technol.* **2006**, *40* (23), 7228-7235.
41. Dodd, M. C.; Shah, A. D.; Von Gunten, U.; Huang, C.-H., Interactions of fluoroquinolone antibacterial agents with aqueous chlorine: Reaction kinetics, mechanisms, and transformation pathways. *Environ. Sci. Technol.* **2005**, *39* (18), 7065-7076.
42. Glassmeyer, S. T.; Shoemaker, J. A., Effects of chlorination on the persistence of pharmaceuticals in the environment. *Bull. Environ. Contam. Toxicol.* **2005**, *74* (1), 24-31.
43. Bedner, M.; MacCrehan, W. A., Transformation of acetaminophen by chlorination produces the toxicants 1,4-benzoquinone and N-acetyl-*p*-benzoquinone imine. *Environ. Sci. Technol.* **2006**, *40* (2), 516-522.
44. Hu, J.-y.; Aizawa, T.; Ookubo, S., Products of aqueous chlorination of bisphenol A and their estrogenic activity. *Environ. Sci. Technol.* **2002**, *36* (9), 1980-1987.
45. Gueymard, C. A., *SMARTS, A Simple Model of the Atmospheric Radiative Transfer of Sunshine: Algorithms and Performance Assessment*; Professional Paper FSEC-PF-270-95; Florida Solar Energy Center: Cocoa, FL, 1995.
46. Gueymard, C. A., Parameterized transmittance model for direct beam and circumsolar spectral irradiance. *Solar Energy* **2001**, *71* (5), 325-346.
47. Latch, D. E.; Stender, B. L.; Packer, J. L.; Arnold, W. A.; McNeill, K., Photochemical fate of pharmaceuticals in the environment: cimetidine and ranitidine. *Environ. Sci. Technol.* **2003**, *37* (15), 3342-3350.
48. Werner, J. J.; McNeill, K.; Arnold, W. A., Environmental photodegradation of mefenamic acid. *Chemosphere* **2005**, *58* (10), 1339-1346.

49. Werner, J. J.; Arnold, W. A.; McNeill, K., Water hardness as a photochemical parameter: tetracycline photolysis as a function of calcium concentration, magnesium concentration, and pH. *Environ. Sci. Technol.* **2006**, *40* (23), 7236-7241.
50. Boreen, A. L.; Arnold, W. A.; McNeill, K., Photodegradation of pharmaceuticals in the aquatic environment: a review. *Aquat. Sci.* **2003**, *65* (4), 320-341.
51. Boreen, A. L.; Arnold, W. A.; McNeill, K., Triplet-sensitized photodegradation of sulfa drugs containing six-membered heterocyclic groups: Identification of an SO₂ extrusion photoproduct. *Environ. Sci. Technol.* **2005**, *39* (10), 3630-3638.
52. Tixier, C.; Singer Heinz, P.; Canonica, S.; Muller Stephan, R., Phototransformation of ticlosan in surface waters: A relevant elimination process for this widely used biocide--laboratory studies, field measurements, and modeling. *Environ. Sci. Technol.* **2002**, *36* (16), 3482-9.
53. Edhlund, B. L.; Arnold, W. A.; McNeill, K., Aquatic photochemistry of nitrofurantoin antibiotics. *Environ. Sci. Technol.* **2006**, *40* (17), 5422-5427.
54. Packer, J. L.; Werner, J. J.; Latch, D. E.; McNeill, K.; Arnold, W. A., Photochemical fate of pharmaceuticals in the environment: naproxen, diclofenac, clofibric acid, and ibuprofen. *Aquat. Sci.* **2003**, *65* (4), 342-351.
55. DellaGreca, M.; Iesce, M. R.; Isidori, M.; Montanaro, S.; Previtera, L.; Rubino, M., Phototransformation of amlodipine in aqueous solution: Toxicity of the drug and its photoproduct on aquatic organisms. *Int. J. Photoenergy* **2007**, *2*, 63459/1-63459/6.
56. Jiao, S.; Zheng, S.; Yin, D.; Wang, L.; Chen, L., Aqueous photolysis of tetracycline and toxicity of photolytic products to luminescent bacteria. *Chemosphere* **2008**, *73* (3), 377-382.
57. Leiker, T. J.; Abney, S. R.; Goodbred, S. L.; Rosen, M. R., Identification of methyl triclosan and halogenated analogues in male common carp (*Cyprinus carpio*) from Las Vegas Bay and semipermeable membrane devices from Las Vegas Wash, Nevada. *Sci. Total Environ.* **2009**, *407* (6), 2102-2114.
58. Richardson, S. D., Water Analysis: Emerging contaminants and current issues. *Anal. Chem.* **2009**, *81* (12), 4645-4677.
59. Petrovic, M.; Barcelo, D., Application of liquid chromatography/quadrupole time-of-flight mass spectrometry (LC-QqTOF-MS) in the environmental analysis. *J. Mass Spectrom.* **2006**, *41* (10), 1259-1267.
60. Vanderford, B. J.; Snyder, S. A., Analysis of pharmaceuticals in water by isotope dilution liquid chromatography/tandem mass spectrometry. *Environ. Sci. Technol.* **2006**, *40* (23), 7312-7320.

Chapter 2 References

1. Daughton, C. G.; Ternes, T. A., Pharmaceuticals and personal care products in the environment: Agents of subtle change? *Environ. Health Perspect.* **1999**, *107* (6), 907-938.
2. Halling-Sorensen, B.; Nielsen, S. N.; Lanzky, P. F.; Ingerslev, F.; Lutzht, H. C. H.; Jorgensen, S. E., Occurrence, fate and effects of pharmaceutical substances in the environment - A review. *Chemosphere* **1997**, *36* (2), 357-393.
3. Heberer, T., Occurrence, fate, and removal of pharmaceutical residues in the aquatic environment: A review of recent research data. *Toxicol. Lett.* **2002**, *131* (1-2), 5-17.
4. Soulet, B.; Tauxe, A.; Tarradellas, J., Analysis of acidic drugs in swiss wastewaters. *Int. J. Environ. Anal. Chem.* **2002**, *82* (10), 659-667.
5. Andreozzi, R.; Raffaele, M.; Nicklas, P., Pharmaceuticals in STP effluents and their solar photodegradation in aquatic environment. *Chemosphere* **2003**, *50* (10), 1319-1330.
6. Kolpin, D. W.; Furlong, E. T.; Meyer, M. T.; Thurman, E. M.; Zaugg, S. D.; Barber, L. B.; Buxton, H. T., Pharmaceuticals, hormones, and other organic wastewater contaminants in U.S. streams, 1999-2000: A national reconnaissance. *Environ. Sci. Technol.* **2002**, *36* (6), 1202-1211.
7. Ternes, T. A., Occurrence of drugs in German sewage treatment plants and rivers. *Water Res.* **1998**, *32* (11), 3245-3260.
8. Stumpf, M.; Ternes, T. A.; Wilken, R.-D.; Silvana Vianna, R.; Baumann, W., Polar drug residues in sewage and natural waters in the state of Rio de Janeiro, Brazil. *Sci. Total Environ.* **1999**, *225* (1-2), 135-141.
9. Dodd, M. C.; Huang, C.-H., Transformation of the antibacterial agent sulfamethoxazole in reactions with chlorine: Kinetics, mechanisms, and pathways. *Environ. Sci. Technol.* **2004**, *38* (21), 5607-5615.
10. Dodd, M. C.; Shah, A. D.; Von Gunten, U.; Huang, C.-H., Interactions of fluoroquinolone antibacterial agents with aqueous chlorine: Reaction kinetics, mechanisms, and transformation pathways. *Environ. Sci. Technol.* **2005**, *39* (18), 7065-7076.
11. Rule, K. L.; Ebbett, V. R.; Vikesland, P. J., Formation of chloroform and chlorinated organics by free-chlorine-mediated oxidation of triclosan. *Environ. Sci. Technol.* **2005**, *39* (9), 3176-3185.

12. Glassmeyer, S. T.; Shoemaker, J. A., Effects of chlorination on the persistence of pharmaceuticals in the environment. *Bull. Environ. Contam. Toxicol.* **2005**, *74* (1), 24-31.
13. Bedner, M.; MacCrehan, W. A., Transformation of acetaminophen by chlorination produces the toxicants 1,4-benzoquinone and N-acetyl-*p*-benzoquinone imine. *Environ. Sci. Technol.* **2006**, *40* (2), 516-522.
14. Shah, A. D.; Kim, J.-H.; Huang, C.-H., Reaction kinetics and transformation of carbadox and structurally related compounds with aqueous chlorine. *Environ. Sci. Technol.* **2006**, *40* (23), 7228-7235.
15. Bedner, M.; MacCrehan, W. A., Reactions of the amine-containing drugs fluoxetine and metoprolol during chlorination and dechlorination processes used in wastewater treatment. *Chemosphere* **2006**, *65* (11), 2130-2137.
16. Pinkston, K. E.; Sedlak, D. L., Transformation of aromatic ether- and amine-containing pharmaceuticals during chlorine disinfection. *Environ. Sci. Technol.* **2004**, *38* (14), 4019-4025.
17. Hu, J.-y.; Aizawa, T.; Ookubo, S., Products of aqueous chlorination of bisphenol A and their estrogenic activity. *Environ. Sci. Technol.* **2002**, *36* (9), 1980-1987.
18. Anderson, P. D.; D'Aco, V. J.; Shanahan, P.; Chapra, S. C.; Buzby, M. E.; Cunningham, V. L.; DuPlessie, B. M.; Hayes, E. P.; Mastrocco, F. J.; Parke, N. J.; Rader, J. C.; Samuelian, J. H.; Schwab, B. W., Screening analysis of human pharmaceutical compounds in U.S. surface Wwaters. *Environ. Sci. Technol.* **2004**, *38* (3), 838-849.
19. Cash, G. G.; Nabholz, J. V., *Ecosar, v0.99g*. US Environmental Protection Agency: Washington, DC, 2001.
20. 4500-Cl B. Iodometric Method 1. *Standard Methods for the Examination of Water and Wastewater*. 2nd ed.; American Public Health Association, American Water Works Association, Water Environmental Federation: Washington, D.C., 1998.
21. Kuzel, R. A.; Bhasin, S. K.; Oldham, H. G.; Damani, L. A.; Murphy, J.; Camilleri, P.; Hutt, A. J., Investigations into the chirality of the metabolic sulfoxidation of cimetidine. *Chirality* **1994**, *6* (8), 607-614.
22. Aiken, G.; Kaplan, L. A.; Weishaar, J., Assessment of relative accuracy in the determination of organic matter concentrations in aquatic systems. *J. Environ. Monit.* **2002**, *4* (1), 70-74.

23. Gerhardt, P. M., R. G. E.; Wood, W. A.; Krieg, R. R., *Methods for General and Molecular Bacteriology*. American Society of Microbiology: Washington, D.C., 1994; pp 541-542.
24. U.S. Environmental Protection agency. Ecological Structure Activity Relationships. <http://www.epa.gov/oppintr/newchems/tools/21ecosar.htm> (accessed July 2007).
25. Jones, O. A. H.; Voulvoulis, N.; Lester, J. N., Aquatic environmental assessment of the top 25 English prescription pharmaceuticals. *Water Res.* **2002**, *36* (20), 5013-5022.
26. Lopez, A.; Mascolo, G.; Tiravanti, G.; Passino, R., Degradation of herbicides (ametryn and isoproturon) during water disinfection by means of two oxidants (hypochlorite and chlorine dioxide). *Water Sci. Technol.* **1997**, *35* (4), 129-136.
27. Kodama, S.; Yamamoto, A.; Matsunaga, A., S-Oxygenation of thiobencarb in tap water processed by chlorination. *J. Agric. Food. Chem.* **1997**, *45* (3), 990-994.
28. Gallard, H.; von Gunten, U., Chlorination of phenols: kinetics and formation of chloroform. *Environ. Sci. Technol.* **2002**, *36* (5), 884-890.
29. Rebenne, L. M.; Gonzalez, A. C.; Olson, T. M., Aqueous chlorination kinetics and mechanism of substituted dihydroxybenzenes. *Environ. Sci. Technol.* **1996**, *30* (7), 2235-2242.
30. Castela-Papin, N.; Cai, S.; Vatie, J.; Keller, F.; Souleau, C. H.; Farinotti, R., Drug interactions with diosmectite: a study using the artificial stomach-duodenum model. *Int. J. Pharm.* **1999**, *182* (1), 111-119.
31. Cinquini, M.; Colonna, S.; Landini, D., Kinetics of α -chlorination of sulfoxides by iodobenzene dichloride. *J. Chem. Soc., Perkin Trans. 2* **1972**, (3), 296-300.
32. Klein, J.; Stollar, H., Stereochemistry of chlorination of thiane 1-oxides. *J. Am. Chem. Soc.* **1973**, *95* (22), 7437-7444.
33. Schwan, A. L.; Strickler, R. R.; Dunn-Dufault, R.; Brillon, D., Oxidative fragmentations of 2-(trimethylsilyl)ethyl sulfoxides - routes to alkane-, arene-, and highly substituted 1-alkenesulfinyl chlorides. *Eur. J. Org. Chem.* **2001**, (9), 1643-1654.
34. Murai, T.; Saeki, T.; Satou, S.; Miura, S.; Takashige, T.; Ikeda, Y.; Kano, N. Process for synthesizing 4-halo-5-(hydroxymethyl)imidazole compounds and certain novel 4-halo-5-(hydroxymethyl) imidazole compounds. *Eur. Pat. Appl.* 611758, Aug. 24, 1994.

35. Miller, R., A.; Hoerrner, R. S., Iodine as a chemoselective reoxidant of TEMPO: application to the oxidation of alcohols to aldehydes and ketones. *Org. Lett.* **2003**, *5* (3), 285-287.
36. Sarkanen, K. V.; Dence, C. W., Reactions of *p*-hydroxybenzyl alcohol derivatives and their methyl ethers with molecular chlorine. *J. Org. Chem.* **1960**, *25*, 715-720.

-

Chapter 3 References

1. Daughton, C. G.; Ternes, T. A., Pharmaceuticals and personal care products in the environment: Agents of subtle change? *Environ. Health Perspect.* **1999**, *107* (6), 907-938.
2. Halling-Sorensen, B.; Nors Nielsen, S.; Lanzky, P. F.; Ingerslev, F.; Holten Lutzhoft, H. C.; Jorgensen, S. E., Occurrence, fate and effects of pharmaceutical substances in the environment--A review. *Chemosphere* **1998**, *36* (2), 357-393.
3. Kolpin, D. W.; Furlong, E. T.; Meyer, M. T.; Thurman, E. M.; Zaugg, S. D.; Barber, L. B.; Buxton, H. T., Pharmaceuticals, hormones, and other organic wastewater contaminants in U.S. streams, 1999-2000: A national reconnaissance. *Environ. Sci. Technol.* **2002**, *36* (6), 1202-1211.
4. Bedner, M.; MacCrehan, W. A., Transformation of acetaminophen by chlorination produces the toxicants 1,4-benzoquinone and N-acetyl-*p*-benzoquinone imine. *Environ. Sci. Technol.* **2006**, *40* (2), 516-522.
5. Hu, J.-y.; Aizawa, T.; Ookubo, S., Products of aqueous chlorination of bisphenol A and their estrogenic activity. *Environ. Sci. Technol.* **2002**, *36* (9), 1980-1987.
6. Latch, D. E.; Packer, J. L.; Arnold, W. A.; McNeill, K., Photochemical conversion of triclosan to 2,8-dichlorodibenzo-*p*-dioxin in aqueous solution. *J. Photochem. Photobiol., A* **2003**, *158* (1), 63-66.
7. Jiao, S.; Zheng, S.; Yin, D.; Wang, L.; Chen, L., Aqueous photolysis of tetracycline and toxicity of photolytic products to luminescent bacteria. *Chemosphere* **2008**, *73* (3), 377-382.
8. Onodera, S.; Ogawa, M.; Suzuki, S., Chemical changes of organic compounds in chlorinated water. XIII. Gas chromatographic-mass spectrometric studies of the reactions of Irgasan DP 300 [5-chloro-2-(2,4-dichlorophenoxy)phenol] with chlorine in dilute aqueous solution. *J. Chromatogr.* **1987**, *392*, 267-275.
9. Rule, K. L.; Ebbett, V. R.; Vikesland, P. J., Formation of chloroform and chlorinated organics by free-chlorine-mediated oxidation of triclosan. *Environ. Sci. Technol.* **2005**, *39* (9), 3176-3185.
10. Canosa, P.; Morales, S.; Rodriguez, I.; Rubi, E.; Cela, R.; Gomez, M., Aquatic degradation of triclosan and formation of toxic chlorophenols in presence of low concentrations of free chlorine. *Anal. Bioanal. Chem.* **2005**, *383* (7-8), 1119-1126.
11. McAvoy, D. C.; Schatowitz, B.; Jacob, M.; Hauk, A.; Eckhoff, W. S., Measurement of triclosan in wastewater treatment systems. *Environ. Toxicol. Chem.* **2002**, *21* (7), 1323-1329.

12. Leiker, T. J.; Abney, S. R.; Goodbred, S. L.; Rosen, M. R., Identification of methyl triclosan and halogenated analogues in male common carp (*Cyprinus carpio*) from Las Vegas Bay and semipermeable membrane devices from Las Vegas Wash, Nevada. *Sci. Total Environ.* **2009**, *407* (6), 2102-2114.
13. Tixier, C.; Singer Heinz, P.; Canonica, S.; Muller Stephan, R., Phototransformation of ticlosan in surface waters: a relevant elimination process for this widely used biocide--laboratory studies, field measurements, and modeling. *Environ. Sci. Technol.* **2002**, *36* (16), 3482-3489.
14. Nilsson, C.-A.; Andersson, K.; Rappe, C.; Westermark, S.-O., Chromatographic evidence for the formation of chlorodioxins from chloro-2-phenoxyphenols. *J. Chromatogr. A* **1974**, *96* (1), 137-147.
15. Freeman, P. K.; Srinivasa, R., Photochemistry of polyhaloarenes. 4. Phototransformations of perchloro-*o*-phenoxyphenol in basic media. *J. Org. Chem.* **1986**, *51* (21), 3939-3942.
16. Kanetoshi, A.; Ogawa, H.; Katsura, E.; Kaneshima, H.; Miura, T., Study on the environmental hygienic chemistry of chlorinated 2-hydroxydiphenyl ethers: photolytic conversion to polychlorinated dibenzo-*p*-dioxins. *Kankyo Kagaku* **1992**, *2* (3), 515-522.
17. Mezcua, M.; Gomez, M. J.; Ferrer, I.; Aguera, A.; Hernando, M. D.; Fernandez-Alba, A. R., Evidence of 2,7/2,8-dibenzodichloro-*p*-dioxin as a photodegradation product of triclosan in water and wastewater samples. *Anal. Chim. Acta* **2004**, *524* (1-2), 241-247.
18. Aranami, K.; Readman, J. W., Photolytic degradation of triclosan in freshwater and seawater. *Chemosphere* **2007**, *66* (6), 1052-1056.
19. McConnell, E. E.; Moore, J. A.; Haseman, J. K.; Harris, M. W., The comparative toxicity of chlorinated dibenzo-*p*-dioxins in mice and guinea pigs. *Toxicol. Appl. Pharmacol.* **1978**, *44* (2), 335-356.
20. Poland, A.; Glover, E., Studies on the mechanism of toxicity of the chlorinated dibenzo-*p*-dioxins. *Environ. Health Perspect.* **1973**, *5*, 245-251.
21. Wisk, J. D.; Cooper, K. R., Comparison of the toxicity of several polychlorinated dibenzo-*p*-dioxins and 2,3,7,8-tetrachlorodibenzofuran in embryos of the Japanese medaka (*Oryzias latipes*). *Chemosphere* **1990**, *20* (3-4), 361-377.
22. Mason, G.; Farrell, K.; Keys, B.; Piskorska-Pliszczynska, J.; Safe, L.; Safe, S., Polychlorinated dibenzo-*p*-dioxins: Quantitative in vitro and in vivo structure-activity relationships. *Toxicology* **1986**, *41* (1), 21-31.

23. Kanetoshi, A.; Ogawa, H.; Katsura, E.; Kaneshima, H., Chlorination of Irgasan DP300 and formation of dioxins from its chlorinated derivatives. *J. Chromatogr.* **1987**, *389* (1), 139-153.
24. Kanetoshi, A.; Ogawa, H.; Katsura, E.; Kaneshima, H.; Miura, T., Formation of polychlorinated dibenzo-*p*-dioxin from 2,4,4'-trichloro-2'-hydroxydiphenyl ether (Irgasan DP300) and its chlorinated derivatives by exposure to sunlight. *J. Chromatogr.* **1988**, *454*, 145-155.
25. Leifer, A., *The Kinetics of Environmental Aquatic Photochemistry: Theory and Practice*. American Chemical Society: Washington, DC, 1988; pp 333-362.
26. Dulin, D.; Mill, T., Development and evaluation of sunlight actinometers. *Environ. Sci. Technol.* **1982**, *16* (11), 815-820.
27. Gueymard, C. A., Parameterized transmittance model for direct beam and circumsolar spectral irradiance. *Solar Energy* **2001**, *71* (5), 325-346.
28. Gueymard, C. A., *SMARTS, A Simple Model of the Atmospheric Radiative Transfer of Sunshine: Algorithms and Performance Assessment*; Professional Paper FSEC-PF-270-95; Florida Solar Energy Center: Cocoa, FL, 1995.
29. Schwarzenbach, R. P.; Gschwend, P. M.; Imboden, D. M., *Environmental Organic Chemistry*. John Wiley & Sons: Hoboken, NJ, 2003.
30. Benitez, F. J.; Beltran-Heredia, J.; Acero, J. L.; Rubio, F. J., Oxidation of several chlorophenolic derivatives by UV irradiation and hydroxyl radicals. *J. Chem. Technol. Biotechnol.* **2001**, *76* (3), 312-320.
31. Latch, D. E.; Packer, J. L.; Stender, B. L.; VanOverbeke, J.; Arnold, W. A.; McNeill, K., Aqueous photochemistry of triclosan: Formation of 2,4-dichlorophenol, 2,8-dichlorodibenzo-*p*-dioxin, and oligomerization products. *Environ. Toxicol. Chem.* **2005**, *24* (3), 517-525.
32. Rayne, S.; Wan, P.; Ikonomou, M. G.; Konstantinov, A. D., Photochemical mass balance of 2,3,7,8-TeCDD in aqueous solution under UV light shows formation of chlorinated dihydroxybiphenyls, phenoxyphenols, and dechlorination products. *Environ. Sci. Technol.* **2002**, *36* (9), 1995-2002.
33. Choudhry, G. G.; Webster, G. R. B., Environmental photochemistry of polychlorinated dibenzofurans (PCDFs) and dibenzo-*p*-dioxins (PCDDs): A review. *Toxicol. Environ. Chem.* **1987**, *14* (1-2), 43-61.

34. Ferrer, I.; Mezcua, M.; Gomez, M. J.; Thurman, E. M.; Agueera, A.; Hernando, M. D.; Fernandez-Alba, A. R., Liquid chromatography/time-of-flight mass spectrometric analyses for the elucidation of the photodegradation products of triclosan in wastewater samples. *Rapid Commun. Mass Spectrom.* **2004**, *18* (4), 443-450.
35. Sanchez-Prado, L.; Llompart, M.; Lores, M.; Garcia-Jares, C.; Bayona, J. M.; Cela, R., Monitoring the photochemical degradation of triclosan in wastewater by UV light and sunlight using solid-phase microextraction. *Chemosphere* **2006**, *65* (8), 1338-1347.
36. Aguera, A.; Fernandez-Alba, A. R.; Piedra, L.; Mezcua, M.; Gomez, M. J., Evaluation of triclosan and biphenylol in marine sediments and urban wastewaters by pressurized liquid extraction and solid phase extraction followed by gas chromatography mass spectrometry and liquid chromatography mass spectrometry. *Anal. Chim. Acta* **2003**, *480* (2), 193-205.
37. Bester, K., Fate of triclosan and triclosan-methyl in sewage treatment plants and surface waters. *Arch. Environ. Contam. Toxicol.* **2005**, *49* (1), 9-17.
38. Sabaliunas, D.; Webb, S. F.; Hauk, A.; Jacob, M.; Eckhoff, W. S., Environmental fate of triclosan in the River Aire Basin, UK. *Water Res.* **2003**, *37* (13), 3145-3154.
39. Ontario Ministry of the Environment., *Scientific Criteria Document for Standard Development, no. 4-84. Polychlorinated Dibenzo-p-dioxins (PCDDs) and Polychlorinated Dibenzofurans (PCDFs)*; Ontario Ministry of the Environment: Toronto, Ontario, 1984.
40. Fiedler, H., National PCDD/PCDF release inventories under the Stockholm Convention on persistent organic pollutants. *Chemosphere* **2007**, *67* (9), S96-108.

-

Chapter 4 References

1. McAvoy, D. C.; Schatowitz, B.; Jacob, M.; Hauk, A.; Eckhoff, W. S., Measurement of triclosan in wastewater treatment systems. *Environ. Toxicol. Chem.* **2002**, *21* (7), 1323-1329.
2. Singer, H.; Mueller, S.; Tixier, C.; Pillonel, L., Triclosan: occurrence and fate of a widely used biocide in the aquatic environment: Field measurements in wastewater treatment plants, surface waters, and lake sediments. *Environ. Sci. Technol.* **2002**, *36* (23), 4998-5004.
3. Thomas, P. M.; Foster, G. D., Tracking acidic pharmaceuticals, caffeine, and triclosan through the wastewater treatment process. *Environ. Toxicol. Chem.* **2005**, *24* (1), 25-30.
4. Lindstrom, A.; Buerge Ignaz, J.; Poiger, T.; Bergqvist, P.-A.; Muller Markus, D.; Buser, H.-R., Occurrence and environmental behavior of the bactericide triclosan and its methyl derivative in surface waters and in wastewater. *Environ. Sci. Technol.* **2002**, *36* (11), 2322-2329.
5. Heidler, J.; Halden, R. U., Mass balance assessment of triclosan removal during conventional sewage treatment. *Chemosphere* **2006**, *66* (2), 362-369.
6. Bester, K., Triclosan in a sewage treatment process--balances and monitoring data. *Water Res.* **2003**, *37* (16), 3891-3896.
7. Sabaliunas, D.; Webb, S. F.; Hauk, A.; Jacob, M.; Eckhoff, W. S., Environmental fate of triclosan in the River Aire Basin, UK. *Water Res.* **2003**, *37* (13), 3145-3154.
8. Vanderford, B. J.; Snyder, S. A., Analysis of pharmaceuticals in water by isotope dilution liquid chromatography/tandem mass spectrometry. *Environ. Sci. Technol.* **2006**, *40* (23), 7312-7320.
9. Tixier, C.; Singer Heinz, P.; Canonica, S.; Muller Stephan, R., Phototransformation of ticlosan in surface waters: A relevant elimination process for this widely used biocide--laboratory studies, field measurements, and modeling. *Environ. Sci. Technol.* **2002**, *36* (16), 3482-3489.
10. Latch, D. E.; Packer, J. L.; Arnold, W. A.; McNeill, K., Photochemical conversion of triclosan to 2,8-dichlorodibenzo-*p*-dioxin in aqueous solution. *J. Photochem. Photobiol., A* **2003**, *158* (1), 63-66.
11. Kanetoshi, A.; Ogawa, H.; Katsura, E.; Kaneshima, H.; Miura, T., Study on the environmental hygienic chemistry of chlorinated 2-hydroxydiphenyl ethers: Photolytic conversion to polychlorinated dibenzo-*p*-dioxins. *Kankyo Kagaku* **1992**, *2* (3), 515-522.

12. Mezcua, M.; Gomez, M. J.; Ferrer, I.; Aguera, A.; Hernando, M. D.; Fernandez-Alba, A. R., Evidence of 2,7/2,8-dibenzodichloro-*p*-dioxin as a photodegradation product of triclosan in water and wastewater samples. *Anal. Chim. Acta* **2004**, *524* (1-2), 241-247.
13. Aranami, K.; Readman, J. W., Photolytic degradation of triclosan in freshwater and seawater. *Chemosphere* **2007**, *66* (6), 1052-1056.
14. Onodera, S.; Ogawa, M.; Suzuki, S., Chemical changes of organic compounds in chlorinated water. XIII. Gas chromatographic-mass spectrometric studies of the reactions of Irgasan DP 300 [5-chloro-2-(2,4-dichlorophenoxy)phenol] with chlorine in dilute aqueous solution. *J. Chromatogr.* **1987**, *392*, 267-275.
15. Rule, K. L.; Ebbett, V. R.; Vikesland, P. J., Formation of chloroform and chlorinated organics by free-chlorine-mediated oxidation of triclosan. *Environ. Sci. Technol.* **2005**, *39* (9), 3176-3185.
16. Canosa, P.; Morales, S.; Rodriguez, I.; Rubi, E.; Cela, R.; Gomez, M., Aquatic degradation of triclosan and formation of toxic chlorophenols in presence of low concentrations of free chlorine. *Anal. Bioanal. Chem.* **2005**, *383* (7-8), 1119-1126.
17. Greyshock, A. E.; Vikesland, P. J., Triclosan reactivity in chloraminated waters. *Environ. Sci. Technol.* **2006**, *40* (8), 2615-2622.
18. Leiker, T. J.; Abney, S. R.; Goodbred, S. L.; Rosen, M. R., Identification of methyl triclosan and halogenated analogues in male common carp (*Cyprinus carpio*) from Las Vegas Bay and semipermeable membrane devices from Las Vegas Wash, Nevada. *Sci. Total Environ.* **2009**, *407* (6), 2102-2114.
19. Nilsson, C.-A.; Andersson, K.; Rappe, C.; Westermark, S.-O., Chromatographic evidence for the formation of chlorodioxins from chloro-2-phenoxyphenols. *J. Chromatogr. A* **1974**, *96* (1), 137.
20. Kanetoshi, A.; Ogawa, H.; Katsura, E.; Kaneshima, H., Chlorination of Irgasan DP300 and formation of dioxins from its chlorinated derivatives. *J. Chromatogr.* **1987**, *389* (1), 139-153.
21. Kanetoshi, A.; Ogawa, H.; Katsura, E.; Kaneshima, H.; Miura, T., Formation of polychlorinated dibenzo-*p*-dioxin from 2,4,4'-trichloro-2'-hydroxydiphenyl ether (Irgasan DP300) and its chlorinated derivatives by exposure to sunlight. *J. Chromatogr.* **1988**, *454*, 145-155.
22. Ontario Ministry of the Environment., *Scientific Criteria Document for Standard Development, no. 4-84. Polychlorinated Dibenzo-*p*-dioxins (PCDDs) and Polychlorinated Dibenzofurans (PCDFs)*; Ontario Ministry of the Environment: Toronto, Ontario, 1984.

Chapter 5 References

1. Kolpin, D. W.; Furlong, E. T.; Meyer, M. T.; Thurman, E. M.; Zaugg, S. D.; Barber, L. B.; Buxton, H. T., Pharmaceuticals, hormones, and other organic wastewater contaminants in U.S. streams, 1999-2000: A national reconnaissance. *Environ. Sci. Technol.* **2002**, *36* (6), 1202-1211.
2. Singer, H.; Mueller, S.; Tixier, C.; Pillonel, L., Triclosan: occurrence and fate of a widely used biocide in the aquatic environment: Field measurements in wastewater treatment plants, surface waters, and lake sediments. *Environ. Sci. Technol.* **2002**, *36* (23), 4998-5004.
3. Lindstrom, A.; Buerge Ignaz, J.; Poiger, T.; Bergqvist, P.-A.; Muller Markus, D.; Buser, H.-R., Occurrence and environmental behavior of the bactericide triclosan and its methyl derivative in surface waters and in wastewater. *Environ. Sci. Technol.* **2002**, *36* (11), 2322-2329.
4. Nakada, N.; Kiri, K.; Shinohara, H.; Harada, A.; Kuroda, K.; Takizawa, S.; Takada, H., Evaluation of pharmaceuticals and personal care products as water-soluble molecular markers of sewage. *Environ. Sci. Technol.* **2008**.
5. Geigy., Preparation of halogenated 2-hydroxydiphenyl ethers. Eur. Patent NL6401526 (A), Aug. 24, 1964.
6. Susman, E., Too Clean for Comfort. *Environ. Health Perspect.* **2001**, *109* (1), A18.
7. First toothpaste approved for reducing gum disease. *FDA Consumer* [Online] **1997**.
8. Reiss, R.; Mackay, N.; Habig, C.; Griffin, J., An ecological risk assessment for triclosan in lotic systems following discharge from wastewater treatment plants in the United States. *Environ. Toxicol. Chem.* **2002**, *21* (11), 2483-2492.
9. McAvoy, D. C.; Schatowitz, B.; Jacob, M.; Hauk, A.; Eckhoff, W. S., Measurement of triclosan in wastewater treatment systems. *Environ. Toxicol. Chem.* **2002**, *21* (7), 1323-1329.
10. Heidler, J.; Halden, R. U., Mass balance assessment of triclosan removal during conventional sewage treatment. *Chemosphere* **2007**, *66* (2), 362-369.
11. Thomas, P. M.; Foster, G. D., Tracking acidic pharmaceuticals, caffeine, and triclosan through the wastewater treatment process. *Environ. Toxicol. Chem.* **2005**, *24* (1), 25-30.

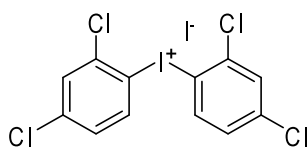
12. Kanetoshi, A.; Ogawa, H.; Katsura, E.; Kaneshima, H.; Miura, T., Study on the environmental hygienic chemistry of chlorinated 2-hydroxydiphenyl ethers: photolytic conversion to polychlorinated dibenzo-*p*-dioxins. *Kankyo Kagaku* **1992**, 2 (3), 515-522.
13. Latch, D. E.; Packer, J. L.; Arnold, W. A.; McNeill, K., Photochemical conversion of triclosan to 2,8-dichlorodibenzo-*p*-dioxin in aqueous solution. *J. Photochem. Photobiol., A* **2003**, 158 (1), 63-66.
14. Mezcua, M.; Gomez, M. J.; Ferrer, I.; Aguera, A.; Hernando, M. D.; Fernandez-Alba, A. R., Evidence of 2,7/2,8-dibenzodichloro-*p*-dioxin as a photodegradation product of triclosan in water and wastewater samples. *Anal. Chim. Acta* **2004**, 524 (1-2), 241-247.
15. Tixier, C.; Singer Heinz, P.; Canonica, S.; Muller Stephan, R., Phototransformation of triclosan in surface waters: A relevant elimination process for this widely used biocide--laboratory studies, field measurements, and modeling. *Environ. Sci. Technol.* **2002**, 36 (16), 3482-3489.
16. Onodera, S.; Ogawa, M.; Suzuki, S., Chemical changes of organic compounds in chlorinated water. XIII. Gas chromatographic-mass spectrometric studies of the reactions of Irgasan DP 300 [5-chloro-2-(2,4-dichlorophenoxy)phenol] with chlorine in dilute aqueous solution. *J. Chromatogr.* **1987**, 392, 267-275.
17. Rule, K. L.; Ebbett, V. R.; Vikesland, P. J., Formation of chloroform and chlorinated organics by free-chlorine-mediated oxidation of triclosan. *Environ. Sci. Technol.* **2005**, 39 (9), 3176-3185.
18. Leiker, T. J.; Abney, S. R.; Goodbred, S. L.; Rosen, M. R., Identification of methyl triclosan and halogenated analogues in male common carp (*Cyprinus carpio*) from Las Vegas Bay and semipermeable membrane devices from Las Vegas Wash, Nevada. *Sci. Total Environ.* **2009**, 407 (6), 2102-2114.
19. Mhin, B. J.; Lee, J. E.; Choi, W., Understanding the congener-specific toxicity in polychlorinated dibenzo-*p*-dioxins: Chlorination pattern and molecular quadrupole moment. *J. Am. Chem. Soc.* **2002**, 124 (1), 144-148.
20. Triplett, L.; Engstrom, D.; Conley, D.; Schellhaass, S., Silica fluxes and trapping in two contrasting natural impoundments of the upper Mississippi River. *Biogeochemistry* **2008**, 87 (3), 217-230.
21. Vanderford, B. J.; Snyder, S. A., Analysis of pharmaceuticals in water by isotope dilution liquid chromatography/tandem mass spectrometry. *Environ. Sci. Technol.* **2006**, 40 (23), 7312-7320.
22. U.S. Environmental Protection Agency., *Method 1613: Tetra- through Octa-Chlorinated Dioxins and Furans by Isotope Dilution HRGC/HRMS*, U.S. Environmental Protection Agency: Washington, D.C., 1994.

23. Green, N. J. L.; Jones, J. L.; Jones, K. C., PCDD/F Deposition Time Trend to Esthwaite Water, U.K., and Its Relevance to Sources. *Environ. Sci. Technol.* **2001**, *35* (14), 2882-2888.
24. Beck, H.; Dross, A.; Eckart, K.; Mathar, W.; Wittkowski, R., Determination of PCDDs and PCDFs in Irgasan DP 300. *Chemosphere* **1989**, *19* (1-6), 167-170.
25. Yang, Z.-j.; Ni, Y.-w.; Zhang, Z.-p.; Zhang, Q.; Chen, J.-p.; Liang, X.-m., Fingerprint of polychlorinated dibenzo-p-dioxins and dibenzofurans congeners in triclosan. *Jingxi Huagong* **2005**, *22* (1), 36-38.
26. Ni, Y.; Zhang, Z.; Zhang, Q.; Chen, J.; Wu, Y.; Liang, X., Distribution patterns of PCDD/Fs in chlorinated chemicals. *Chemosphere* **2005**, *60* (6), 779-784.
27. Hites, R. A.; Lopez-Avila, V., Identification of organic compounds in an industrial waste water. *Anal. Chem.* **1979**, *51* (14), 1452A-1456A.
28. Jungclaus, G. A.; Lopez-Avila, V.; Hites, R. A., Organic compounds in an industrial waste water: a case study of their environmental impact. *Environ. Sci. Technol.* **1978**, *12* (1), 88-96.
29. Lopez-Avila, V.; Hites, R. A., Organic compounds in an industrial wastewater. Their transport into sediments. *Environ. Sci. Technol.* **1980**, *14* (11), 1382-1390.
30. Liem, A. K. D.; Van de Berg, R.; Bremmer, H. J.; Hesse, J. M.; Slooff, W. *Integrated criteria document dioxins*; RIVM: Bilthoven, 1993.
31. Ontario Ministry of the Environment., *Scientific Criteria Document for Standard Development, no. 4-84. Polychlorinated Dibenzo-p-dioxins (PCDDs) and Polychlorinated Dibenzofurans (PCDFs)*; Ontario Ministry of the Environment: Toronto, Ontario, 1984.
32. Van den Berg, M.; Birnbaum, L.; Bosveld, A. T. C.; Brunstrom, B.; Cook, P.; Feeley, M.; Giesy, J. P.; Hanberg, A.; Hasegawa, R.; Kennedy, S. W.; Kubiak, T.; Larsen, J. C.; Van Leeuwen, F. X. R.; Liem, A. K. D.; Nolt, C.; Peterson, R. E.; Poellinger, L.; Safe, S.; Schrenk, D.; Tillitt, D.; Tysklind, M.; Younes, M.; Waern, F.; Zacharewsky, T., Toxic Equivalency Factors (TEFs) for PCBs, PCDDs, PCDFs for Humans and Wildlife. *Environ. Health Perspect.* **1998**, *106* (12), 775-792.

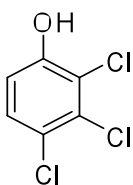
Appendix: Synthesis and Purification of Chlorinated Triclosan Derivatives (CTDs)

(Synthesis of CTDs was performed by Matthew Grandbois, Ph.D. candidate, Chemistry)

The synthesis of CTDs was performed following the general strategy of Marsh et al. [1] for the synthesis of polybrominated diphenyl ethers. All reagents were purchased from commercial suppliers. Solvents were used as received unless otherwise specified. Proton nuclear magnetic resonance spectroscopy (^1H NMR) and carbon nuclear magnetic resonance spectroscopy (^{13}C NMR) utilized a Varian 500 MHz NMR spectrometer. Electrospray ionization time-of-flight mass spectrometry (ESI-TOF-MS) and electrospray ionization time-of-flight high resolution mass spectrometry (ESI-TOF-HRMS) utilized a Bruker BioTOF II mass spectrometer. Preparative HPLC was run on an 1100 series Hewlett-Packard HPLC equipped with UV-absorbance detection. Injections of 100 μL were made on a Supelco Discovery RP-Amide C₁₆, 100 \times 21.1 mm, 5 μm particle size column with an acetonitrile:pH 5 acetate buffer (82:18, v/v) mobile phase run at 5 mL/min and 230 nm detection.

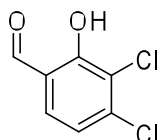


2,2',4,4'-Tetrachlorodiphenyliodonium Iodide (1): Iodine (5.58g, 22.0mmol) was suspended in a mixture of concentrated sulfuric acid (13.0 mL) and fuming sulfuric acid (12.0 mL) added dropwise at room temperature. To this was added a mixture of concentrated sulfuric acid (1.5 mL), fuming sulfuric acid (1.6 mL), and fuming nitric acid (3.3 mL) dropwise and then stirred 75°C for two hours. The mixture was diluted with sulfuric acid (20 mL) and then 1,3-dichlorobenzene (25 g, 106.0mmol) was added dropwise at room temperature. The mixture was stirred at 40°C for twelve hours. Water (100 mL) was added in small portions at 0°C while a stream of N₂(g) was bubbled through the mixture to remove the formed nitric oxides. The resultant mixture was allowed to sit overnight in a freezer. The clear liquid was decanted off and the remaining residue was dissolved in methanol (300 mL). A solution of potassium iodide (10 g, 60.2mmol, 10 mL H₂O) was added dropwise. The crystallized product (18.678 g, 78%) was filtered off and washed with methanol and water. ^1H NMR (500 MHz, acetone-d₆): δ = 8.46 (d, J = 8.5 Hz, 2H, 6-H), 7.81 (d, J = 2.0 Hz, 2H, 5-H), 7.52 (dd, J = 2.5, 8.5 Hz, 2H, 3-H) ppm.

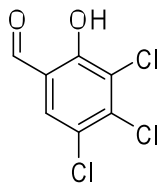


2,3,4-Trichlorophenol (2): 2,3,4-Trichloroaniline (1.0108g, 5.159 mmol) was dissolved in concentrated sulfuric acid (10 mL). To this was added sodium nitrite (0.35517g, 5.15 mmol) in water (3 mL). The solution was brought to reflux and allowed to stir for 4 hours, upon which the solution was cooled to room temperature and

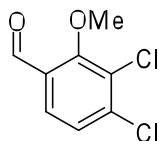
extracted with diethyl ether (100 mL, 3x). The combined organic fractions were dried over Na_2SO_4 and the solvents were removed *in vacuo*. Flash column chromatography (3:1 CH_2Cl_2 :hexanes) gave the crude desired product (0.5547g, 55%) as white crystals. ^1H NMR (500 MHz, CDCl_3): δ = 7.29 (d, J = 9.0 Hz, 1H, 5-H), 6.91 (d, J = 9.0 Hz, 1H, 6-H), 5.88 (s, 1H, OH) ppm. ESI-MS m/z [ion] (rel. int%): 195.2 [$\text{M}-\text{H}$] $^-$ (100), 197.2 [$\text{M}-\text{H}+2$] $^-$ (94), 199.2 [$\text{M}-\text{H}+4$] $^-$ (30). ESI-HRMS: m/z = 194.9175, 2.1 ppm [$\text{C}_6\text{H}_2\text{Cl}_3\text{O}$] $^-$.



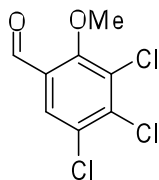
2,3-Dichlorosalicylaldehyde (3): 2,3-Dichlorophenol (5.093g, 31.2 mmol) and anhydrous MgCl_2 (4.570g, 48.0 mmol) were suspended in a round bottom flask equipped with a reflux condenser with dry acetonitrile (70 mL, from CaH_2). To this mixture was added dry triethylamine (16.0 mL, 113.9 mmol, from Na) and dry paraformaldehyde (6.431g, 214.4mmol, 5.0 M in acetonitrile, from P_2O_5). The solution was refluxed for 3 hours, upon which hydrochloric acid (5%, 50 mL) was added. The solution was extracted with diethyl ether (50 mL, 3x) and dried over Na_2SO_4 . The solvents were removed *in vacuo*. Flash column chromatography (1:4 EtOAc:hexanes, R_f = 0.4) gave the desired product (4.5863g, 77%) as a white solid. ^1H NMR (500 MHz, CDCl_3) δ = 11.79 (s, 1H, OH), 9.88 (s, 1H, CHO), 7.44 (d, J = 8.5 Hz, 1H, 6-H), 7.16 (d, J = 8.5 Hz, 1H, 4-H) ppm. ^{13}C NMR (500 NMR, CDCl_3) δ = 195.37 (CHO), 131.50 (6-C), 128.08 (2-C), 122.17 (4-C), 121.52 (5-C), 119.47 (1-C), 114.40 (1-C) ppm.



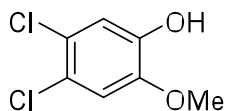
2,3,4-Trichlorosalicylaldehyde (4): In a round bottom flask equipped with a reflux condenser were suspended **2** (0.7680g, 4.79 mmol) and anhydrous MgCl_2 (0.7680g, 8.07 mmol) with dry acetonitrile (70 mL, from CaH_2). To this mixture was added dry triethylamine (2.6 mL, 18.52 mmol, from Na) and dry paraformaldehyde (1.0654g, 35.5mmol, 5.0 M in acetonitrile, from P_2O_5). The solution was refluxed for 3 hours, upon which hydrochloric acid (5%, 50 mL) was added. The solution was extracted with diethyl ether (50 mL, 3x) and dried over Na_2SO_4 . The solvents were removed *in vacuo*. Flash column chromatography (1:4 EtOAc:hexanes, R_f = 0.4) gave the desired product (0.1562g, 14%) as a yellow solid. ^1H NMR (500 MHz, CDCl_3) δ = 11.79 (s, 1H, OH), 9.88 (s, 1H, CHO), 7.44 (d, J = 8.5 Hz, 1H, 6-H), 7.16 (d, J = 8.5 Hz, 1H, 4-H) ppm. ^{13}C NMR (500 NMR, CDCl_3) δ = 195.37 (CHO), 131.50 (6-C), 128.08 (2-C), 122.17 (4-C), 121.52 (5-C), 119.47 (1-C), 114.40 (1-C) ppm. ESI-MS m/z [ion] (rel. int%): 223.0 [$\text{M}-\text{H}$] $^-$ (100), 225.0 [$\text{M}+2-\text{H}$] $^-$ (95), 227.0 [$\text{M}+4-\text{H}$] $^-$ (33). ESI-HRMS: m/z = 222.9138, 8.1 ppm [$\text{C}_7\text{H}_2\text{Cl}_3\text{O}_2$] $^-$.



3,4-Dichloro-2-methoxybenzaldehyde (5): In a round bottom flask equipped with magnetic stir bar, **3** (4.5863g, 24.0 mmol), sodium hydroxide (5.316g, 132.9 mmol), and tetrabutylammonium hydroxide (20.008g, 25.0 mmol) were partitioned between methylene chloride (50 mL) and water (50 mL). To this bright yellow solution was added iodomethane (7.5mL, 120.5 mmol). The solution was allowed to stir at room temperature until colorless, upon which the layers were separated. The aqueous layer was extracted with methylene chloride (50 mL, 3x) and the organic layers were combined and dried over Na₂SO₄. The solvents were removed *in vacuo*. Flash column chromatography (3:1 CH₂Cl₂:hexanes) gave the desired product (2.5956g, 53%) as a white powder. ¹H NMR (500 MHz, CDCl₃): δ = 10.32 (s, 1H, CHO), 7.71 (d, J = 8.5 Hz, 1H, 6-H), 7.37 (d, J = 8.5 Hz, 1H, 5-H), 4.03 (s, 3H, CH₃) ppm. ¹³C NMR (500 NMR, CDCl₃) δ = 188.23 (CHO), 164.01 (2-C), 140.54 (4-C), 129.05 (3-C), 126.65 (6-C), 126.44 (5-C), 114.88 (1-C), 63.42 (CH₃) ppm.

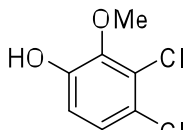


3,4,5-Trichloro-2-methoxybenzaldehyde (6): In a round bottom flask equipped with magnetic stir bar, **4** (0.0556g, 0.26 mmol) and tetrabutylammonium hydroxide (0.4256g, 0.53 mmol) were partitioned between methylene chloride (8 mL) and 1 M NaOH (8 mL). To this bright yellow solution was added iodomethane (100μL, 1.60 mmol). The solution was allowed to stir at room temperature for 48 hours, upon which the layers were separated. The aqueous layer was extracted with methylene chloride (50 mL, 3x) and the organic layers were combined and dried over Na₂SO₄. The solvents were removed *in vacuo*. Flash column chromatography (3:1 CH₂Cl₂:hexanes) gave the desired product (0.0573g, 97%) as a white powder. ¹H NMR (500 MHz, CDCl₃): δ = 10.28 (s, 1H, CHO), 7.86 (s, 1H, 6-H), 4.02 (s, 3H, CH₃) ppm. ¹³C NMR (500 NMR, CDCl₃) δ = 187.10 (CHO), 158.35 (2-C), 138.99 (4-C), 130.49 (5-C), 127.92 (1-C), 127.03 (6-C), 110.32 (3-C), 63.54 (CH₃) ppm.

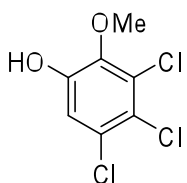


4,5-Dichloroguaiacol (7): Sulphuryl chloride (46.8 mL, 578 mmol) was added drop wise to a round bottom flask containing guaiacol (32.522g, 262.0 mmol). The reaction solution was allowed to stand overnight, upon which the resulting solid was washed with petroleum ether. Recrystallization from hexanes resulted in the desired product (13.8143g, 27%) as fine white crystals. ¹H NMR (500 MHz, CDCl₃): δ = 8.32 (s, 1H, CHO), 7.11 (s, 1H, 3-H), 6.99 (s, 1H, 6-H), 3.88 (s, 3H,

OCH₃) ppm. ESI-MS m/z [ion] (rel. int%): 191.1 [M-H]⁻ (100), 193.1 [M-H+2]⁻ (61). ESI-HRMS: m/z = 190.9657, 5.2 ppm [C₇H₅Cl₂O₂]⁻.

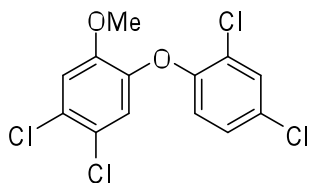


3,4-Dichloro-2-methoxyphenol (8): In a round bottom flask with magnetic stir bar were suspended **5** (2.5606g, 12.5 mmol) and KH₂PO₄ (34.5116g, 253 mmol) in methylene chloride (100 mL). In another flask was added hydrogen peroxide (2.0918g, 18.5 mmol, 30%) and methylene chloride (2 mL). The peroxide solution was cooled to 0°C, upon which trifluoroacetic acid anhydride (13.0 mL, 92.0 mmol) was added drop wise and then allowed to stir for an additional hour at 0°C. The aldehyde mixture was cooled to 0°C and then the peroxide solution added drop wise. The reaction mixture was allowed to stir for two hours, upon which brine (25 mL) and aqueous NaHSO₃ (25 mL, 20%) were added to quench the reaction. The layers were separated and the aqueous layer was extracted with methylene chloride (30 mL, 3x). The organic layers were combined and the solvent was removed *in vacuo*. The residue was dissolved in methanol (20 mL) with one drop of concentrated hydrochloric acid. The reaction mixture was allowed for twelve hours and then the solvents were removed *in vacuo*. Flash column chromatography (4:1 CH₂Cl₂:hexanes) gave the desired product (2.2724g, 94%) as a colorless oil. ¹H NMR (500 NMR, CDCl₃): δ = 7.13 (d, J = 8.5 Hz, 1H, 5-H), 6.85 (d, J = 8.5 Hz, 1H, 6-H), 5.74 (s, 1H, OH), 3.93 (s, 3H, CH₃) ppm. ¹³C NMR (500 NMR, CDCl₃) δ = 148.57 (2-C), 144.43 (1-C), 126.14 (4-C), 125.79 (5-C), 124.15 (3-C), 114.44 (6-C), 61.17 (CH₃) ppm. ESI-MS m/z [ion] (rel. int%): 191.1 [M]⁻ (100), 193.1 [M+2]⁻ (69.8), 195.1 [M+4]⁻ (7.8). ESI-HRMS: m/z = 190.9675, 4.2 ppm [C₇H₅Cl₂O₂]⁻.

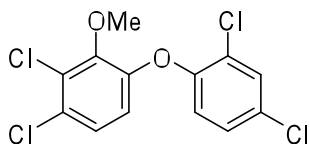


3,4,5-Trichloro-2-methoxyphenol (9): In a round bottom flask with equipped with magnetic stir bar were suspended **6** (0.1123g, 0.47 mmol) and KH₂PO₄ (0.2667g, 1.96 mmol) were suspended in methylene chloride (10 mL). In another flask was added hydrogen peroxide (0.1162g, 1.02 mmol, 30%) and methylene chloride (1 mL). The peroxide solution was cooled to 0°C, upon which trifluoroacetic acid anhydride (500 μL, 3.53 mmol) was added drop wise and then allowed to stir for an additional hour at 0°C. The aldehyde mixture was cooled to 0°C and then the peroxide solution added dropwise. The reaction mixture was allowed to stir for two hours, upon which brine (10 mL) and aqueous NaHSO₃ (10 mL, 20%) were added to quench the reaction. The layers were separated and the aqueous layer was extracted with methylene chloride (30 mL, 3x). The organic layers were combined and the solvent was removed *in vacuo*. The residue was dissolved in methanol (10 mL) with one drop of concentrated hydrochloric acid. The reaction mixture was allowed for twelve hours and then the solvents were removed *in vacuo*. Flash column chromatography (4:1

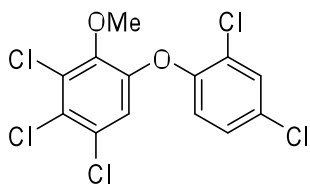
CH₂Cl₂:hexanes) gave the desired product (0.0892g, 84%) as a white solid. ¹H NMR (500 NMR, CDCl₃): δ = 7.06 (s, 1H, 6-H), 5.85 (s, 1H, OH), 3.92 (s, 3H, CH₃) ppm. ¹³C NMR (500 NMR, CDCl₃) δ = 148.36 (2-C), 143.33 (1-C), 129.31 (3-C), 127.51 (5-C), 115.56 (6-C), 114.38 (4-C), 61.30 (CH₃) ppm. ESI-MS m/z [ion] (rel. int%): 225.0 [M-H]⁻ (100), 227.0 [M-H+2]⁻ (99), 229.0 [M-H+4]⁻ (30). ESI-HRMS: m/z = 224.9277, 1.8 ppm [C₇H₄Cl₃O₂]⁻.



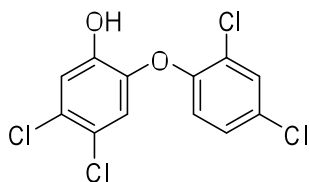
4,5-Dichloro-2-(2,4-dichlorophenoxy)anisole (10): In a round bottom flask were suspended **7** (2.0185g, 10.46 mmol), potassium carbonate (2.9277g, 21.18 mmol), and 18-crown-6 ether (0.2981g, 1.13 mmol) in N,N-dimethylacetamide (25 mL). To this reaction mixture was added **1** (11.494g, 21.06 mmol) and then heated to 80°C where it was stirred for 15 hours. The mixture was cooled to room temperature and diluted with methylene chloride (25 mL) and water (250 mL). The layers were separated and the aqueous layer was extracted with methylene chloride (25 mL, 3x). The organic fractions were combined, washed with aqueous NaHSO₃ (25 mL, 5%), aqueous NaOH (25 mL, 1.0 M, 2x), water (25 mL, 3x), and dried over Na₂SO₄. The solvent was removed *in vacuo*. Flash column chromatography (4:1 hexanes:CH₂Cl₂) gave the desired product (2.4786, 70%) as a colorless resin. ¹H NMR (500 MHz, CDCl₃): δ = 7.45 (d, J = 2.0 Hz, 1H, 3'-H), 7.16 (dd, J = 2.5, 9.0 Hz, 1H, 5'-H), 7.06 (s, 1H, 3-H), 6.94 (s, 1H, 6-H), 6.77 (d, J = 8.5 Hz, 1H, 6'-H) ppm. ¹³C NMR (500 NMR, CDCl₃) δ = 151.15 (2C), 149.85 (1'-C), 143.85 (1-C), 130.54 (3'-C), 130.22 (4-C), 129.19 (4'-C), 128.36 (2'-C), 128.02 (6-C), 125.42 (5-C), 120.90 (5'-C), 119.47 (3-C), 114.52 (6'-C) ppm.



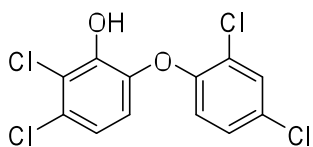
5,6-Dichloro-2-(2,4-dichlorophenoxy)anisole (11): In a round bottom flask were suspended **8** (2.203g, 11.4 mmol), potassium carbonate (3.302g, 23.9 mmol), and 18-crown-6 ether (0.307g, 1.2 mmol) in N,N-dimethylacetamide (50 mL). To this reaction mixture was added **1** (12.619g, 23.1 mmol) and then heated to 80°C where it was stirred for 2 hours. The mixture was cooled to room temperature and diluted with methylene chloride (50 mL) and water (50 mL). The layers were separated and the aqueous layer was extracted with methylene chloride (50 mL, 3x). The organic fractions were combined, washed with aqueous NaHSO₃ (50 mL, 5%), aqueous NaOH (50 mL, 1.0 M, 2x), water (50 mL, 3x), and dried over Na₂SO₄. The solvent was removed *in vacuo*. Flash column chromatography (4:1 hexanes:CH₂Cl₂, R_f = 0.52) gave the desired product (2.882g, 75%) as a colorless resin. ¹H NMR (500 MHz, CDCl₃): δ = 7.47 (d, J = 2.5 Hz, 1H, 3'-H), 7.17 (m, 2H, 6-H, 6'-H), 6.77 (m, 2H, 4-H, 5'-H), 3.93 (s, 3H, CH₃) ppm.



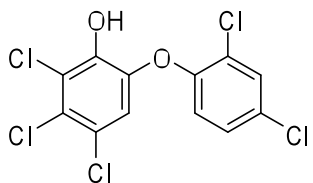
4,5,6-Trichloro-2-(2,4-dichlorophenoxy)anisole (12): In a round bottom flask were suspended **9** (0.1848g, 0.37 mmol), potassium carbonate (0.1117g, 0.81 mmol), and 18-crown-6 ether (0.0437g, 0.17 mmol) in N,N-dimethylacetamide (10 mL). To this reaction mixture was added **1** (0.4237g, 0.78 mmol) and then heated to 80°C where it was stirred for 15 hours. The mixture was cooled to room temperature and diluted with methylene chloride (25 mL) and water (250 mL). The layers were separated and the aqueous layer was extracted with methylene chloride (25 mL, 3x). The organic fractions were combined, washed with aqueous NaHSO₃ (25 mL, 5%), aqueous NaOH (25 mL, 1.0 M, 2x), water (25 mL, 3x), and dried over Na₂SO₄. The solvent was removed *in vacuo*. Flash column chromatography (4:1 hexanes:CH₂Cl₂) gave the desired product (0.1183g, 85%) as a colorless resin. ¹H NMR (500 MHz, CDCl₃): δ = 7.50 (d, J = 2.5 Hz, 1H, 3'-H), 7.24 (dd, J = 2.5, 8.5 Hz, 1H, 5'-H), 6.88 (d, J = 8.5 Hz, 1H, 6'-H), 6.86 (s, 1H, 6-H), 3.93 (s, 3H, CH₃) ppm. ¹³C NMR (500 NMR, CDCl₃) δ = 150.08 (2-C), 148.46 (1'-C), 146.88 (1-C), 130.81 (3'-C), 130.46 (4-C), 130.00 (4'-C), 129.81 (2'-C), 128.42 (6-C), 127.41 (5-C), 120.67 (5'-C), 118.86 (3-C), 118.18 (6'-C) 61.42 (CH₃) ppm.



4,5-Dichloro-2-(2,4-dichlorophenoxy)phenol (13): In a round bottom flask equipped with a reflux condenser and magnetic stir bar was dissolved **10** (1.1730g, 3.47 mmol) in dry methylene chloride (20 mL, from CaH₂). Boron tribromide (3.3 mL, 34.9 mmol) was added and the solution was allowed to stir for 48 hours, upon which the solution was cooled to 0°C and water (10 mL) was carefully added. The solution was extracted with methylene chloride (10 mL, 3x) and dried over Na₂SO₄. The solvents were removed *in vacuo*. Flash column chromatography (1:1 CH₂Cl₂:hexanes) gave the desired product (1.0508g, 93%) as a colorless oil. Further purification (98%) was accomplished by preparative HPLC on a Supelco Discovery RP-Amide C₁₆, 100 × 21.1 mm, 5 μm particle size column with an acetonitrile:pH 5 phosphate buffer (82:18 v/v) mobile phase, a flow rate of 5 mL/min, and detection at 230 nm. ¹H NMR (500 MHz, CDCl₃): δ = 7.51 (d, J = 2.5 Hz, 1H, 3'-H), 7.28 (dd, J = 2.5, 8.5 Hz, 1H, 5'-H), 7.17 (s, 1H, 3-H), 7.02 (d, J = 8.5 Hz, 1H, 6'-H), 6.75 (s, 1H, 6-H), 5.76 (s, 1H, OH) ppm. ¹³C NMR (500 NMR, CDCl₃) δ = 149.60 (1'-C), 145.70 (2-C), 142.82 (1-C), 130.98 (3'-C), 130.62 (4'-C), 128.55 (5'-C), 127.83 (2'-C), 126.75 (4-C), 123.36 (5-C), 121.74 (6'-C), 117.95 (6-C), 117.88 (3-C) ppm. ESI-MS m/z [ion] (rel. int%): 323.1 [M-H]⁻ (100), 321.1 [M-H-2]⁻ (63), 325.1 [M-H+2]⁻ (41). ESI-HRMS: m/z = 322.9003, 3.4 ppm [C₁₂H₅Cl₄O₂].



5,6-Dichloro-2-(2,4-dichlorophenoxy)phenol (14): In a round bottom flask equipped with a reflux condenser and magnetic stir bar was dissolved **11** (1.911g, 5.65 mmol) in dry methylene chloride (25 mL, from CaH₂). Boron tribromide (5.4 mL, 56.5 mmol) was added and the solution was refluxed for 24 hours, upon which the solution was cooled to 0°C and water (50 mL) was carefully added. The solution was extracted with methylene chloride (50 mL, 3x) and dried over Na₂SO₄. The solvents were removed *in vacuo*. Flash column chromatography (1:1 CH₂Cl₂:hexanes, R_f = 0.43) gave the desired product (1.6698g, 91%) as a white solid. Further purification (98%) was accomplished by preparative HPLC on a Supelco Discovery RP-Amide C₁₆, 100 × 21.1 mm, 5 μm particle size column with an acetonitrile:pH 5 phosphate buffer (82:18 v/v) mobile phase, a flow rate of 5 mL/min, and detection at 230 nm. ¹H NMR (500 MHz, CDCl₃): δ = 7.49 (s, 1H, 3'-H), 7.22 (dd, J = 2.5, 8.5 Hz, 1H, 5'-H), 6.97 (d, J = 9.0 Hz, 1H, 5-H), 6.92 (d, J = 9.0 Hz, 1H, 6'-H), 6.65 (d, J = 9.0 Hz, 1H, 6-H), 5.98 (s, 1H, OH) ppm. ¹³C NMR (500 NMR, CDCl₃) δ = 150.31 (1'-C), 144.50 (2-C), 142.62 (1-C), 130.75 (3'-C), 130.21 (4'-C), 128.45 (2'-C), 128.27 (5'-C), 126.241 (5-C), 120.96 (4-C), 120.76 (6'-C), 120.42 (6-C), 116.38 (3-C) ppm. ESI-MS m/z [ion] (rel. int%): 323.0 [M-H]⁻ (100), 321.0 [M-2-H]⁻ (71.5), 325.0 [M+2-H]⁻ (45.6), 327.0 [M+4-H]⁻ (7.3). ESI-HRMS: m/z = 322.9056, 13 ppm [C₁₂H₅Cl₄O₂]⁻.

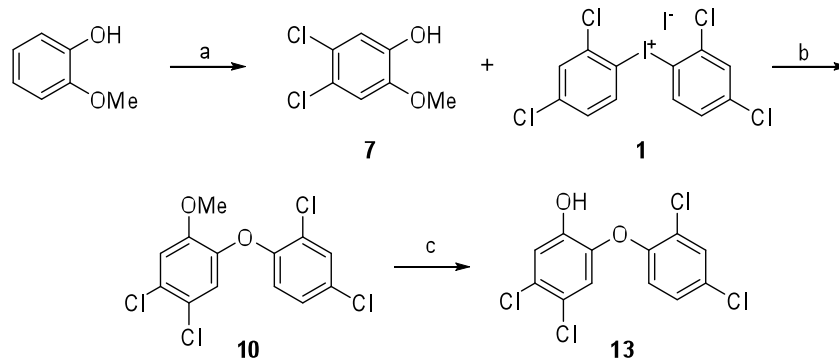


4,5,6-Trichloro-2-(2,4-dichlorophenoxy)phenol (15): In a round bottom flask equipped with a reflux condenser and magnetic stirbar was dissolved **12** (0.1163g, 0.31 mmol) in dry methylene chloride (5 mL, from CaH₂). Boron tribromide (300 μL, 3.17 mmol) was added and the solution was refluxed for 24 hours, upon which the solution was cooled to 0°C and water (5 mL) was carefully added. The solution was extracted with methylene chloride (10 mL, 3x) and dried over Na₂SO₄. The solvents were removed *in vacuo*. Flash column chromatography (1:1 CH₂Cl₂:hexanes, R_f = 0.41) gave the desired product (0.1066g, 95%) as a colorless oil. Further purification (97%) was accomplished by preparative HPLC on a Supelco Discovery RP-Amide C₁₆, 100 × 21.1 mm, 5 μm particle size column with an acetonitrile:pH 5 phosphate buffer (82:18 v/v) mobile phase, a flow rate of 5 mL/min, and detection at 230 nm. ¹H NMR (500 MHz, CDCl₃): δ = 7.51 (d, J = 2.5 Hz, 1H, 3'-H), 7.27 (dd, J = 2.5, 8.5 Hz, 1H, 5'-H), 7.00 (d, J = 8.5 Hz, 1H, 6'-H), 6.77 (s, 1H, 6-H), 6.04 (s, 1H, OH) ppm. ¹³C NMR (500 NMR, CDCl₃) δ = 149.50 (1'-C), 143.01 (2-C), 142.76 (1-C), 130.98 (3'-C), 130.65 (4'-C), 128.52 (5'-C), 126.99 (2'-C), 126.68 (4-C), 124.26 (5-C), 121.63 (6'-C), 121.52 (3-C), 116.53 (6-C) ppm. ESI-MS m/z [ion]

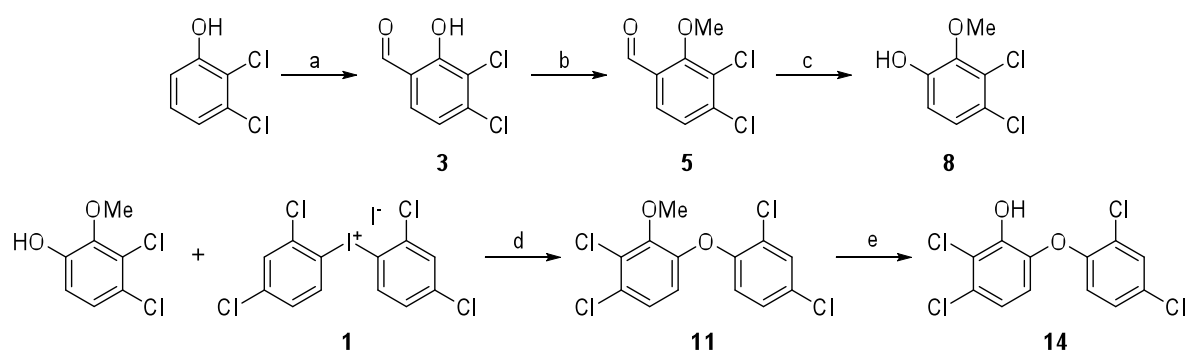
(rel. int%): 357.0 [M-H]⁻ (100), 359.0 [M-H+2]⁻ (61.3), 355.0 [M-H-2]⁻ (54.9), 361.0 [M-H+4]⁻ (16.2). ESI-HRMS: m/z = 356.8624, 2.5 ppm [C₁₂H₄Cl₅O₂]⁻.

Reference

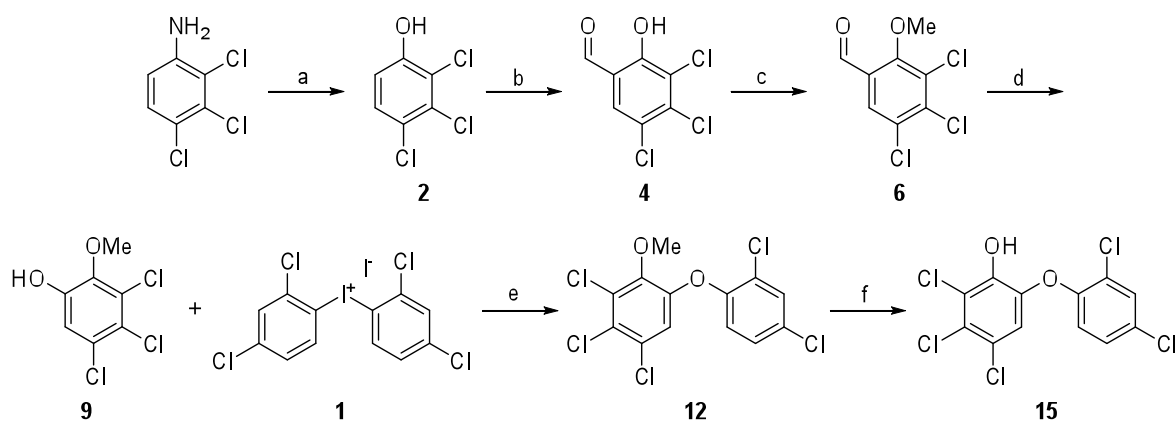
1. Marsh, G.; Hu, J.; Jakobsson, E.; Rahm, S.; Bergman, A. Synthesis and characterization of 32 polybrominated diphenyl ethers. *Environ. Sci. Technol.* **1999**, *33*, 3033-3037.



Scheme S1. Synthesis of 4,5-Dichloro-2-(2,4-Dichlorophenoxy)phenol. Reaction conditions: a) sulfuryl chloride, 27%; b) NaOH, dioxane, H₂O, 70%; c) BBr₃, CH₂Cl₂, r.t., 93%.



Scheme S2. Synthesis of 5,6-Dichloro-2-(2,4-Dichlorophenoxy)phenol (19). Reaction conditions: a) MgCl₂, paraformaldehyde, TEA, CH₃CN, 77%; b) (C₄H₉)₄NOH, NaOH, MeI, CH₂Cl₂, H₂O, 53%; c) 1) H₂O₂, (CF₃CO)₂O, KH₂PO₄, CH₂Cl₂, 2) MeOH, HCl, 94%; d) K₂CO₃, 18-crown-6, DMAC, 75%; f) BBr₃, CH₂Cl₂, 91%.



Scheme S3. Synthesis of 4,5,6-Trichloro-2-(2,4-Dichlorophenoxy)phenol. Reaction conditions: a) H₂SO₄, NaNO₂, 55%; b) MgCl₂, paraformaldehyde, TEA, CH₃CN, 14%; c) (C₄H₉)₄NOH, NaOH, MeI, CH₂Cl₂, H₂O, 97%; d) 1) H₂O₂, (CF₃CO)₂O, KH₂PO₄, CH₂Cl₂, 2) MeOH, HCl, 84%; e) K₂CO₃, 18-crown-6, DMAC, 85%; f) BBr₃, CH₂Cl₂, 95%.